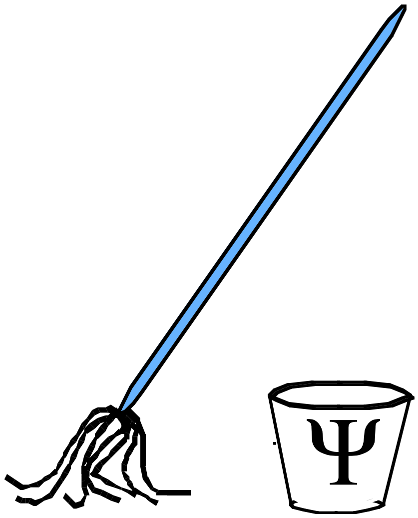

QM for AMOP

Chapter 5
Waves in Per-Spacetime: (k,ω)-Dispersion

W. G. Harter

A fundamental axiom of wave-phase invariance leads to a logical development of the principles of quantum theory and relativistic dynamics that are the current foundations of modern physics. Careful examination of wavevector and frequency leads to their relativistic properties that mirror those of space and time developed in the preceding chapters. The Planck's axiom E=hν then leads directly to momentum-energy , rest energy Mc^2, and other key ideas such as a wave dispersion interpretation of inertial mass and classical dynamics. The Schrodinger equation is seen as an approximation and it limitations are discussed. Relativistic accelerative dynamics are introduced from both classical and quantum points of view.

Chapter 5. Waves in Per-Spacetime: (k,ω)-Dispersion

5.1 Relativistic invariant hyperbolas

So much of physics held dear in Newtonian theory seems to soften in relativity and quantum wave theory. As modern physics mixes time and space or per-time (frequency ω) and per-space (k-vector), the hard and precise classical world might seem to be melting into shifting sands as wave relativism trumps cherished absolutes. However, any idea that classical measurement may have absolute precision is a myth.

In fact, modern coherent wave and pulse optics has achieved a precision that puts any classical "hard edge" meter rods to shame. Imagine building a Global Positioning System out of steel girders even for a *1 km* asteroid! Without optically aided stabilization, such a frame would be next to useless.

Optics owes much of its tremendous precision to *invariants* that are constant for all observers. Lightspeed in (4.3.1) is one invariant and *wave phase* in (4.3.6) is another. Other invariants, including the hyperbolic geometry introduced in Sec. 4.4 and reviewed below, are related to these. Any and all invariants are welcome and useful additions to spacetime wave theory. A port, any port, in a storm!

(a) Hyperbolic wavevector geometry: "baseball diamond" invariants

The "baseball-diamond" geometry of counter-propagating laser waves introduced in Fig. 4.3.2 and Fig. 4.4.3 is repeated again in the following Fig. 5.1.1. This has per-spacetime plots or frequency-ω-*versus*-wavevector-*ck* graphs of the interfering output waves between a pair dueling lasers of identical frequency $\omega_0=2c$ and opposite wavevectors $ck_0=\pm 2c$. ($1c$ unit is 300 THz.) Fig. 5.1.1(a) displays green light *ck*-wavevectors pointing in opposite directions at 600 THz, as seen by the lasers. Fig. 5.1.1(b), is the view of an atom traveling right to left in the frame where it sees the right-moving laser beam Doppler blue shifted up to 1200 THz while the left-moving wave is red shifted down to 300THz.

The color-invariant lightspeed axiom (4.3.1) confines laser (ck,ω) vectors to the $\pm 45°$ baselines or "foul ball lines" while the time-reversal axiom demands that Doppler red shift $r=e^{-\rho}$ be inverse to the blue shift $b=e^{\rho}$ in (4.3.5b). The right baseline stretches by $b=2$ while the left baseline shrinks by $1/b$. So a product of foul-line hypotenuses $\sqrt{2}\omega_0 b$ and $\sqrt{2}\omega_0 r$ must be a constant $2\omega_0^2$. So, the diagonal of the $\sqrt{2}\omega_0 b$–by–$\sqrt{2}\omega_0 r$ rectangle follows a hyperbola of radius $2\omega_0$ traced by "2nd base" in Fig. 5.1.1(b) as blue shift b or relativistic speed $\beta=u/c$ of the atom increases.

Baseball diamond half-diagonals follows a hyperbola of radius ω_0, on which lies the "pitcher's mound" at diamond center. Half-diagonal vectors $\mathbf{K}'_{phase}=(\mathbf{K}'_{\rightarrow}+\mathbf{K}'_{\leftarrow})/2$ and $\mathbf{K}'_{group}=(\mathbf{K}'_{\rightarrow}-\mathbf{K}'_{\leftarrow})/2$ are half-sum (difference) of laser vectors $\mathbf{K}'_{\rightarrow}$ and $\mathbf{K}'_{\leftarrow}$. They define phase and group waves in (4.2.10) or (4.3.4).

$$\mathbf{K}'_{phase}=((k'_{\rightarrow}+k'_{\leftarrow})/2,\ (\omega'_{\rightarrow}+\omega'_{\leftarrow})/2) \quad (5.1.1a) \qquad \mathbf{K}'_{group}=((k'_{\rightarrow}-k'_{\leftarrow})/2,\ (\omega'_{\rightarrow}-\omega'_{\leftarrow})/2)) \quad (5.1.1b)$$

Vectors $\mathbf{K}'_{phase}$ and $\mathbf{K}'_{group}$ define a Lorentz-Einstein-Minkowski coordinate grid in *both* spacetime (4.3.5e) *and* per-spacetime (4.3.10). A wave-produced spacetime grid is shown in Fig. 4.3.3(a) for the lasers and in Fig. 4.3.3(b) for the atom speeding through the laser field at $\beta=u/c=-3/5$. Per-spacetime grid vectors for lasers in Fig. 5.1.1(a) and for the atom in Fig. 5.1.1(b) are shown along with invariant hyperbolic curves.

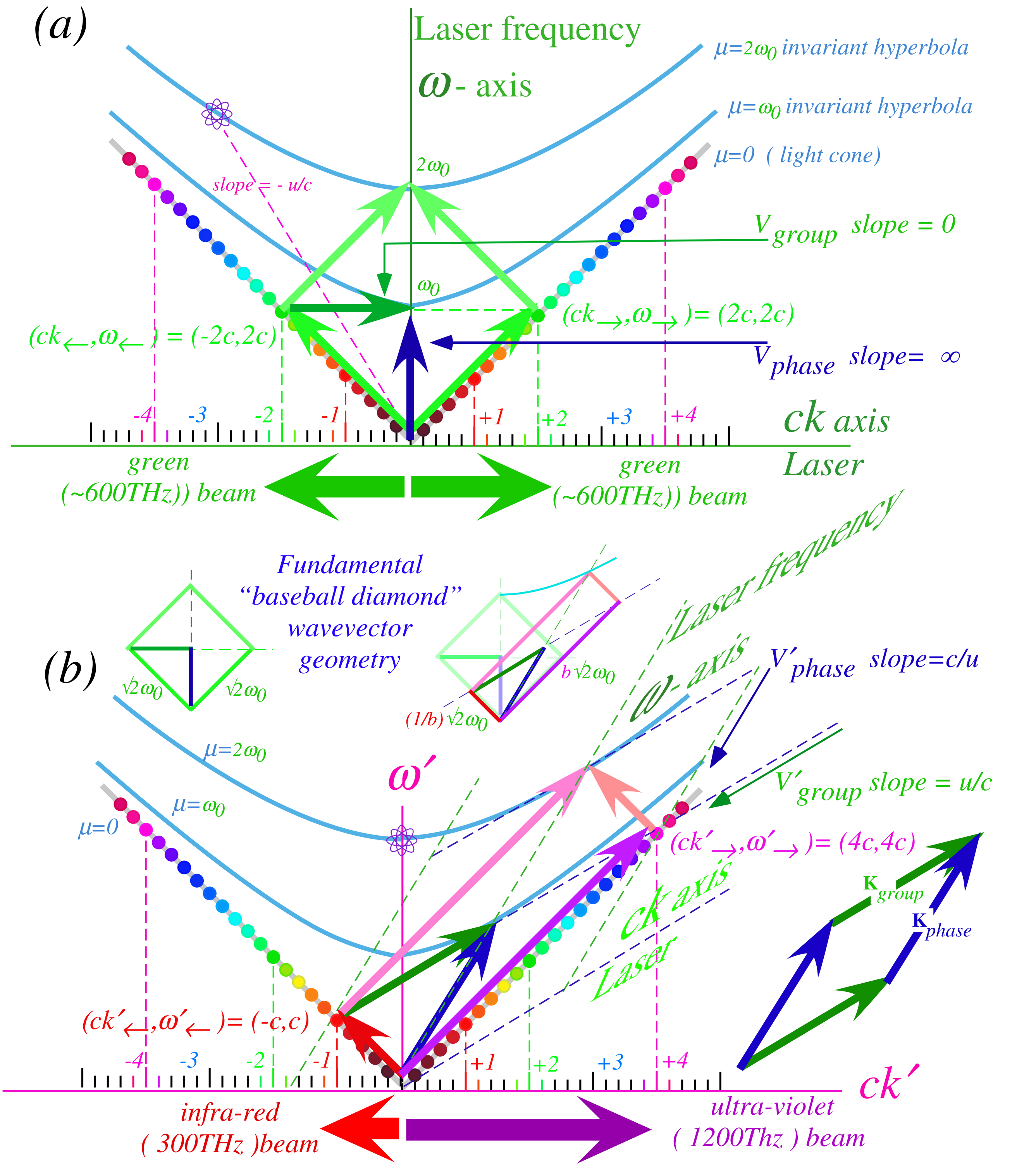

Fig. 5.1.1 Baseball wavevector geometry. (a) Laser view with atom at velocity u=-3c/5. (b) Atom view.

The hyperbolas, derived in (4.3.11), look the same in either atom *(ck′,ω′)* or laser *(ck,ω)* coordinates.

$$\omega^2{}_{12} - \left(ck_{12}\right)^2 = \omega'^2{}_{12} - \left(ck'_{12}\right)^2 = \mu^2 = 0, \pm\omega_0^2, \pm 2\omega_0^2, \ldots \tag{5.1.2}$$

Each hyperbolic radius $\mu=0,\ \omega_0,\ 2\omega_0,\ \ldots$ is the *invariant* or *proper frequency* of that hyperbola.

Proper or invariant quantities are key descriptors of physical objects or waves that do not depend upon the reference frame or coordinates used to define the object. Below is a discussion of a spacetime invariant called *proper time* τ. Later it is compared with proper frequency μ defined above.

Any quantity, invariant or otherwise, defined in spacetime, has a similar quantity defined in per-spacetime with an inverse physical interpretation. Particle velocity has units of x/t (*meters*)-per-(*second*), while wave velocity has the units ω/k (*per-second*)-per-(*per-meter*). A time t *vs.* space x plot in Fig. 4.2.11(a) keeps the same slope-velocity correspondence as a per-space k *vs.* per-time ω plot of Fig. 4.2.11(b) by switching ck and ω axes. Note also that phase velocity and group velocity (4.3.5a) are inverses of each other so our ω *vs.* ck per-spacetime plots have $\mathbf{K}_{phase}$ and $\mathbf{K}_{group}$ define ω and ck axes, respectively, but they switch roles in spacetime plots where $\mathbf{K}_{group}$ and $\mathbf{K}_{phase}$ define the t and x-axis.

(b) Spacetime invariants: Proper time

The area of a unit rectangular *(b)-by-(1/b)* cell in Fig. 5.1.2(a) is *1* for any speed u of the atom. The Lorentz rhombic graph in Fig. 5.1.2(a) is just a square graph stretched by a Doppler factor of b along the x-ct or $+45°$ diagonal and compressed by the inverse factor $1/b$ along the other diagonal so its area stays the same. As speed u varies, all grid points trace hyperbolas with UV=constant where $U=x+ct$ and $V=x-ct$ are $\pm 45°$ diagonal coordinates that might be used in Fig. 5.1.2(a) in place of x and ct.

It is easy to check that the product UV is unchanged by Lorentz transformation (4.3.5e).

$$-UV = -(x+ct)(x-ct) = (ct)^2 - (x)^2 = (ct')^2 - (x')^2 \qquad (5.1.3)$$

For an atom who carries its origin $x=0$ this quantity is called its *proper time* τ or *own-time* or *age*.

$$c^2\tau^2 = (ct)^2 - (x)^2 = (ct')^2 - (x')^2 \qquad (5.1.4)$$

Except for light, these are equations of hyperbolas in spacetime. Light has $\tau=0$ on straight $\pm 45°$ lines called the *light cone* where age τ is forever zero. *Light never ages.* It just can't grow up! If you could accompany light along the $45°$ path in Fig. 4.2.10(c) then you, too, would see all phasors frozen at one time.

Grids and invariants are plotted in Fig. 5.1.2. Notice how the hyperbolas serve as grid markers for both the square unsqueezed diamond as well as any squeezed or Lorentz-transformed rhombus.

(c) Per-spacetime invariants: Proper frequency

The per-spacetime invariant (5.1.2) is called *proper frequency* μ or *own frequency*.

$$\mu^2 = (\omega)^2 - (ck)^2 = (\omega')^2 - (ck')^2 \qquad (5.1.5a)$$

Proper frequency is the flip side of proper time (5.1.4), that is, if τ is an *age*, then μ is the *rate* of aging. Light never ages, so its proper frequency μ is identically zero. Having $\mu=0$ implies a constant-c speed.

$$(\omega)^2-(kc)^2 = (\omega')^2-(k'c)^2 = 0 \text{ implies:} \qquad c=|\omega/k|=|\omega'/k'|. \qquad (5.1.5b)$$

The *null-invariant* $\mu=0$ or *light cone* in (kc,ω)-per-spacetime is the $\pm 45°$ "X" in Fig. 5.1.2 (b) as is $\tau=0$ for (x,ct)-spacetime in Fig. 5.1.2(a). Non-zero-μ-invariant hyperbolas in Fig. 5.1.2(b) serve as grid markers in per-spacetime just as do τ-invariant hyperbolas in spacetime of Fig. 5.1.2(a).

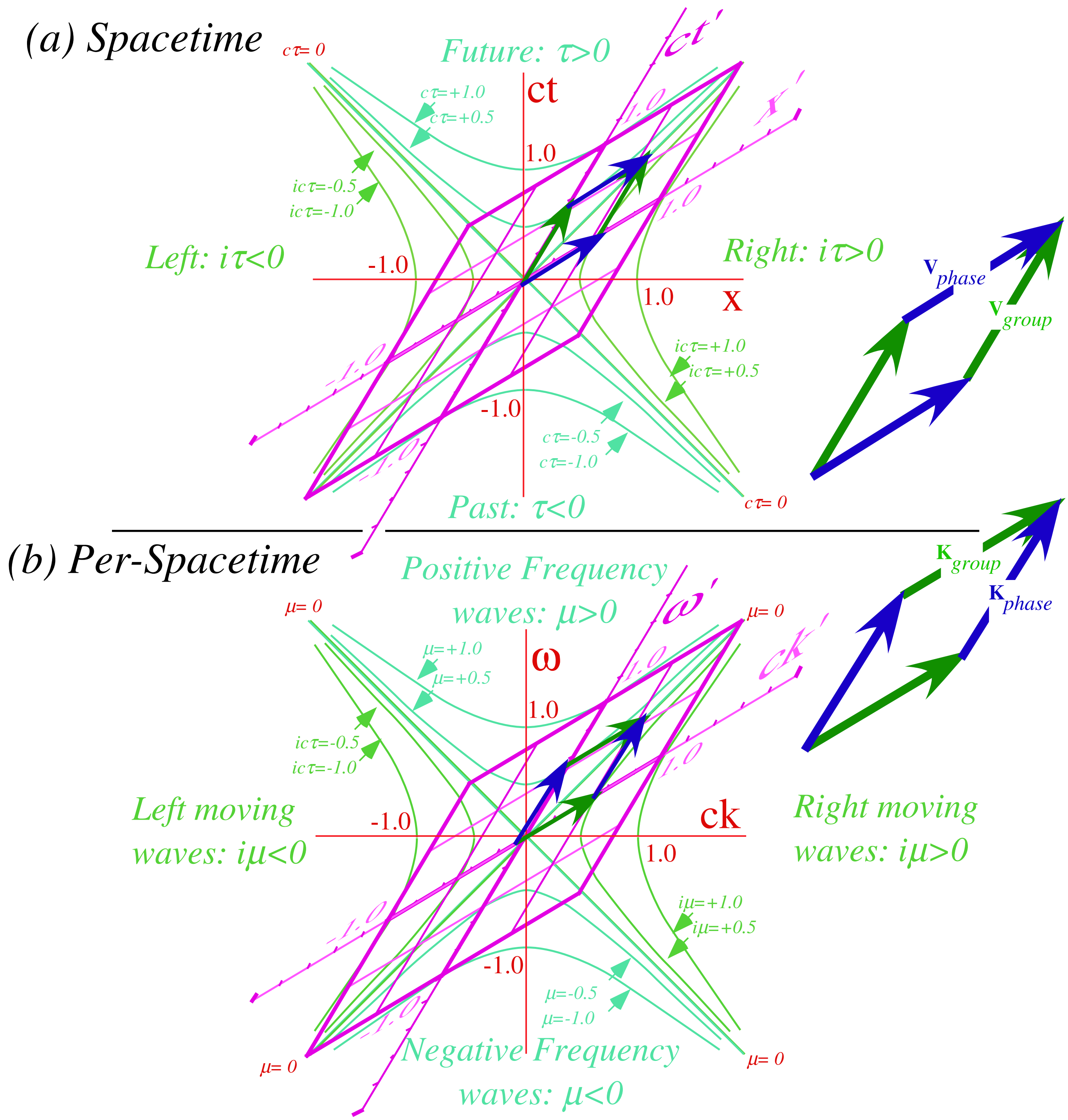

Fig. 5.1.2(a) Space-time grid plot with proper time invariant hyperbolas $c\tau^2 = ct^2 - x^2 = 0, \pm 0.5, \pm 1.0,..$
Fig. 5.1.2(b) Wavevector-frequency plot with proper frequency invariants $\mu^2 = \omega^2 - (ck)^2 = 0, \pm 0.5, \pm 1.0,..$

Proper time versus frequency: γ-waves never age!

Non-degenerate τ-hyperbolas with real τ such that $c^2\tau^2 = 1, 4, \ldots$ serve to mark temporal grid points $ct' = \pm 1, \pm 2, \ldots$ for any ct'-axis. Imaginary τ such as $c^2\tau^2 = -1, -4, \ldots$ serve to mark spatial axis grid points $x' = \pm 1, \pm 2, \ldots$ As shown in Fig. 5.1.2(a), real proper time τ values demark time in the past or future while imaginary $\tau=ix$ demark distance to the right or left. Proper time τ means "own" time or "eigen" time. τ is an "age" $\tau=t'$ or $\tau=t''$ of any object that is holding its "own" origin $x'=0$ or $x''=0$, respectively.

Light cone residents always have zero proper time in (5.1.3b). It is as though they never age. Free photons or γ-waves, from below radio frequency to ExaHertz and above, are all forever young!

But, μ-waves do age!

However, we seem to be made of other "stuff" than simple γ-waves. Unfortunately, for those of us who would like to live forever, our "stuff" ages. The μ-waves, which we call *matter*, have intrinsic τ-clocks running at a *non*-zero proper frequency μ. This allows μ-waves to have any speed *but* the speed c of light. In contrast, a light wave (γ-wave) travels at only its speed c but with internal clocks frozen like an $x=ct$ line of phasors in Fig. 4.2.10(c). Having zero proper frequency $\mu=0$, means you just don't tick!

The μ-hyperbolas with real μ such that $\mu^2=1, 4,\ldots$ serve to mark frequency grids at points $,\omega'=\pm 1, \pm 2,\ldots$ for an observant atom in a general $(k'c,\omega')$-frame of Fig. 5.1.2(b). The positive frequency side ages normally while those on the negative frequency side un-age, that is, appear to *go back in time*! (We will have more to say about such *anti-matter* behavior later.)

The μ-hyperbolas with imaginary μ with $\mu^2=-1, -4,\ldots$ mark points $,ck'=\pm 1, \pm 2,\ldots$ on the wavevector axis of the $(k'c,\omega')$-frame with $\pm k$ labeling right or left-moving waves. Imaginary-μ-waves correspond to faster-than-light or so-called *tachyonic* waves. For example, phase waves with $\mathbf{K}_{phase}$ in (5.1.1a) have to go faster-than-light in order to trace the x-coordinate grids or *NOW*-lines in Fig. 4.3.3(b).

γ-waves versus μ-waves

Since all colors go c, a rocket ship cannot ever catch-up to a light or γ-wave. As shown in Fig. 5.1.3 below, an ever-faster rocket may only Doppler shift the light more and more to the red, but it never can achieve exactly zero for either the frequency ω of a γ-wave or for a γ-wave's wavevector k.

However, a rocket ship may catch-up and even pass a matter or μ-wave as sketched in Fig. 5.1.4. A μ-wave has $\mathbf{K}_{phase}=(ck_p,\omega_p)$ on a hyperbola of radius $\omega_0=\mu=2c$ that tracks the center "pitcher's mound" of the "baseball diamond" in Fig. 5.1.1.

As the rocket speeds up, it sees k_p swing from $k_p=1.5$ (Fig. 5.1.4(a)) through zero (Fig. 5.1.4(b)) to a negative value $k_p=-1.5$ (Fig. 5.1.4(c)) while the frequency ω_p dips from $\omega_p=2.5c$ to a minimum $\omega_p=\mu=2$ (Fig. 5.1.4(b)) and then back to $\omega_p=2.5c$. This makes the phase velocity $V_{phase} = \omega_p/k_p$ go from $5c/3$ to infinity, then to minus infinity and finally to a fast negative value V_{phase} =-5c/3 in the final frame of Fig. 5.1.4(c).

Meanwhile, group velocity $V_{group} =\omega_g/k_g$ simply goes from $3c/5$ to zero in Fig. 5.1.4(b) to $-3c/5$ in Fig. 5.1.4(c). This group wave dynamics is more like what one sees when passing a classical object of matter. But, group *and* phase dynamics underlie all waves that make our world, light or matter.

Wave behavior is, perhaps, one of the deepest and most fundamentally unifying ideas in all of modern physics. Indeed, with 20-20 hindsight, we find beginnings of the idea of matter-as-waves going back centuries to works of Huygens, Hamilton, and Poincare′ as discussed later in Sec. 5.4. In order to understand and derive quantum theory, the concept of phase invariance and its related *Colorful Relativity* axiom (4.3.1) is essential and fundamental. Now, let us put these concepts to work!

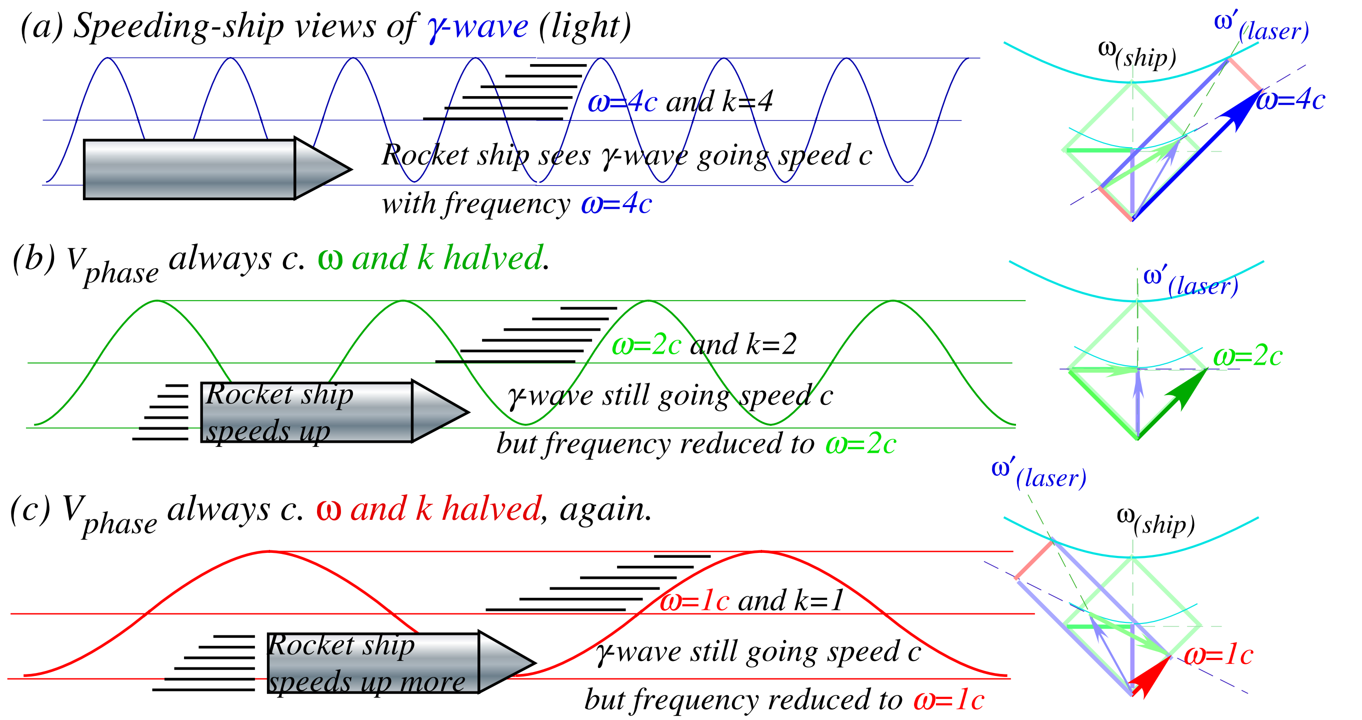

Fig. 5.1.3 Light γ-wave cannot be passed by rocket but ω may appear Doppler-shifted (almost) to zero.

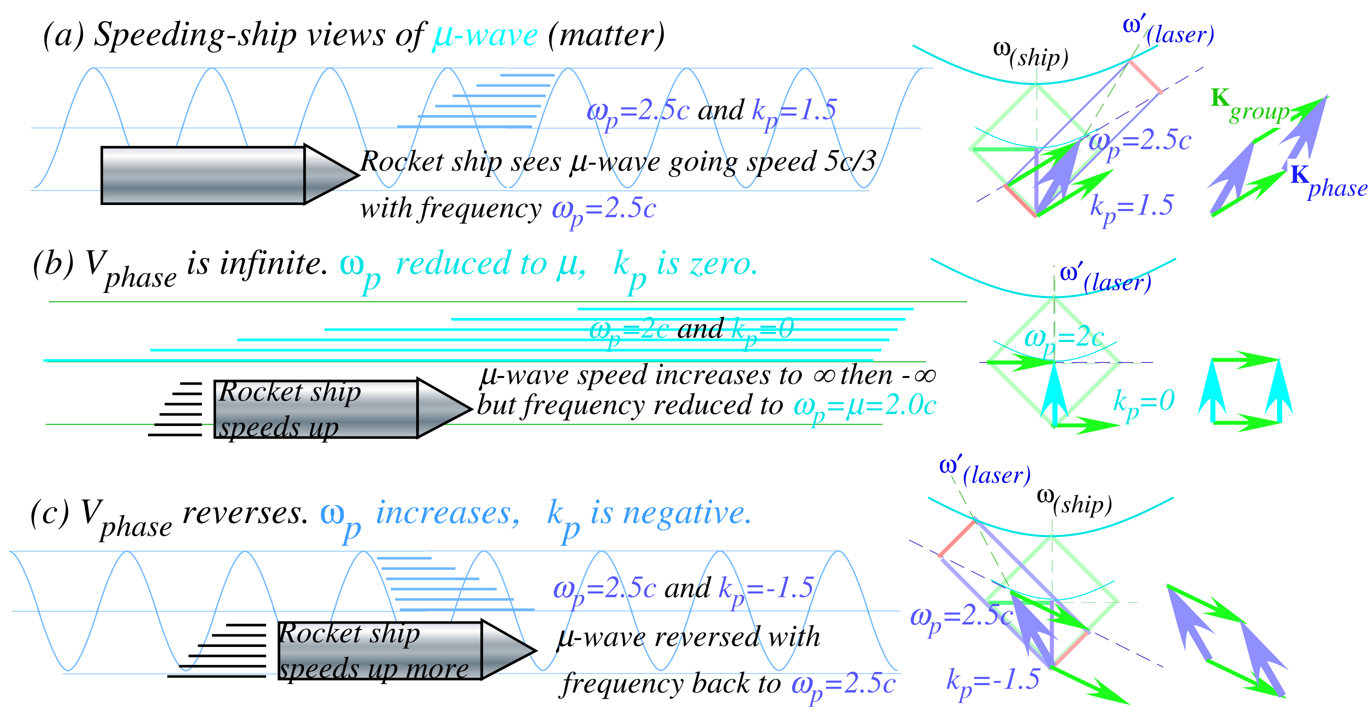

Fig. 5.1.4 Matter μ-wave is caught (b) and passed (c) by rocket but ω_p cannot be Doppler-shifted below μ.

5.2. CW relativistic energy-momentum: Quantum theory

This section is an important one. It derives fundamental quantum dynamics using the continuous wave (CW) theory of just two "colors" developed so far. As seen in the following Sec. 5.3, pulse wave (PW) or optical pulse train (OPT) dynamics require many frequencies. So, CW theory is simpler. Also, it is not predjudiciously encumbered by ideas of Newtonian "particles" of matter or "corpuscles" of light.

(a) To catch a μ-wave...(or "particle")

Relativistic symmetry of the continuous wave (CW) development is based on invariance of phase Φ (4.3.6) and proper frequency μ (5.1.5). This applies to *matter* or *μ-waves* as well as to light or γ-waves. Matter waves age at some invariant proper frequency μ that, unlike that of light, is *non*-zero. Lab frequency ω of a *μ-wave* lies on a non-degenerate hyperbola (5.1.5) in (ck,ω)-per-spacetime.

$$(\omega)^2-(kc)^2 =(\omega')^2-(k'c)^2 = \mu^2 >0 \qquad (5.2.1)$$

Consider a wave that has positive real proper frequency, say, the $(\mu=1)$-hyperbola in Fig. 5.1.2(b). Each point (ck,ω) on the $(\mu=1)$-hyperbola corresponds to one wave state of $(\mu=1)$-"stuff" with a wavevector k and a frequency ω. That point also defines another frame such as the tilted one labeled $(k'c,\omega')$ in Fig. 5.1.2(b). In the $(k'c,\omega')$-frame the wavevector k' is zero and frequency ω' is μ, that is, $(k'c,\omega')=(0,\mu)$ by (5.2.1). It looks like the rocket-view sketched in Fig. 5.1.4(b): a "kinkless" wave with infinite phase speed.

That wave point (kc,ω) also defines a space-time (x',ct')-frame of speed $u=\beta c$ such as the one in Fig. 5.1.2(a) that has exactly the same velocity tilt $\beta=u/c$ as the frame in Fig. 5.1.2(b). (They both have our familiar $\beta=3/5$.) It is a *rest-frame* of the matter wave or "particle" defined by having the wavevector k "Doppler-shifted" to zero as in Fig. 5.1.4(b) $(k'c,\omega')=(0,\mu)$.Any (kc,ω)-state is a "kinkless" $(k'=0)$-wave in the one frame that has "caught up" with it by going the velocity u that is a special velocity for the wave, namely its group velocity V_{group} (4.3.2). That u is the classical Newtonian "particle" or matter velocity.

Lab view of a μ-wave

The frequency ω' in atom frame where $k'=0$ is the *proper frequency* $\mu=\omega'$ by (5.2.1). Lorentz equations (4.3.10a) then give lab values (k,ω) of the $((k',\omega')=(0,\mu))$-wave that "has" velocity u in the lab.

$$ck = \frac{ck' + \beta\omega'}{\sqrt{1-\beta^2}} = \frac{0+\mu u/c}{\sqrt{1-(u/c)^2}} \cong \mu\frac{u}{c} - \frac{1}{2}\mu\left(\frac{u}{c}\right)^3 + \ldots \qquad (5.2.2)$$

$$\omega = \frac{\beta ck' + \omega'}{\sqrt{1-\beta^2}} = \frac{0+\mu}{\sqrt{1-(u/c)^2}} \cong \mu + \frac{1}{2}\mu\left(\frac{u}{c}\right)^2 + \ldots \qquad (5.2.3)$$

Binomial expansion $(1-x)^{-1/2}\sim 1+x/2+\ldots$ approximates waves of low group velocity ($u<<c$).

Our difficult work is now done and it is only necessary to apply *Planck's axiom* ($E=\hbar\omega$) of quantum theory. This, however, is a step far less trivial than it might seem. Indeed, Planck proposed $E=\hbar\omega$ or its Hertz equivalent, $E=h\nu$, as a "trick" to solve vexing cold-blackbody radiation problems. But, upon reconsideration, he actually sought to discard it. Taking Planck's axiom ($E=\hbar\omega$) seriously demands the *equivalence of energy and frequency*. Energy IS some ω wiggle rate! So, what's wiggling? That's the hard question. Is it space time itself? That $E=\hbar\omega$ seemed wacky to Planck. Energy of a classical oscillator goes as frequency *squared*. ($E_{HO}=k\omega^2$) We now use of his curious $E=\hbar\omega$, but we do not just take it lightly!

(b) Planck-DeBroglie-Einstein relations

Planck's axiom *($E=\hbar\omega$)* of energy-frequency equivalence is applied to (5.2.3).

$$E=\hbar\omega=\frac{\hbar\mu}{\sqrt{1-(u/c)^2}}\cong\hbar\mu+\frac{1}{2}\hbar\mu\left(\frac{u}{c}\right)^2+\ldots \tag{5.2.4}$$

Energy E rises quadratically in velocity u *($E\sim[\hbar\mu/c^2]u^2$)* as should kinetic energy $^1/_2Mu^2$ for a classical mass M. Setting M to the coefficient $\hbar\mu/c^2$ in (5.2.4) fixes the invariant proper frequency constant μ.

$$\hbar\mu=Mc^2 \tag{5.2.5a}$$

So, $\hbar\mu$ is *Einstein rest energy* Mc^2, the first term in an expansion of exact *total relativistic energy* E.

$$E=\hbar\omega=\frac{Mc^2}{\sqrt{1-(u/c)^2}}\cong Mc^2+\frac{1}{2}Mu^2+\ldots \tag{5.2.5b}$$

Classical kinetic energy $^1/_2Mu^2$ is the lowest order u-term in $\hbar\omega$. Now by (5.2.2) the lowest order u-term in $\hbar k$ is classical *momentum Mu* (using $\mu= Mc^2/\hbar$). So, $\hbar k=p$ is the exact *relativistic momentum*.

$$p=\hbar k=\frac{M\,u}{\sqrt{1-(u/c)^2}}\cong Mu+\frac{1}{2}Mc^2\left(\frac{u}{c}\right)^3+\ldots \tag{5.2.5c}$$

Momentum, or *impego* as Galileo called it, falls out as the *DeBroglie momentum-wavevector equivalence*: momentum *IS* so many kinks in space. It is analogous to the Planck energy-frequency equivalence: energy *IS* so many wiggles in time. Perhaps, Planck's axiom isn't so wacky, after all!

(c) Quantum dispersion relations

Einstein and DeBroglie energy and momentum relations (5.2.5) follow directly from the continuous wave (CW) phase invariance axiom (5.2.1) and Planck's frequency-energy equivalence axiom *($E=\hbar\omega$)*. Next we derive the quantum matter or μ-wave dispersion relation that governs the world's dynamics.

Energy and momentum equations (5.2.5b-c) each solve for wave group velocity u or slope $\beta=u/c$.

$$\frac{u}{c}=\frac{\sqrt{E^2-\left(Mc^2\right)^2}}{E}=\frac{cp}{E}=\frac{cp}{\sqrt{\left(Mc^2\right)^2+(cp)^2}} \tag{5.2.6}$$

The preceding uses an energy-momentum μ-invariant (5.2.1) or they come directly from (5.2.5b-c).

$$E^2-(cp)^2=(Mc^2)^2=\mu^2\hbar^2 \tag{5.2.7}$$

Solving for energy $E=\hbar\omega$ gives a *relativistic matter-energy dispersion function $\omega(k)$* plotted in Fig. 5.2.1a.

$$E=\hbar\omega=\sqrt{\left(Mc^2\right)^2+(cp)^2}=\sqrt{\left(Mc^2\right)^2+(c\hbar k)^2}\cong Mc^2+\frac{p^2}{2M}+\ldots \tag{5.2.8}$$

The dispersion function $\omega(k)$ gives wave velocities. Here V_{phase} formula (4.3.2c) is used with equal same sign wavevectors *($k_1=k=k_2$)* and equal frequency ($\omega_1=\omega=\omega_2$) to give the conventional *(ω/k)*-formula for phase velocity. It checks with the value derived before in (4.3.5a).

$$V_{phase} = \lim \frac{\omega_1 + \omega_2}{k_1 + k_2}\bigg|_{(k_1)=k=(k_2)} = \frac{\omega}{k} = \frac{E}{p} = \frac{c^2}{u} \tag{5.2.9a}$$

Using (4.2.12) with k_1 *approaching* k_2 gives the conventional group velocity or "particle" velocity u.

$$V_{group} = \lim \frac{\omega_1 - \omega_2}{k_1 - k_2}\bigg|_{(k_1)\to(k_2)} = \frac{d\omega}{dk} = \frac{dE}{dp} = \frac{c^2 p}{E} = u \tag{5.2.9b}$$

The conventional definition of group velocity is a slope of a tangent to a dispersion function. Fig. 5.2.1(a) shows an $E'=1$ line tangent to an $Mc^2=1$ dispersion. Its slope of $u/c=-3/5$ is that of the p'-axis for a frame moving from right to left at $u=-3c/5$. As in Fig. 5.1.2, a μ-hyperbola crosses the ω'-axis at $\omega'=\mu$.

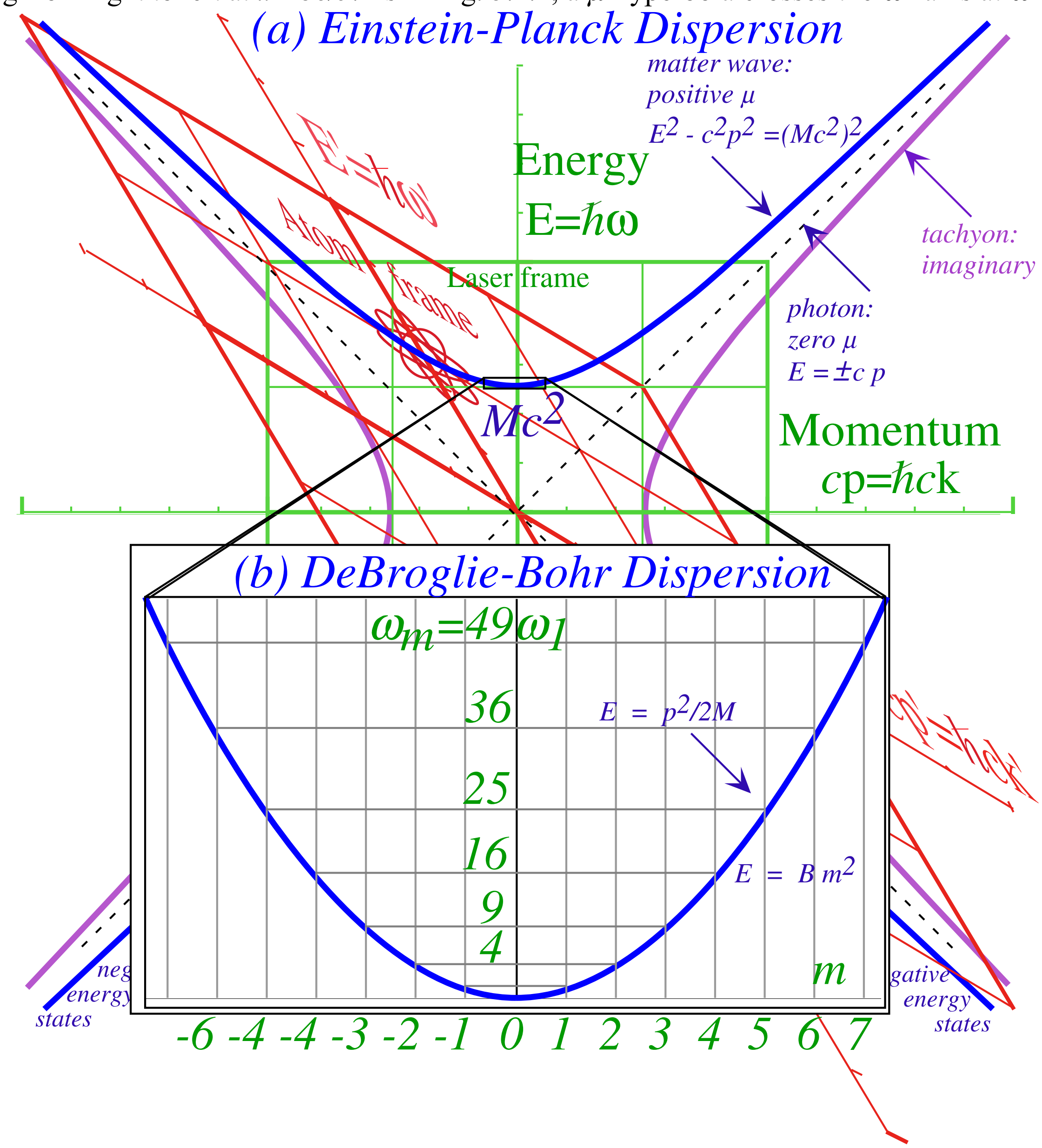

Fig. 5.2.1 Energy vs. momentum dispersion functions including mass M, photon, and tachyon.

(a) Relativistic (Einstein-Planck) case: $(Mc^2)^2=E^2-(cp)^2 = 1$ or $\mu^2=\omega^2-(ck)^2 = 1/\hbar^2$.

(b) Non-relativistic (Schrodinger-DeBroglie-Bohr) case: $E=-(1/2M)p^2$ or $\omega=\hbar k^2/2M$

Feynman showed energy and momentum arise from transformation of a *(k=0)* wave. That is, energy-momentum states are boosts of zero-momentum "particles" by *(cp,E)*-Lorentz relations.

$$cp = \frac{cp' + \beta E'}{\sqrt{1-\beta^2}} = cp' \cosh\theta + E' \sinh\theta \qquad (5.2.10a)$$

$$E = \frac{\beta cp' + E'}{\sqrt{1-\beta^2}} = cp' \sinh\theta + E' \cosh\theta \qquad (5.2.10b)$$

Energy-momentum relations are simply (ck,ω)-relations (4.3.10) or (5.2.2) multiplied by $\hbar$. It's an easy derivation of such important equations if based on CW states having well defined energy-momentum.

Non-relativistic (Schrodinger-Bohr) dispersion

In the non-relativistic limit $(u<<c)$, approximations of energy, such as (5.2.8) or Fig. 5.2.1b, usually drop the Mc^2 term since neither absolute energy nor absolute phase are physically observable. Only energy *difference* is physically important for classical mechanics, and only *relative* phase and phase velocity is observed in quantum mechanics. Neglecting a constant term like Mc^2 in energy expression (5.2.5b) does not change the group velocity $d\omega/dk = u$ or any wave behavior given by a probability envelope $\Psi^*\Psi$. The envelope $\Psi^*\Psi$ always has group velocity u according to equations (4.7.2).

On the other hand, phase velocity ω/k, is reduced by neglecting Mc^2 and changes from an enormous value c^2/u to a value near $u/2$ that is quite small in the non-relativistic limit $(u<<c)$, indeed, it is about half of the group velocity as in (4.7.8) and Fig. 4.7.3. This, however, is not inconsistent with classical physics or experiments based on observing $\Psi^*\Psi$ since the phase cancels out of $\Psi^*\Psi$. Phase velocity is more easily detectible for light, but then for $Mc^2=0$, all velocities are c, anyway.

(d) Quantum count rates suffer Doppler shifts, too

Doppler shifts, galloping waves, and electromagnetic wave coordinates made by CW lasers have been the basis of the development of relativity in Chapter 4 and of quantum theory in the present Chapter 5. A discussion of wave coordinates seen by arbitrarily moving sources and observers is given now. The discussion revolves around the question, *"Can a laser-pair in a frame-A produce the Minkowski coordinate grid of a frame B suitable for viewing by a third observer in a frame-C?"*

A simpler question is, "Can the laser-pair in frame *A* produce a grid for a moving observer's frame *B* so that it is seen by *B* as a Cartesian space-time grid?" This would seem easy. Simply tune up the laser shining along *B*'s velocity $u=\beta c$ by Doppler factor $b=\sqrt{(1+\beta)}/\sqrt{(1-\beta)}$ to frequency $\omega_{\rightarrow} = (b)\omega_0$ and de-tune the oppositely moving wave to $\omega_{\leftarrow} = (1/b)\omega_0$. However, we must also adjust laser wave *amplitudes* as well as frequencies in order that the intended observer *B* sees a standing wave like Fig. 4.3.3(a) and not a galloping one like Fig. 4.5.1 or Fig. 4.6.1. The same applies to the more complex *A*, *B*, and *C* question.

Relativistic Fourier amplitude shifts

Spacetime simulations in Fig. 4.3.3 and particularly those in Fig. 4.3.3(b) show that Lorentz-Minkowski wave coordinate lines are obtained from balanced Fourier combinations of plane waves. In Fig. 4.3.3, the amplitude $E_{\rightarrow}$ of the left-to-right wave must equal the amplitude $E_{\leftarrow}$ of the right-to-left wave. Otherwise, wave galloping arises as shown in Fig. 4.5.1 and Fig. 4.6.1.

However, balanced amplitudes in the laser lab frame do *not* translate into balanced amplitudes in a boosted atom frame or *vice-versa*. Both the frequencies *and the amplitudes* are affected by Lorentz transformation. Surprisingly, it turns out that amplitudes of light waves transform in the same way as their frequency, that is, by a Doppler blue-shift factor $b=e^{\rho}$ (or red-shift $1/b$) of (4.3.5b) repeated here.

$$\omega_{\leftarrow} = \sqrt{\frac{1-\beta}{1+\beta}}\omega_0 = e^{-\rho}\omega_0 , \qquad \omega_{\rightarrow} = \sqrt{\frac{1+\beta}{1-\beta}}\omega_0 = e^{+\rho}\omega_0 , \tag{5.2.11}$$

Relativistic tensor analysis [AJP **53** 671(1985)] of electromagnetic plane wave amplitudes gives the following.

$$E_{\leftarrow} = \sqrt{\frac{1-\beta}{1+\beta}}E_0 = e^{-\rho}E_0 , \qquad E_{\rightarrow} = \sqrt{\frac{1+\beta}{1-\beta}}E_0 = e^{+\rho}E_0 . \tag{5.2.12}$$

But, E-amplitude shifts (5.2.12) can be derived more easily by revisiting the Doppler shift while imagining light corpuscles or "photons." Pulse rates and photon count rates transform in the same way as any frequency. Doppler formulas (5.2.11) determine the atom's photon or pulse count rate $N_{\leftarrow}$ of right-to-left (red) photons and $N_{\rightarrow}$ of left-to-right (blue) photons, if N_0 (green) photons per second are emitted by each PW laser in Fig. 5.2.2(a) boosted to velocity $u=\beta c=3c/5$ in Fig. 5.2.2(b).

$$N_{\leftarrow} = \sqrt{\frac{1-\beta}{1+\beta}}N_0 = e^{-\rho}N_0 , \qquad N_{\rightarrow} = \sqrt{\frac{1+\beta}{1-\beta}}N_0 = e^{+\rho}N_0 , \tag{5.2.13}$$

Recall Fig. 4.2.5 where $N_0 =1.0Hz$ lasers hit the atom with "red" at $N_{\leftarrow}=0.5Hz$ and "blue" at $N_{\rightarrow}=2.0Hz$.

The quantum count rate N is related to Poynting flux S or electromagnetic field energy density U.

$$S = |\mathbf{E}\times\mathbf{B}| = cU \;\; [Joule/(m^2 s)]$$

The e.m. field energy $U[Jm^{-3}]$ is product of photon number $N\,[m^{-3}]$ and Planck's energy $\hbar\omega$ per photon

$$U = \varepsilon_0 |E|^2 = N\,\hbar\omega \;\; [Joule/(m^3)], \tag{5.2.14a}$$

where N is the expected photon number

$$N = |\Psi|^2 . \tag{5.2.14b}$$

This relates the classical electric field E to a quantum field or wave probability amplitude Ψ.

$$E = \sqrt{\frac{\hbar\omega}{\varepsilon_0}}\Psi \tag{5.2.14c}$$

Since the energy density $|E|^2$ is a product of N and ω which each shift factor by Doppler factor b, the E-field also shifts by b for a moving observer as in (5.2.12) while the energy density shifts by b^2.

$$U_{\leftarrow} = \frac{1-\beta}{1+\beta}U_0 , \qquad U_{\rightarrow} = \frac{1+\beta}{1-\beta}U_0 \tag{5.2.15}$$

Broadcasting optical coordinates: SWR transforms like velocity

It is interesting to derive the amplitude settings that are needed to broadcast a 50-50 Minkowski wave (4.6.3) to a moving atom so it sees a laser space-time coordinate system as a Minkowski grid like Fig. 4.3.3(b). A 50-50 wave in one frame has unit ratio of left and right moving amplitudes. The amplitude ratio in a β-moving frame is the square of a Doppler shift factor given by (5.2.12).

$$\frac{E_{\leftarrow}}{E_{\rightarrow}} = \frac{1-\beta}{1+\beta}. \tag{5.2.16}$$

Solving for $\beta=u/c$ shows that the relativity parameter β is just the *SWR* (4.5.1b) in the broadcasting frame.

$$\beta = \frac{E_{\leftarrow} - E_{\rightarrow}}{E_{\leftarrow} + E_{\rightarrow}} = SWR_{broadcast} . \tag{5.2.17}$$

This shows that the broadcaster must match the minimum galloping wave speed (4.5.1c), that is, its *SWR*, to the speed of the frame containing the intended recipient.

The optical *SWR* has a transformation relation based on (5.2.12).

$$E'_{\leftarrow} = \sqrt{\frac{1-\beta}{1+\beta}}E_{\leftarrow}\,, \qquad E'_{\rightarrow} = \sqrt{\frac{1+\beta}{1-\beta}}E_{\rightarrow}\,. \tag{5.2.18a}$$

$$SWR' = \frac{E'_{\rightarrow} - E'_{\leftarrow}}{E'_{\rightarrow} - E'_{\leftarrow}} = \frac{SWR+\beta}{1+SWR\cdot\beta}\,. \tag{5.2.18b}$$

So *SWR* transforms like velocity $\beta_0 = u_0/c$ in (4.4.3b) as it must since velocity is determined by *SWR*.

$$\beta_0{}' = \frac{\beta_0+\beta}{1+\beta_0\cdot\beta} \tag{5.2.19}$$

All this shows that perfect standing waves *(SWR=0)* and linear wave coordinates are possible in only one Lorentz frame at a time. For the atom's waves to look like Fig. 4.3.3(b), lasers must tune the *SWR* to the atom's β-value of *–3/5*. Then the lasers have galloping waves like Fig. 4.5.1(e) and not Fig. 4.3.3(a) where *SWR=0*. If the lasers leave their *SWR* at zero, then the atom sees *SWR′=3/5* with galloping waves like Fig. 4.6.1(b) and not a perfect Minkowski grid. (But, the atom could recover a perfect grid by simply attenuating the blue-shifted UV beam by *b=2*.)

By detuning frequencies as well as *SWR*, the lasers can present the speeding atom with its own Cartesian coordinate frame. An ultraviolet laser on the right with twice the argon frequency and twice the amplitude meeting an infrared beam with half the frequency and half the amplitude would make a square green grid like Fig. 4.3.3(a) *for the atom*. The result is the same as the atom would see if it had its own pair of argon lasers. In the original laser frame the atom's lasers would yield an intense UV beam counter-propagating right-to-left with a weak IR beam going left-to-right, just the reverse of Fig. 4.3.3(b). That results in a coordinate grid like the one labeled "*Atom Frame*" in Fig. 5.2.2(a).

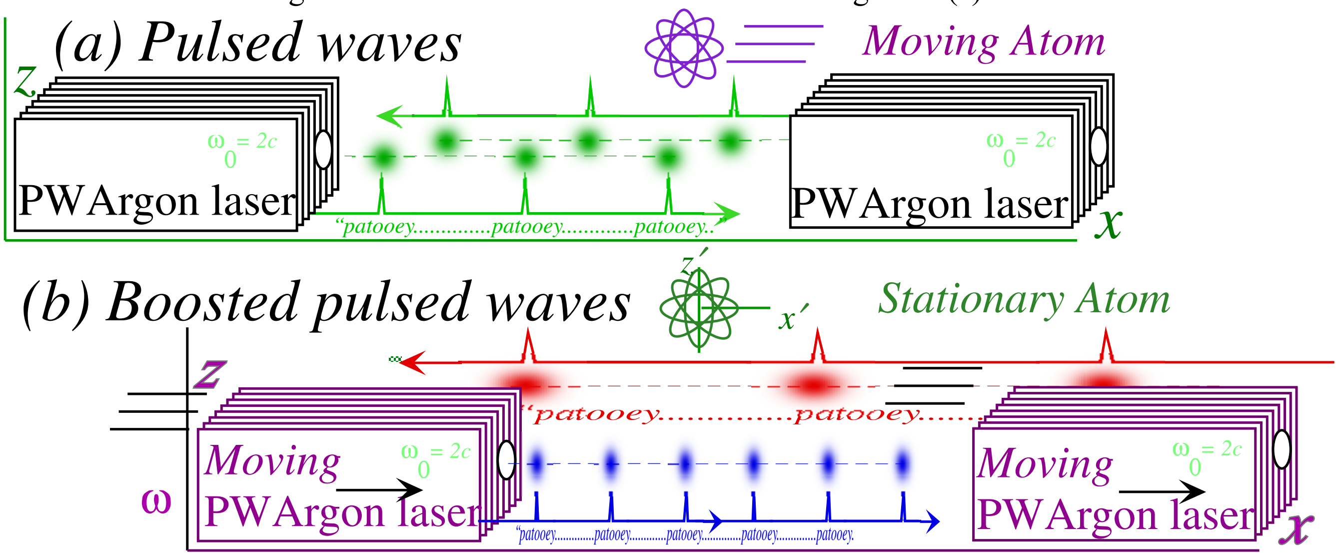

Fig. 5.2.2 Doppler shifting pulsed wave (PW) output. (a) Laser view. (b) Atom view.

(e) Imprisoned light ages (And gets heavier)

Each two-laser field depicted so far may be replaced by single inter-cavity laser field or, in principle, by a field between a pair of perfect mirrors. When a pair of counter-propagating waves add together as they do inside a cavity the resultant (ck,ω)-vector $\mathbf{K}_+ = \mathbf{K}_\rightarrow + \mathbf{K}_\leftarrow$ points to a positive frequency hyperbola as in Fig. 5.2.3, which is a copy of Fig. 5.2.1 with cavity mirrors added.

Shown also are the hyperbolas associated with the difference vector $\mathbf{K}_- = \mathbf{K}_\rightarrow - \mathbf{K}_\leftarrow$ and the group and phase vectors $\mathbf{K}_{group} = (\mathbf{K}_\rightarrow - \mathbf{K}_\leftarrow)/2$ and $\mathbf{K}_{phase} = (\mathbf{K}_\rightarrow + \mathbf{K}_\leftarrow)/2$ whose sum and difference are the original primitive $\mathbf{K}_\rightarrow$ and $\mathbf{K}_\leftarrow$ laser source vectors.

Other observers such as the atom see the vectors $\mathbf{K}_{group}$, $\mathbf{K}_{phase}$, $\mathbf{K}_+$ and $\mathbf{K}_-$ differently, but always on their respective hyperbolas ($\mathbf{K}_\rightarrow$ and $\mathbf{K}_\leftarrow$ stick to $\pm 45°$ light cones) as shown in Fig. 5.2.1(b). The atom-viewed vectors $\mathbf{K}'_\rightarrow$ and $\mathbf{K}'_\leftarrow$ define particle paths as in Fig. 4.2.11(b) while $\mathbf{K}'_{group}$ and $\mathbf{K}'_{phase}$ span a wave coordinate lattice as in Fig. 4.2.11(a). Fig. 5.2.3(b) shows the Lorentz-Minkowski lattice of Fig. 4.3.3(b) or energy-momentum wave lattices of Fig. 5.2.1 or Fig. 5.1.1 in a cavity that is Lorentz-contracted and time skewed to fit the waves it contains (as well as the matter-waves that make its box).

This brings the (continuous wave) CW development of relativistic quantum theory full circle and shows that a combination of two γ-waves having **K**-vectors $\mathbf{K}_\rightarrow = (ck_0,\omega_0)$ and $\mathbf{K}_\leftarrow = (-ck_0,\omega_0)$ is like a μ-wave with proper frequency $\mu = 2\omega_0$. In fact, combinations in a box are μ-waves with many of the wave properties of a massive "particles." Trapped light acquires a non-zero proper frequency $\mu = 2\omega_0$ and that is the same as acquiring mass according to (5.2.5b). "Light-plus-Light" acts like "matter."

But, why twice as heavy?

To accelerate the box to a small velocity *u* requires momentum associated with twice the photon frequency ω_0 since it has to be turned around and bounced forward. So a proper frequency $\mu = 2\omega_0$ gives the correct rest mass $M_{rest} = \hbar\mu / c^2 = 2\hbar\omega_0 / c^2$ of this arrangement.

Still, it seems that a laser cavity operating at the frequency ω_0 should only have proper frequency ω_0 and not twice that. Adding up two waves of frequency ω_0 is still just frequency ω_0.

The trick is to note that this must be (at least) a *two*-photon state involving *products* of the two wave states in a correlated or "entangled" sum in order to make this heavier "light-particle" box which responds with increased inertia. A product $\psi_{K\rightarrow}\psi_{K\leftarrow}$ of the two plane wave states gives a state with the K-vector $\mathbf{K}_+ = \mathbf{K}_\rightarrow + \mathbf{K}_\leftarrow$ that has proper frequency $\mu = 2\omega_0$. Exciting more photons means more wave or state factors and a heavier box. Frequency is energy is mass is (for a moving observer) momentum.

Several things are missing that prevent us from giving a precise discussion of trapped photons. First, the one-dimensional cavity sketched in Fig. 5.2.3 lacks another pair of walls with floor and ceiling. It's not maximum-security incarceration! Two and 3-dimensional box modes will be discussed in Chapter 6. Second, we need the quantum mechanics of wave products or "multi-particle" states to be introduced in Chapter 21. Finally, theory of quantum states of radiation, that is, "multi-photon" states, will be taken up in Chapter 22. We've got a ways to go. Newton's corpuscles aren't entirely dead yet!

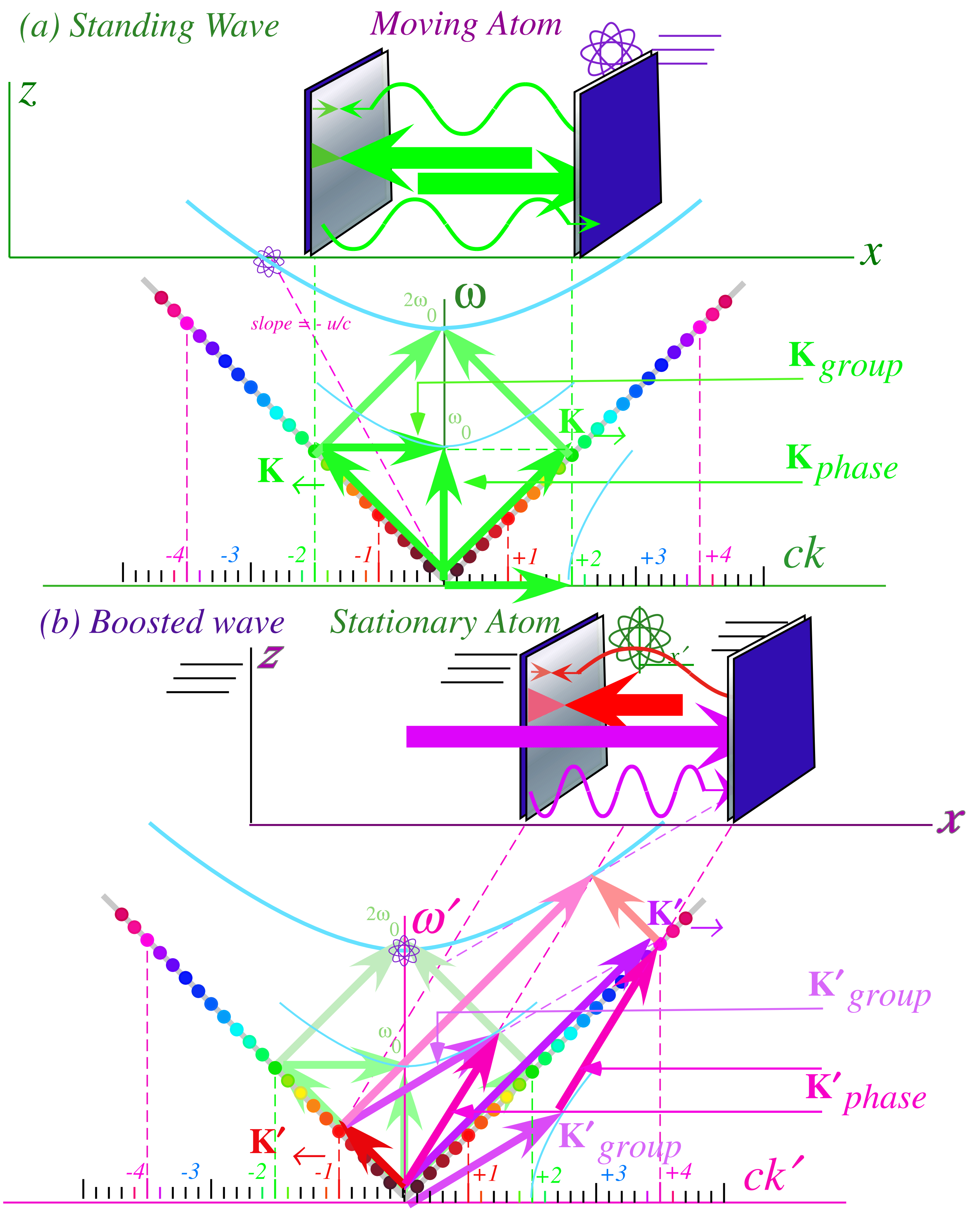

Fig. 5.2.3 Different views of a "photon(s)-in-a-box" and atom. (a) Box view. (b) Atom view.

(f) Effective mass

Classical mechanics is concerned with particle velocity u and momentum p that, in the non-relativistic limit $(u<<c)$, are directly proportional to the wave group velocity (5.2.9b). (Relativistic phase velocity c^2/u (5.2.9a) is *inversely* proportional to group velocity u.) Classical dynamics equates rate of change of momentum ($\dot{p} = \hbar\dot{k}$) to a force F introduced by Newton's Second Law $F=ma$. This "law" or axiom (It used to be taught in high school.) introduces inertial mass m as a ratio F/a of force to acceleration. How is this mass m related to wave proper-frequency μ or rest-mass $M=\hbar\mu/c^2$ in (5.2.5a)?

Effective mass M_{eff} is the ratio of wave force $F = \hbar\dot{k}$ (or $\dot{p}$) and wave group acceleration $a = \dot{V}_{group} = \dot{u}$. Then M_{eff} is inversely proportional to the curvature of the dispersion function (5.2.8).

$$M_{eff} = \frac{F}{a} = \frac{\hbar\dot{k}}{\left(\frac{dV_{group}}{dt}\right)} = \frac{\hbar\dot{k}}{\left(\frac{dV_{group}}{dk}\frac{dk}{dt}\right)} = \frac{\hbar}{\left(\frac{d^2\omega}{dk^2}\right)} \qquad (5.2.20a)$$

The relativistic quantum dispersion (5.2.8) gives M_{eff}, for low velocity, as approaching the rest mass M.

$$M_{eff} = \frac{F}{a} = \frac{1}{\left(\frac{d^2E}{dp^2}\right)} = \frac{M}{\left(1-\beta^2\right)^{3/2}} \xrightarrow[\beta\approx 0]{} M \qquad (5.2.20b)$$

These results may seem paradoxical in light of the observation that a photon dispersion function is a straight line ($\omega = c|k|$). So, is photon effective mass really infinite? Yes! Pure photon group and phase velocity never change no matter what "force" is encountered. ("Pure" means no μ-waves combining with γ-waves to change dispersion (5.2.8).) γ-wave effective mass is indeed infinite. Effective mass of a massive particle (μ-waves) also approaches infinity as it nears the speed of light $(\beta\to 1)$. Here mass means inertia.

The invariant mass M of a particle is its *rest mass*, that is, its effective mass at zero wavevector. This means inertial mass is due to a $(k=0)$ wave wiggle rate: the proper frequency $\mu = Mc^2/\hbar$ from (5.2.5a). Waves that wiggle faster are harder to accelerate, except for photons whose proper frequency is zero. The photon dispersion function ($\omega = c|k|$) in Fig. 5.2.1 has a $90°$ "corner" with infinite curvature at the origin. So its rest mass, according to the equation (5.2.20a), is indeed zero.

It may be difficult to tell the difference between a very "light" particle and light itself. The dispersion function of a low-μ matter wave differs from that of light only near the origin ($k=0$) as sketched in Fig. 5.2.4. Elsewhere, the dispersion function hugs the light cone so closely that a light particle might as well be light.

It may help to visualize a $(k=0)$-photon as a nearly uniform ("kinkless" like the wave in Fig. 5.1.4(b)) electric field oscillating at a very low frequency $\mu=\omega_0$. A boost of such a system (or of an observer viewing this system) results in a finite wavevector because of the asimultaneity effect. For small ω_0, a small change in k makes a wave with speed near c. It is as though a very tiny mass briefly underwent an enormous acceleration to near c. Then the electric rest-wave acquires near-light speed and "recovers" its near-infinite inertia so it can no longer accelerate. Further acceleration causes little further change in apparent wavespeed *c* since *(k'c,ω')* is so close to the light-cone-asymptote of the dispersion hyperbola.

However, no observer can get into a true photon's *(k=0)* frame without going at exactly the speed *c* of light, while, as shown in Fig. 5.1.4, one can catch up with a matter μ-wave. In fact, we do it every day whenever you pass somebody! As we have noted, the lightspeed "horizon" may be approached but never reached. In Sec. 5.6 we will see what happens if we to approach it with enormous acceleration.

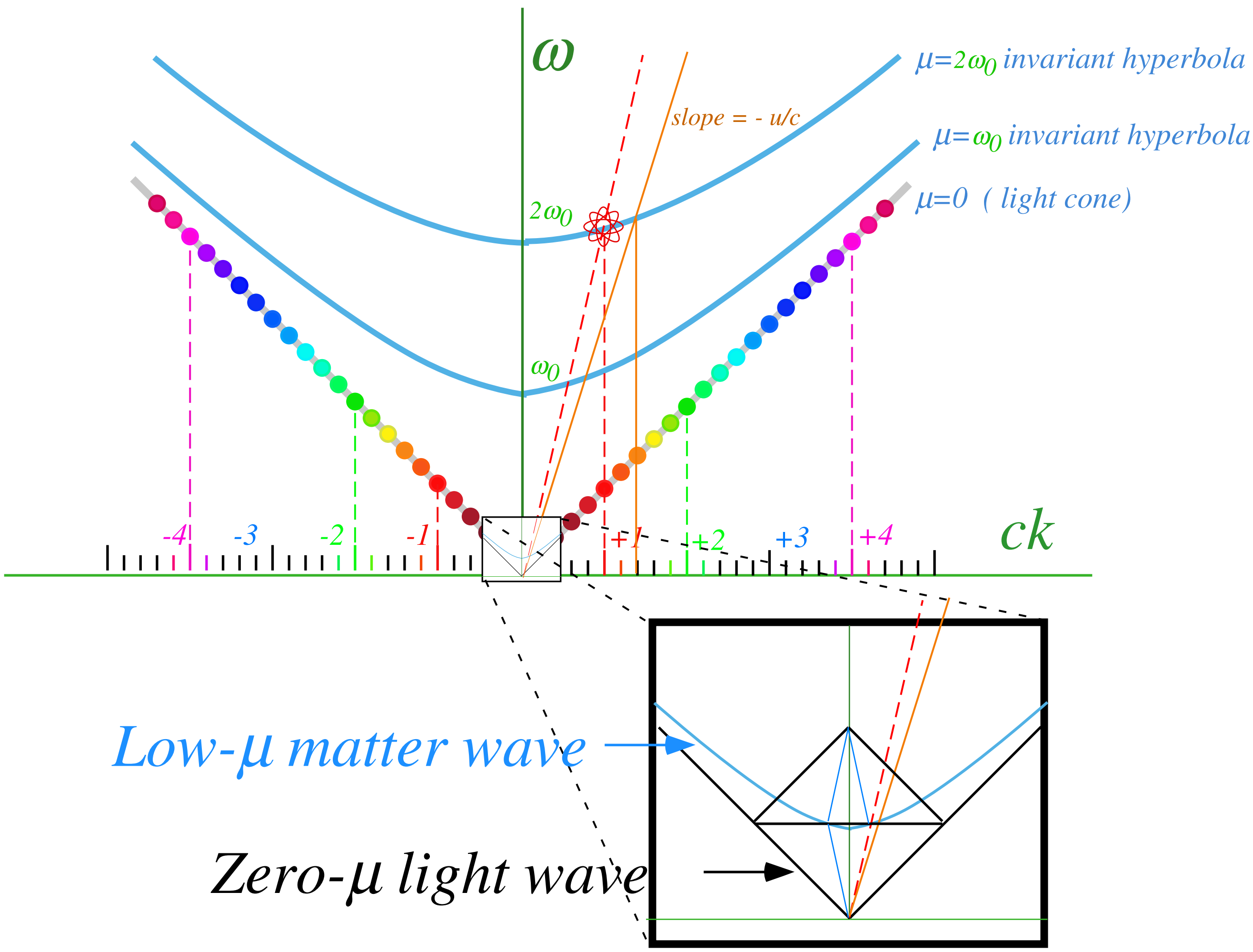

Fig. 5.2.4 Comparing light and very light matter.

(g) Two photons for every mass: Compton recoil

An optical cavity sketched in Fig. 5.2.3 decays to a lower energy (frequency) states by emitting light and is an analogy for a molecular, atomic, or nuclear *photoemission process* sketched in Fig. 5.2.5.

Feynman tells of a question his father asked him when he visited home after completing a (pricey) education at MIT. Feynman's father had heard that an atom can emit a photon and wanted to know where that photon was before it "came out." Feynman said he was sorry he didn't have a good answer for his father who had funded his MIT tuition for many years. Standard answers seemed unsatisfying. One such answer is that photons are "manufactured" by an atom occupying at once states $E_1=\hbar\mu_1$ and $E_0=\hbar\mu_0$ so its charge cloud "beats" at the difference frequency $\Delta= \mu_1 -\mu_0$ thus broadcasting light at this frequency.

Feynman's father's question has a Newtonian flavor, but it can be answered nicely by the wave "baseball diamond" geometry developed in this chapter. This also gives a more precise photoemission frequency $\omega_\gamma(final)$ that is shifted from Δ by a relativistic *Compton recoil shift* $\delta\omega$ that we derive now.

The trick is to imagine the excited μ_1 atom is "made" of two monstrous counter-propagating photon waves represented by big $\mathbf{K}_{\rightarrow}(\mu_1)$ and $\mathbf{K}_{\leftarrow}(\mu_1)$ vectors each taking up length $\mu_1/\sqrt{2}$ along the baselines of the diamond in Fig. 5.2.6(a). By "monstrous" we mean $E_1=\hbar\mu_1 =M_1c^2$ or trillions of *Volts (TeV)*.

Similarly, the de-excited μ_0 atom is "made" of two smaller (but still monstrous) photons having $\mathbf{K}_{\rightarrow}(\mu_0)$ and $\mathbf{K}_{\leftarrow}(\mu_0)$ vectors in Fig. 5.2.6(b-c). In contrast, typical atomic photoemission is tiny $\mathbf{K}(\omega_\gamma)$, a few *eV*, or so. That would be too small to draw in Fig. 5.2.6 so instead we imagine a nuclear or high-energy process with a big $\mathbf{K}(\omega_\gamma)$. Then, relativistic shifts are comparable to the energy values themselves.

The emission $\mathbf{K}(\omega_\gamma)$ is the difference between the sum of the excited and de-excited atom vectors according to a *phase conservation* rule requiring equality of **K**-vector sums before and after emission.

$$\mathbf{K}(\textit{initial total}) = \mathbf{K}_{\rightarrow}(\mu_1)+\mathbf{K}_{\leftarrow}(\mu_1) = \mathbf{K}_{\rightarrow}(\mu_0)+\mathbf{K}_{\leftarrow}(\mu_0)+\mathbf{K}\ (\omega_\gamma) = \mathbf{K}(\textit{final total}) \tag{5.2.21}$$

That is equivalent to conservation of *both* total energy (frequency) *and* momentum (wavevector) and so represents fundamental axioms of Newtonian mechanics. However, as will be shown later, (5.2.21) is an *approximate* consequence of wave interference. (Reducing **K**-vector uncertainty nearer to CW limit makes it a better approximation.) Quantum theory "proves" Newtonian axioms, but only *approximate*ly.

To make the final total-**K** match the initial one, we Doppler lengthen the 1st baseline $\mathbf{K}_{\rightarrow}(\mu_0)$ vector (length $\mu_0/\sqrt{2}$) by a factor $b=e^\rho$ so as to equal the length $\mu_1/\sqrt{2}$ of initial $\mathbf{K}_{\rightarrow}(\mu_1)$ vector of the atom. This in turn shortens the $\mathbf{K}_{\leftarrow}(\mu_0)$ vector to 3rd base by inverse factor $b^{-1}=e^{-\rho}$ leaving a larger deficit $\omega_\gamma\sqrt{2}$ between the length $\mu_1/\sqrt{2}$ of $\mathbf{K}_{\leftarrow}(\mu_1)$ and the new 3rd baseline $e^{-\rho}\mu_0/\sqrt{2}$. That ω_γ is the exact *photoemission frequency.*

$$\mu_1/\sqrt{2}=e^\rho\mu_0/\sqrt{2} \quad \text{or:}\quad \mu_1/\mu_0=e^\rho \quad (5.2.22a) \qquad\qquad \omega_\gamma=\frac{\mu_1-e^{-\rho}\mu_0}{2}=\mu_0\frac{e^\rho-e^{-\rho}}{2}=\mu_0\sinh\rho \quad (5.2.22b)$$

We relate ω_γ to the non-relativistic beat frequency $\Delta= \mu_1 -\mu_0$, and the recoil shift $\delta\omega$ in Fig. 5.2.6(c).

$$\omega_\gamma=\mu_0\frac{e^\rho-e^{-\rho}}{2}=\frac{\mu_0}{2}\left(\frac{\mu_1}{\mu_0}-\frac{\mu_0}{\mu_1}\right)=\frac{(\mu_1-\mu_0)(\mu_1+\mu_0)}{2\mu_1}=\frac{\Delta}{2}\left(1+\frac{\mu_0}{\mu_1}\right) \tag{5.2.23a}$$

$$\delta\omega=\Delta-\omega=\frac{\Delta}{2}\left(1-\frac{\mu_0}{\mu_1}\right)=\frac{\Delta^2}{2\mu_1} \tag{5.2.23b}$$

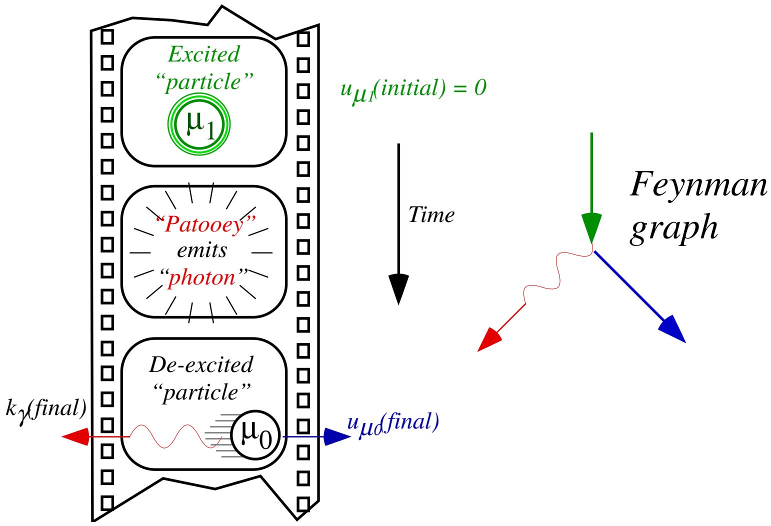

Fig. 5.2.5 Photoemission process

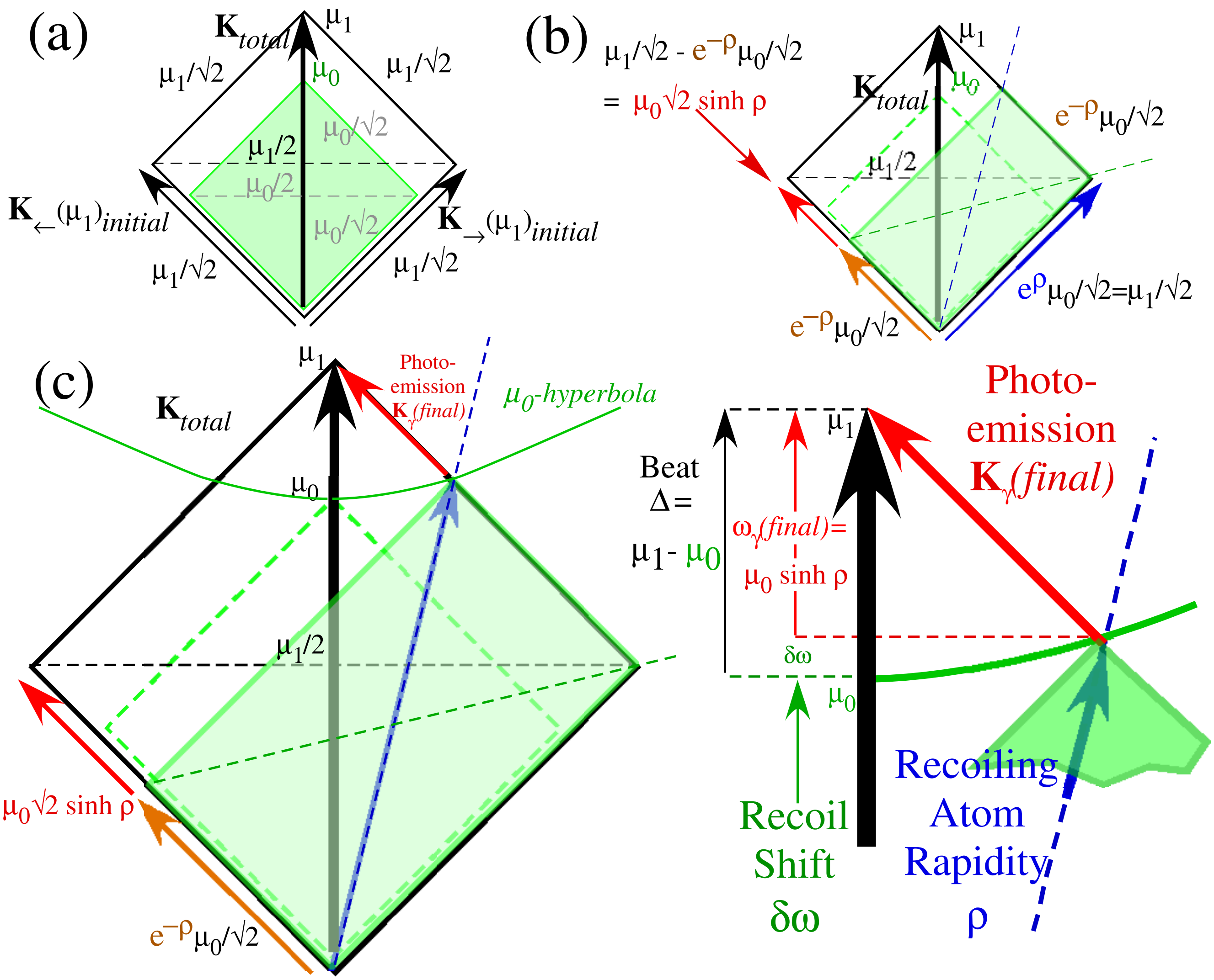

*Fig. 5.2.6 Diamond geometry of photoemission **K**-vectors derives recoil shift and atomic recoil velocity.*

5.3. Pulse Wave (PW) Dynamics :Wave-Particle Duality

The continuous wave (CW) approach to relativity and quantum theory used so far in this Chapter 5 and the preceding Chapter 4 takes full advantage of all parts including the "inside" and "outside" of a simple two-component wave interference first sketched in Fig. 4.2.4. Experimentalists rarely get such an ideal and coherent view. If they did, this CW theoretical approach would have been noticed long before.

Instead, we are usually restricted to an "outside only" view of waves made of many spectral components that are often incoherent. This is simply the usual classical world; a big incoherent mess! The book and pencil you may be holding now, and you, too, are combinations of unimaginably enormous numbers of so many insanely tiny waves that the wave nature of it all is about *last* thing you'd notice.

Now let us add up some number *2, 3, 4,…, N* waves to make pulse waves (PW) with "bumps" that resemble a classical "particles." We imagining a Newtonian "corpuscle spitter" in Fig. 5.2.2 and analyze pulses alluded to in discussing Fig. 4.2.11 and Fig. 4.3.5. (*"patooey..patooey..patooey…"*)

(a) Taming the phase: Wavepackets and pulse trains

In graphs like Fig. 4.6.1 a real wave $\mathrm{Re}\Psi(x,t)$ is plotted in spacetime. If the intensity $\Psi^*\Psi$ or envelope $|\Psi|$ is plotted, the part of the wave having the fast and wild phase velocity disappears leaving only its envelope moving constantly at the slower and more "tame" group velocity.

For example, the complicated dynamics of the (SWR=-1/8) switchback of Fig. 4.6.1(d) is reduced to parallel grooves by a $|\Psi|$-plot in Fig. 5.3.1(a). The grooves follow the group envelope motion that has only a steady group velocity . The lower part of Fig. 4.6.1 is thus tamed. Pure plane wave states Fig. 4.6.1 (a) and Fig. 4.6.1(f) are tamed even more in a $|\Psi|$-plot to become featureless and flat like their envelopes.

One gets a glimpse of phase behavior in an envelope or $\Phi^*\Phi$ plot by adding the lowest scalar DC fundamental *(m=0)*-wave $\Psi_0=1$ to a galloping combination wave such as $\Psi = a\,\Psi_{+4} + b\,\Psi_{-1}$. The result

$$\begin{aligned}\Phi^*\Phi &= \left(1 + a\Psi_{+4} + b\Psi_{-1}\right)^*\left(1 + a\Psi_{+4} + b\Psi_{-1}\right) = \left(1 + a\Psi_{+4} + b\Psi_{-1} + a^*\Psi^*_{+4} + b^*\Psi^*_{-1} + \Psi^*\Psi\right)\\ &= 1 + 2\,\mathrm{Re}\,\Psi + \Psi^*\Psi\end{aligned} \tag{5.3.1}$$

is plotted in the upper part of Fig. 5.3.1(b). The DC bias keeps the phase part from canceling itself, and the probability distribution shows signs of, at least half-heartedly, following the fast phase motion of the $\mathrm{Re}\Psi$ wave plotted underneath it. (Dashed lines showing phase and group paths are sketched onto $\Phi^*\Phi$.)

Indeed, (5.3.1) shows that if the $(1+\Psi^*\Psi)$ background could be subtracted, then the real wave $\mathrm{Re}\Psi$ plots of Fig. 4.4.4 would emerge double-strength! However, such a subtraction, while easy for the theorist, is more problematic for the experimentalist. Usually we must be content with results more like the upper than the lower portions of Fig. 5.3.1. It's a bit like watching an orgy ensuing beneath a thick rug.

However, such censorship can be a welcome feature. As more participating Fourier components enter the fray, a simpler view can help to sort out important classical effects that might otherwise be hidden in a cacophonous milieu. We next consider examples of this with regard to sharper wavepackets such as spikey pulse trains as well as the more graceful Gaussian wavepackets.

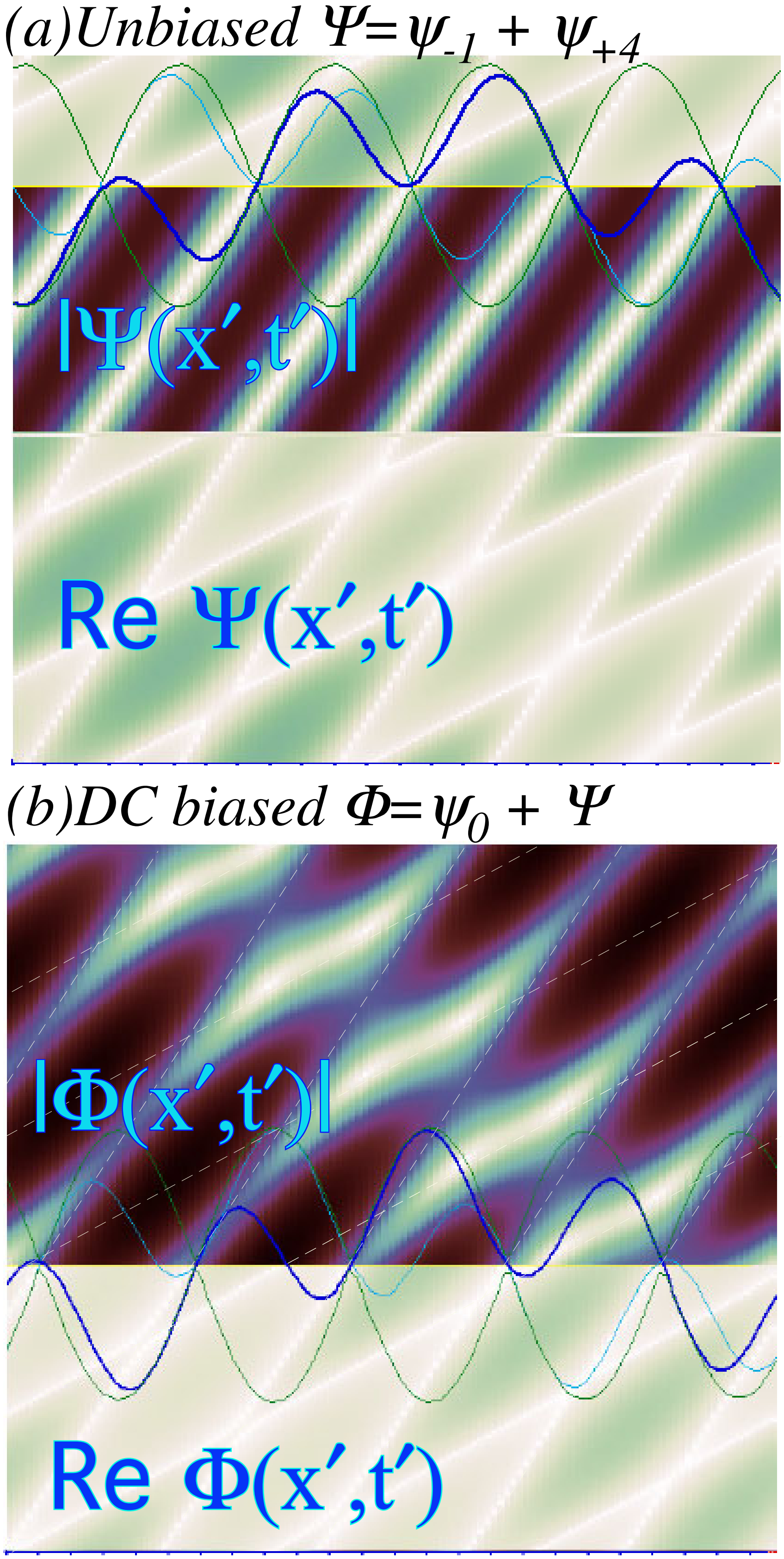

Fig. 5.3.1 Examples of group envelope plots of galloping waves (a) Unbiased. (b) DC biased.

(b) Continuous Wave (CW) vs. Pulsed Wave (PW): colorful versus colorless

Counter-propagating pulsed waves (PW) or Optical pulse trains (OPT), such as are imagined in Fig. 5.2.2, may be written as Fourier series of N continuous wave (CW) ω_1-harmonics.

$$\begin{aligned}\Phi_N(x,t) &= 1+e^{i(k_1x-\omega_1t)}+e^{i(-k_1x-\omega_1t)}+e^{i(k_2x-\omega_2t)}+e^{i(-k_2x-\omega_2t)}+\ldots+e^{i(k_Nx-\omega_Nt)}+e^{i(-k_Nx-\omega_Nt)}\\ &= 1+\quad 2e^{-i\omega_1t}\cos k_1x \quad+\quad 2e^{-i\omega_2t}\cos k_2x \quad+\ldots+\quad 2e^{-i\omega_Nt}\cos k_Nx\end{aligned} \tag{5.3.2}$$

The fundamental OPT or *(N=0-1)* beat wave in Fig. 5.3.2(b) is a rest-frame view of Fig. 5.3.1(b)

$$\Phi_1(x,t) = 1+\quad 2e^{-i\omega_1t}\cos k_1x \tag{5.3.3}$$

Φ_1 should be compared to the pure or unbiased fundamental *(m=±1)*-standing wave Ψ_1 in Fig. 5.3.2(a).

$$\Psi_1(x,t) = 2e^{-i\omega_1t}\cos k_1x \tag{5.3.4}$$

The real part $\mathrm{Re}\,\Psi_1$ is discussed in connection with the Cartesian spacetime wave grid in Fig. 4.3.3(a). The modulus $|\Psi_1|$, unlike $|\Phi_1|$, is constant in time as indicated by the vertical time-grooves at the extreme upper right of Fig. 5.3.2(a). In contrast, the magnitude $|\Phi_1|$ of the DC-biased beat wave makes an "H" or "X" in its spacetime plot of Fig. 5.3.2(b) thereby showing the beats. The width of the fundamental *(0-1)* beat is one fundamental wavelength $\Delta x=2\pi/k_0$ of space and one fundamental period $\Delta t=2\pi/\omega_0$ of time. Including $N=2,3,\ldots$ terms in (5.3.2) reduces the pulse width by a factor of $1/N$ as seen in Fig. 5.3.2 (c-e) below. The spatial ${}^{\sin Nx}/_{x}$ wave shape is the same as is had by adding $N=2,3,\ldots$ slits to an elementary optical diffraction experiment. Adding more frequency harmonics makes the pulse narrower in time, as well as space. Using *12* terms with *11* harmonics reduces the pulse width to *1/11* of a fundamental period. A pico-period pulse would be a sum of a trillion harmonics!

Reducing pulse width or spatial uncertainty Δx and temporal duration Δt of each pulse requires increased wavevector and frequency bandwidth Δk and $\Delta\omega$. The widths obey *Heisenberg relations* $\Delta x\Delta k\sim 2\pi$ or $\Delta t\Delta\omega\sim 2\pi$. The sharper the pulses the more white or colorless they become. Finally, the spacetime plots will simplify to simple equilateral diamonds or *45°*-tipped squares shown in the $N=11$ plots of Fig. 5.3.2(e). Each resembles the baseball diamond of Fig. 5.1.1 or PW paths of Fig. 4.3.5(b).

For $N=11$ there is less distinction between the $\mathrm{Re}\,\Phi$ and $|\Phi|$ plots than there is for the cases of $N=1,2$, or 3 shown in the preceding plots of Fig. 5.3.2(a-c). However, as in Fig. 5.3.1, there is a still a noticeable distinction between $\mathrm{Re}\,\Phi$ and $|\Phi|$ plots with all $\mathrm{Re}\,\Phi$ plots being sharper than $|\Phi|$ plots in all cases including the high-N cases. Having phase information increases precision particularly for low N. The sharpest set of zeros, somewhat paradoxically, are found in the $N=1$ case of Fig. 5.3.2(a) and for the unbiased $\mathrm{Re}\,\Psi$ plot of the Cartesian wave grid. However, plotting zeros by graphics shading is one thing. Finding experimental phase zeros using $\Psi^*\Psi$, that is, $|\Psi|$ *squared*, is quite another thing.

A close look at the center of the $\mathrm{Re}\,\Phi$ plot for $N=11$ in Fig. 5.3.2(e) reveals a tiny Cartesian spacetime grid. It is surrounded by "gallop-scallops" similar to the faster-and-slower-than-light paths shown in Fig. 4.5.1. It is due to the interference of counter-propagating ringing wavelets that surround each counter propagating ${}^{\sin Nx}/_{x}$ –pulse. In contrast note the $|\Phi|$ plots for which the ringing leaves only vertical grooves like those that occupy the entire $N=1$ plot of $|\Psi|$ in Fig. 5.3.2(a).

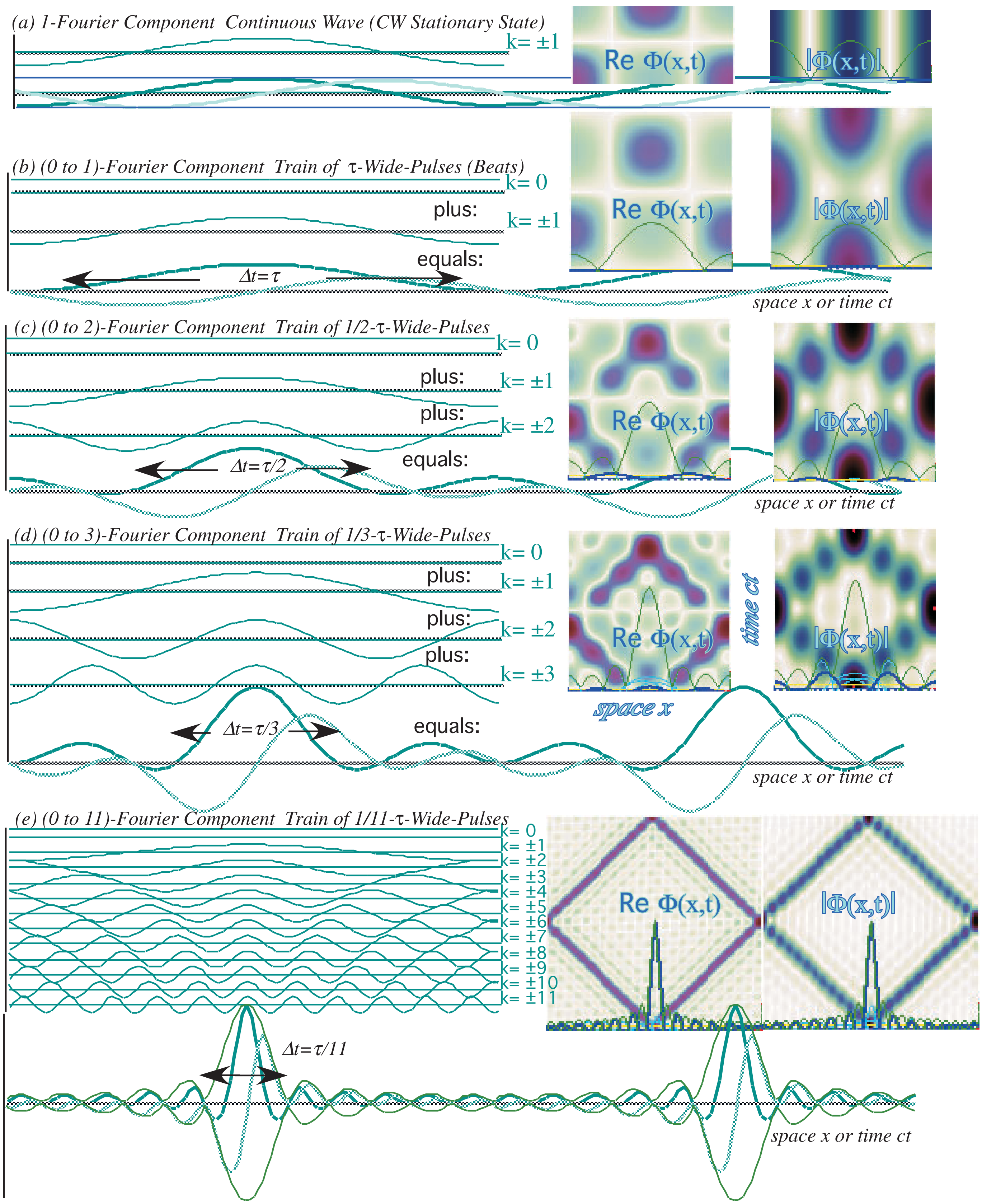

Fig. 5.3.2 Pulse Wave (PW) or Optical Pulse Trains (OPT) and Continuous Wave (CW) Fourier components

Wave ringing: m_{Max}-term cutoff effects

An analysis of wave pulse ringing reveals it may be blamed on the last Fourier component added. There are *11* zeros in the ringing wave envelope in Fig. 5.3.2(e), the same number as in the *11th* and last Fourier component. An integral over $k = m2\pi / N$ approximates a Fourier sum $S(m_{Max})$ up to a maximum $m_{Max}=11$. The unit sum interval $\Delta m=1$ is replaced by a smaller k-differential dk multiplied by $\frac{\Delta m}{dk} = \frac{N}{2\pi}$.

$$S(m_{Max}) = \sum_{m=-m_{Max}}^{m_{Max}} e^{im(\phi-\alpha)} = \sum_{m=-m_{Max}}^{m_{Max}} \Delta m\, e^{im(\phi-\alpha)} \cong \int_{-k_{Max}}^{k_{Max}} dk \frac{\Delta m}{dk} e^{ik\frac{N}{2\pi}(\phi-\alpha)}$$
$$\cong \frac{e^{i\frac{k_{Max}N}{2\pi}(\phi-\alpha)} - e^{-i\frac{k_{Max}N}{2\pi}(\phi-\alpha)}}{i(\phi-\alpha)} = 2\frac{\sin\frac{k_{Max}N(\phi-\alpha)}{2\pi}}{(\phi-\alpha)} = 2\frac{\sin m_{Max}(\phi-\alpha)}{\phi-\alpha} \tag{5.3.5}$$

This geometric sum verifies our suspect's culpability. The sum rings according to the highest m_{Max}-terms while lesser m-terms seem to experience an interference cancellation. The *last-one-in* is what shows!

Ringing suppressed: m_{Max}-term Gaussian packets

Ringing is reduced by *tapering* higher-m waves so they tend to cancel each other's ringing and no single wave dominates. A Gaussian $e^{-(m/\Delta m)^2}$ taper makes cleaner "particle-like" pulses in Fig. 5.3.3.

$$S_{Guass}(m_{Max}) = \frac{1}{2\pi}\sum_{m=-\infty}^{\infty} e^{-\frac{m^2}{\Delta m^2}} e^{im\phi} = \frac{1}{2\pi}\sum_{m=-\infty}^{\infty} e^{-\pi\left(\frac{m}{m_{Max}}\right)^2} e^{im\phi}, \text{ where: } \Delta m = \frac{m_{Max}}{\sqrt{\pi}} \tag{5.3.6a}$$

Completing the square of the exponents extracts a Gaussian ϕ-angle wavefunction $e^{-(\Delta m\phi/2)^2}$ with an angular uncertainty $\Delta\phi$ that is twice the inverse of the momentum quanta uncertainty Δm. $(\Delta\phi = 2/\Delta m)$.

$$S_{Guass}(m_{Max}) = \frac{1}{2\pi}\sum_{m=-\infty}^{\infty} e^{-\left(\frac{m}{\Delta m} - i\frac{\Delta m}{2}\phi\right)^2 - \left(\frac{\Delta m}{2}\phi\right)^2} = \frac{A(\Delta m,\phi)}{2\pi} e^{-\left(\frac{\Delta m}{2}\phi\right)^2} \tag{5.3.6b}$$

Definition $\Delta m = m_{Max}/\sqrt{\pi}$ of momentum uncertainty relates *half-width-($^1/_e$)th-maximum* Δm to the value $m=m_{Max}$ for which the taper $e^{-(m/\Delta m)^2}$ is $e^{-\pi}$. ($e^{-\pi} = 0.04321$ is an easy-to-recall number near *4%*. Waves $e^{im\phi}$ beyond $e^{im_{Max}\phi}$ have $e^{-(m/\Delta m)^2}$ amplitudes below $e^{-\pi}$.) Amplitude $A(\Delta m,\phi)$ becomes an integral for large m_{Max} as does (5.3.5). Then $A(\Delta m,\phi)$ approaches a Gaussian integral whose value itself is m_{Max}.

$$A(\Delta m,\phi) = \sum_{m=-\infty}^{\infty} e^{-\left(\frac{m}{\Delta m} - i\frac{\Delta m}{2}\phi\right)^2} \xrightarrow[\Delta m >> 1]{} \int_{-\infty}^{\infty} dk\, e^{-\left(\frac{k}{\Delta m}\right)^2} = \sqrt{\pi}\Delta m = m_{Max} \tag{5.3.6c}$$

The resulting Gaussian wave $e^{-(\phi/\Delta\phi)^2}$ has angular uncertainty $\Delta\phi = \phi_{Max}/\sqrt{\pi}$ defined analogously to Δm.

$$S_{Guass}(m_{Max}) \cong \frac{1}{2\pi}\sum_{m=-m_{Max}}^{m_{Max}} e^{-\left(\frac{m}{\Delta m}\right)^2} e^{im\phi} = \frac{m_{Max}}{2\pi} e^{-\left(\frac{\Delta m}{2}\phi\right)^2} = \frac{m_{Max}}{2\pi} e^{-\left(\frac{\phi}{\Delta\phi}\right)^2} \text{ where: } \Delta\phi = \frac{\phi_{Max}}{\sqrt{\pi}} \tag{5.3.6d}$$

Uncertainty relations in Fig. 5.3.3 are stated using Δm and $\Delta\phi$ or in terms of *4%* limits m_{Max} and ϕ_{Max}.

$$\Delta m \cdot \Delta\phi = 2 \quad (5.3.7a) \qquad\qquad m_{Max} \cdot \phi_{Max} = 2\pi \quad (5.3.7b)$$

In Fig. 5.3.2, the number of pulse widths in interval 2π is the number m_{Max} of *(>4%)*-Fourier terms.

Are these pulses photons?

No! But each pulse would appear to have photons in them if counters were put in the beams. However, it is *highly* unlikely that you would ever hear a counter tick *"click...click...click..."* with one count for each pulse! Newton's mythical *"patooey...patooey..."* becomes a random distribution of clicks *within* each pulse.

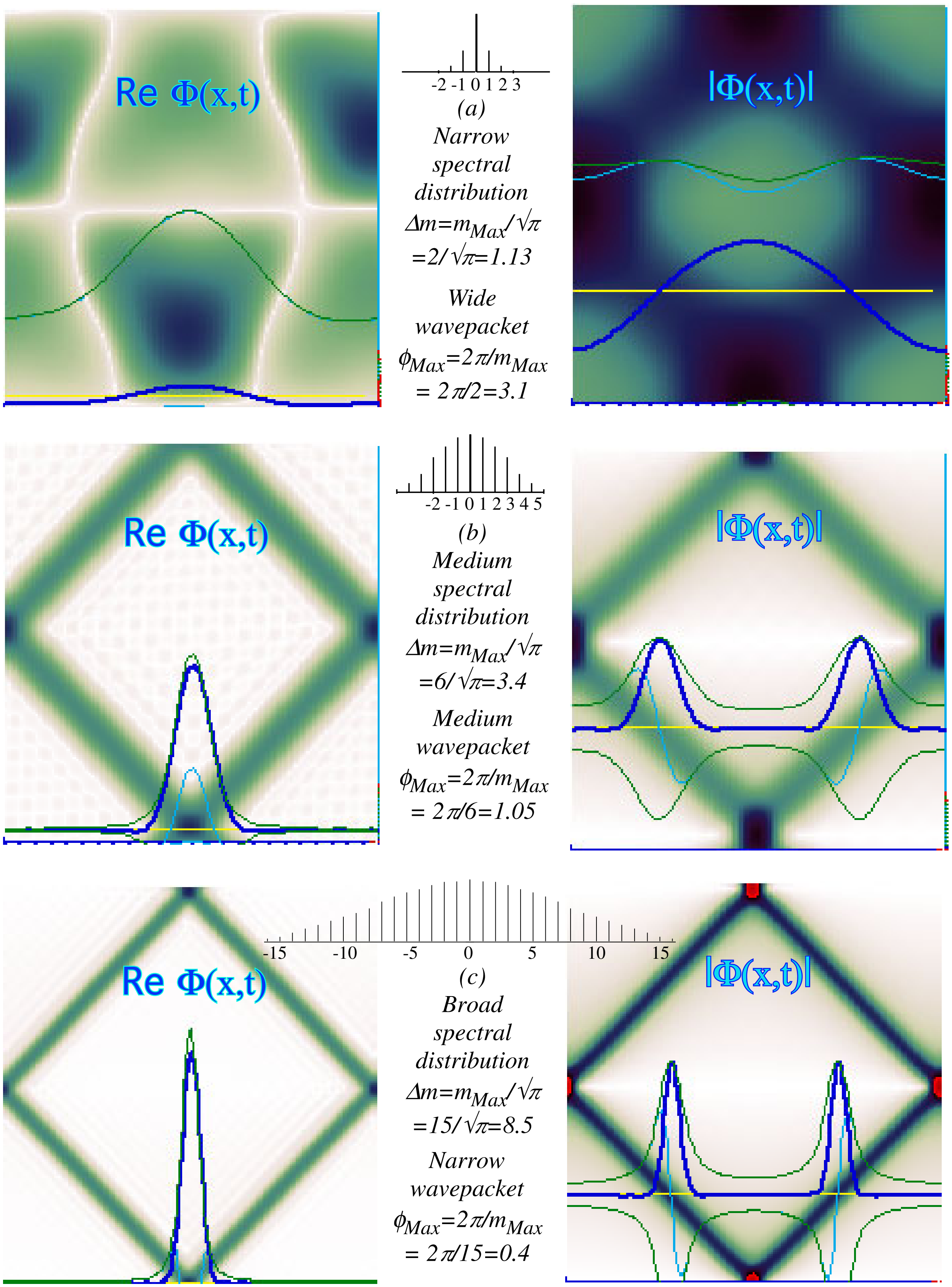

Fig. 5.3.3 Gaussian wavepackets. (Ringing is reduced compared to Fig. 5.3.2.)

(c) PW switchbacks and "anomalous" dispersion

An interesting exercise involves the dynamics associated with *anomalous* or "abnormal" dispersion functions. Often, the term anomalous applies to any dispersion function beyond the elementary optical linear dispersion $\omega=ck$ or quadratic Bohr-Schrodinger dispersion $\omega=Bk^2$. Here, we might so disparage any dispersion that does not fit the relativistic invariant form $\omega^2\text{-}(ck)^2 = \mu^2$ of (5.1.5) or (5.2.7).

What we are looking for here is abnormal wave behavior like that of the galloping and switchback waves displayed in Fig. 4.5.1 and Fig. 4.6.1, but with an important difference. The extraordinary dances in Fig. 4.5.1 and Fig. 4.6.1 involved phase velocity of *phase* waves Re Ψ or Im Ψ and here we ask if such super luminal behavior is possible for *group* velocity and group envelopes $|\Psi|$ or $\Psi^*\Psi$.

Abnormal relativistic dispersion

Faster-than-light group velocity is not possible on the normal positive branch ($\mu>0$) or positive light cone in Fig. 5.2.1 since no two points on the ($\mu>0$) hyperbola make a line of slope greater than one. Branches of imaginary-μ have the opposite problem; their group velocity is never *less* than c. This led Gerald Feinberg to suggest *tachyonic matter* in 1970. No evidence for it was found. Perhaps, it's not so surprising since a time factor $e^{-i\omega t}$ with imaginary frequency $\omega=i\mu$ is a decaying exponential $e^{-\mu t}$.

This leaves the negative frequency branches ($\mu<0$) or negative light cone branches that are hiding behind the inset Bohr dispersion graph in Fig. 5.2.1. For these branches group velocity $d\omega/dk$ is negative and so is the effective mass h/($d^2\omega/dk^2$). This is the domain of Dirac's *anti-matter* as discussed in Sec. 5.7.

Abnormal laboratory dispersion

As described in later chapters, there are no end of abnormal dispersion in waves that involve combination of light and matter. Gases and solids break the Lorentz symmetry of the vacuum by being their own "absolute" frame of reference, and so they are not restricted to the invariant form. The earliest examples of anomalous dispersion involve above-resonance polaron light whose index of refraction n is less than one. (Velocity is defined as c/n so $n<1$ is faster-than-light.)

Still it was not until recently that dispersion control in laser-pumped matter became so powerful that an index could be made zero or negative with phase or group velocities of virtually arbitrary sign and magnitude. This includes "backward waves" whose envelope travels oppositely to the wave phase.

Fig. 5.3.4 sketches dispersion cases of *normal* ($n>1$ and $V<c$), *vacuum* ($n=1$ and $V=c$), *anomalous* ($n<1$ and $V>c$), *evanescent* ($n=0$ and $V=\infty$), and *negative-backward* ($n<0$ and $V<0$). The latter has the peculiar property of emitting a pulse before it arrives! As shown in Fig. 5.3.5, this is an example of a spacetime switchback analogous to the phase switchbacks in Fig. 4.6.1. It plays out like the zeros in Fig. 4.6.1(d) only now it is a whole pulse and envelope instead of a zero that cruises toward its annihilation by its "anti-pulse" or "back-in-time-traveling" part that was produced in an earlier "pair-creation" event.

These hyper-anomalous pulses are set-up-jobs like any Fourier system. Pulses look like they go back in time but they don't "cause" anything before they're sent because they were never really "sent" at all! Wave interference dynamics makes the classical rules we are used to, and on the average, obeys them.

However, that which giveth also taketh away. For quantum waves, classical rules are made to be broken! When matter waves get left alone, as will be shown later in Sec. 5.6, they party like mad!

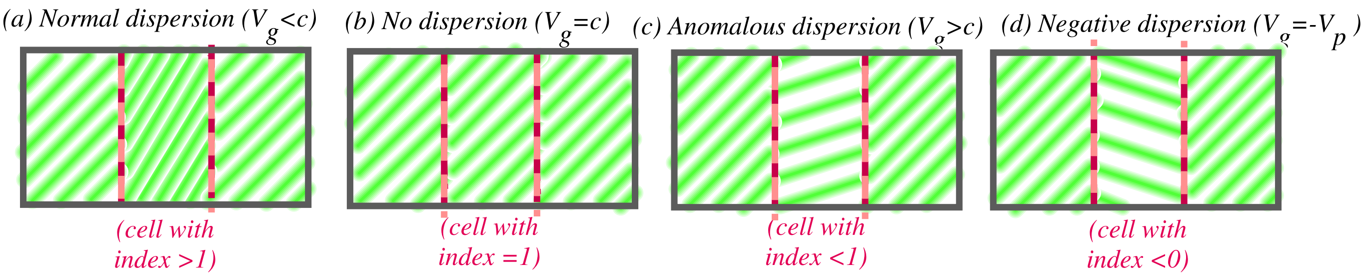

Fig. 5.3.4 Spacetime tracks of wave pulse group envelopes for various dispersion cases

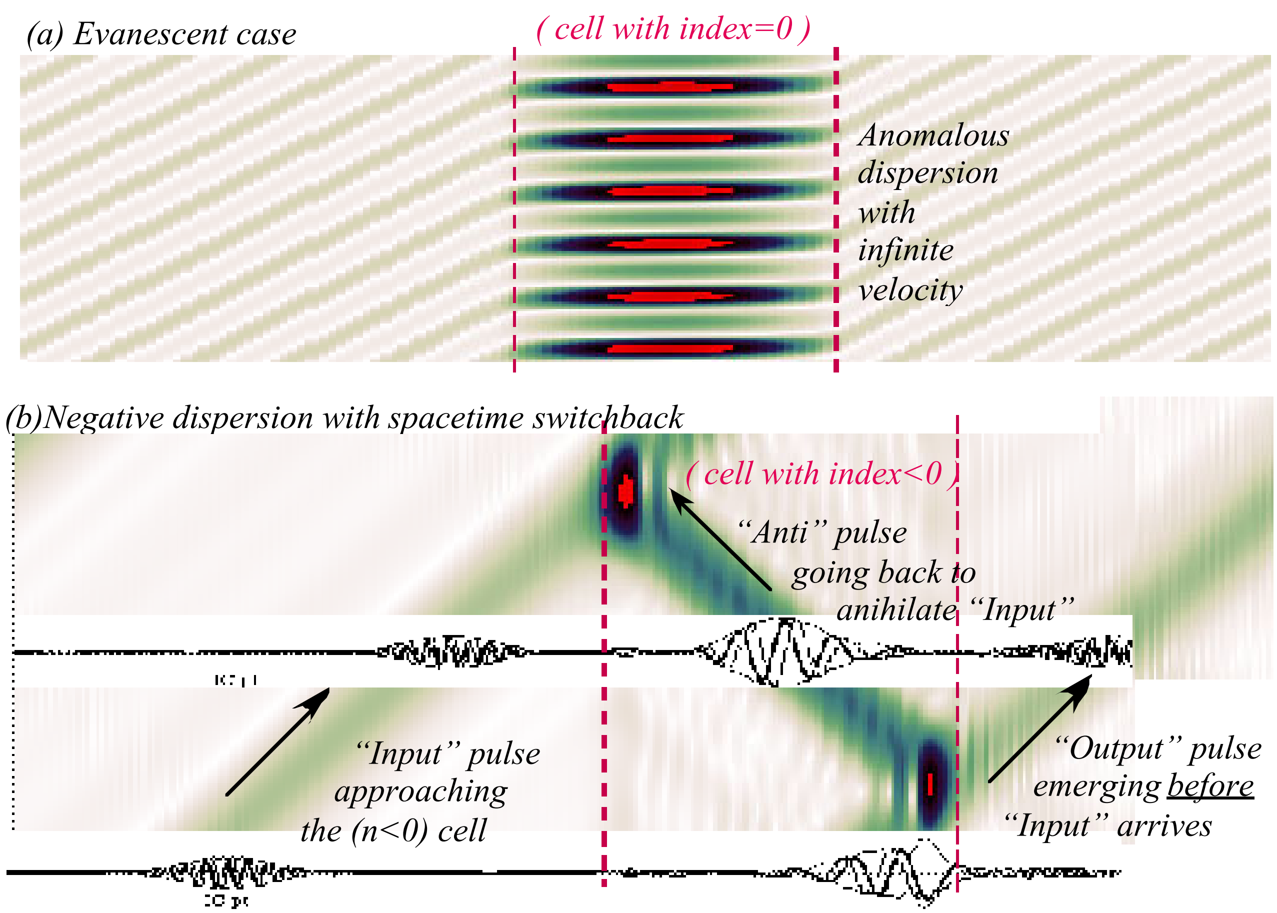

Fig. 5.3.5 Simulations of optical pulse group envelopes for hyper-anomalous dispersion cases

5.4. Quantum-Classical Relationships

Deriving classical mechanical phenomena from quantum mechanics is probably a reasonable strategy given that quantum theory is supposed to supersede the classical. Yet we seem compelled to do the reverse by explaining and even deriving quantum mechanical effects using classical or semi-classical arguments. Such a reverse engineering strategy is most certainly doomed at the most fundamental level.

Nevertheless, it often seemed the only recourse available, particularly in atomic and molecular physics. Also, we often teach quantum theory by saying, " the particle does this...," and relativity pedagogy is still based on old-fashioned classical meter sticks, particles, pulses, and clocks.

The continuous wave (CW) approach of this unit has shown that quantum theory and relativity really need each other. It is possible to learn both with far less effort than struggling with even one of the many apparent paradoxes posed by either one of these subjects taken alone. The only price is an abandonment of a classical "bang-bang-particle" Newtonian paradigm, much as Newtonian physics required disabusing oneself of an Aristotelian one.

(a) Deep classical mechanics: Poincare's invariant

The unified CW approach of Chapters 4-5 is based upon wave mechanics. It appears at first sight to "short-circuit" classical mechanics. However, we will here argue that the CW approach actually brings quantum development closer to the very deepest levels of classical mechanics including the earliest ideas of wave phase due to Christian Huygens and the related invariance principles of Poincare'. These ideas are embodied in the classical *Legendre transformation* that expresses a Lagrangian function L in terms of a Hamiltonian function H.

$$L = p\dot{x} - H \tag{5.4.1}$$

This is rewritten as the *Poincare' differential invariant* which is also called the *differential of action S*.

$$dS = L\,dt = p\,dx - H\,dt \tag{5.4.2}$$

Assuming action $S=\int L\,dt$ is an integrable function leads directly to the *Hamilton-Jacobi equations*, that is, the coefficient of each differential dx and dt must be the respective derivative of action S.

$$p = \frac{\partial S}{\partial x}\ , \qquad (5.4.3a) \qquad\qquad -H = \frac{\partial S}{\partial t} \qquad (5.4.3b)$$

Dirac and Feynman showed that the action is essentially the *quantum phase* Φ in units of $\hbar$.

$$\Psi \approx e^{iS/\hbar} = e^{i\int L\,dt/\hbar} \tag{5.4.4}$$

Quantum relations (5.2.5) for momentum $p= \hbar k$ and energy $H=E= \hbar\omega$ give action-phase differential

$$dS=\hbar d\Phi=\hbar kdx - \hbar\omega dt, \tag{5.4.5a}$$

and a *Hamilton-Dirac-Feynman action-phase equivalence*. For free space-time it is a plane wave phase

$$S/\hbar=\Phi=kx - \omega t. \tag{5.4.5b}$$

So, the notion in Sec. 5.2 of phase invariance actually appears much earlier in the history of classical physics. Unfortunately, it has been quite well disguised by unnecessarily complex formalism.

(b) Classical versus quantum dynamics

Time behavior has similar classical or semi-classical roots. The Hamilton velocity equation

$$\dot{x} = \frac{\partial H}{\partial p} \tag{5.4.6a}$$

is related to the definition (5.2.9b) of group velocity by derivative of the dispersion function.

$$u = \frac{\partial \omega}{\partial k} \tag{5.4.6b}$$

The Hamilton change-of-momentum or "force" equation has a relativistic example discussed later.

$$\dot{p} = -\frac{\partial H}{\partial x} \tag{5.4.7a}$$

It is related to the wave refraction due to spatial gradient of frequency dispersion.

$$\dot{k} = -\frac{\partial \omega}{\partial x} \tag{5.4.7b}$$

As we will see in Sec. 5.5, this is the wave theoretical counterpart of Newton's *(F=ma)*-Law.

A crummy (but quick!) derivation of Schrodinger's equation

We can pretend to derive quantum theory using the ancient classical stuff. As stated previously, this bass-ackwards approach is just a trick. It is by no means an equal to proper Dirac derivations of quantum energy and momentum operators that will be given in *Unit 4 (Wave Equations)*. It is included mainly for historical and pedagogical mnemonics. A slightly improved derivation follows here in Sec. (c).

The reverse-engineering approach takes the x-derivative of the wave (5.4.4) using (5.4.3a).

$$\frac{\partial}{\partial x}\Psi \approx \frac{\partial}{\partial x}e^{iS/\hbar} = \frac{i}{\hbar}\frac{\partial S}{\partial x}e^{iS/\hbar} = \frac{i}{\hbar}p\Psi \tag{5.4.8a}$$

This resembles the *momentum-p-operator* definition that we will derive more clearly in Unit 4.

$$\frac{\hbar}{i}\frac{\partial}{\partial x}\Psi = p\Psi \tag{5.4.8b}$$

The time derivative is similarly related to an "energy-operator" or Hamiltonian operator.

$$\frac{\partial}{\partial t}\Psi \approx \frac{\partial}{\partial t}e^{iS/\hbar} = \frac{i}{\hbar}\frac{\partial S}{\partial t}e^{iS/\hbar} = -\frac{i}{\hbar}H\Psi \tag{5.4.9a}$$

The famous H-J-equation (5.4.3b) makes this into the more famous *Schrodinger time equation*.

$$i\hbar\frac{\partial}{\partial t}\Psi = H\Psi \tag{5.4.9b}$$

Again, a more rigorous development of this awaits a few chapters ahead.

If you now put in a generic off-the-shelf Hamiltonian function $H=p^2/2M+V(x)$ you get

$$i\hbar\frac{\partial}{\partial t}\Psi = \left[\frac{p^2}{2M} + V(x)\right]\Psi = \frac{-\hbar^2}{2M}\frac{\partial^2\Psi}{\partial x^2} + V(x)\Psi \tag{5.4.10}$$

which is the *non-relativistic Schrodinger wave equation*. By non-relativistic we mean it has a potential energy *V(x)* with no momentum part to balance. Also, it treats time as a parameter that cannot mix with spatial coordinate x, and so it cannot manifest the intimate relation of relativity and quantum theory.

The derivation above obtains a famous result using less than rigorous steps. Most notable is the wavy equals sign in (5.4.9a) which indicates that a variable amplitude factor has been left out. When this is fixed the result is Bob Wyatt's useful semi-classical approach to non-relativistic quantum mechanics. It should be noted that substituting $\Psi = e^{iS/h}$ into Schrodinger's equation (5.4.10) does not quite return us to Hamilton-Jacobi equations (5.4.3). Instead the result is a wave equation of the *Riccati* form.

$$-\psi \frac{\partial S}{\partial t} = -\psi \frac{\hbar i}{2m} \nabla^2 S + \psi \left[\frac{1}{2m} \left(\frac{\partial S}{\partial \mathbf{r}} \right)^2 + V(r) \right]$$
$$\frac{\hbar i}{2m} \nabla^2 S = \frac{\partial S}{\partial t} + \left[\frac{1}{2m} \left(\frac{\partial S}{\partial \mathbf{r}} \right)^2 + V(r) \right] = \frac{\partial S}{\partial t} + H\left(\frac{\partial S}{\partial \mathbf{r}}, \mathbf{r} \right) \qquad (5.4.11)$$

In the limit that the left hand double (Laplacian) derivative vanishes, the full quantum Schrodinger equation reduces to the classical H-J equations (5.4.3). This is sometimes called a *semi-classical limit*.

$$\hbar \left| \nabla^2 S \right| << \left(\frac{\partial S}{\partial \mathbf{r}} \right)^2, \text{ or: } \hbar \left| \frac{d^2 S}{dx^2} \right| = \hbar \left| \frac{dp_x}{dx} \right| << p_x^2, \text{ or: } \hbar \left| \frac{dp_x}{dx} \right| / \left| p_x \right| << \left| p_x \right| = \hbar \left| k_x \right| \qquad (5.4.12a)$$

For this to hold, DeBroglie wavelength $\lambda_x/h = 1/\hbar k_x = 1/p_x$ must be small compared to its variation in the space of a wavelength. Equivalently wavevector k_x is large compared to relative rate of change of k_x.

$$\left| \frac{dk_x}{dx} \right| / \left| k_x \right| << \left| k_x \right|, \text{ or: } \left| \frac{d\lambda_x}{dx} \right| << 1 \qquad (5.4.12b)$$

(c) A slightly improved derivation of Schrodinger's equation

A μ-wave dispersion function (5.2.8) *sans* its $(\hbar\mu = Mc^2)$ term gives a Newtonian approximation.

$$KE = \hbar\omega - \hbar\mu \Rightarrow KE_{NR} = \hbar\omega \cong \frac{(\hbar ck)^2}{2\hbar\mu} = \frac{p^2}{2M} \quad \text{where:} \begin{cases} \hbar k = p \\ \hbar\mu = Mc^2 \end{cases}$$

An approximate classical Hamiltonian is a sum of the Newtonian kinetic energy KE and a potential $\mathbf{V}$.

$$\mathbf{H} = \frac{\mathbf{p}^2}{2M} + \mathbf{V} = KE_{NR} + PE_{NR}$$

Presumably, $\mathbf{V}$ is an interaction energy of the μ-wave with whatever else might occupy its vacuum. Fourier plane waves $\psi_{k,\omega}(x,t) = \langle x,t | k,\omega \rangle = e^{i(kx-\omega t)} / \sqrt{N}$ are eigenfunctions of momentum $\mathbf{p}$ or KE only.

$$\langle x,t | \mathbf{p} | k,\omega \rangle = \hbar k \langle x,t | k,\omega \rangle = \frac{\hbar}{i} \frac{\partial}{\partial x} \psi_{k,\omega}(x,t) \qquad (3.4.13a)$$

$$\langle x,t | KE | k,\omega \rangle = \hbar\omega \langle x,t | k,\omega \rangle = \hbar i \frac{\partial}{\partial t} \psi_{k,\omega}(x,t) \qquad (5.4.13a)$$

A wave $\langle x,t | \Psi \rangle$ with Fourier coefficients $\alpha_{k,\omega} = \langle k,\omega | \Psi \rangle$ satisfies a Schrodinger time equation.

$$\sum_{k,\omega} \alpha_{k,\omega} \langle x,t | KE | k,\omega \rangle = \sum_{k,\omega} \alpha_{k,\omega} \langle x,t | H - V | k,\omega \rangle = i\hbar \sum_{k,\omega} \alpha_{k,\omega} \frac{\partial}{\partial t} \psi_{k,\omega}(x,t) \qquad (5.4.14a)$$

$$\langle x,t | KE | \Psi \rangle = \langle x,t | H - V | \Psi \rangle = i\hbar \frac{\partial \Psi(x,t)}{\partial t} \quad \text{where: } \Psi(x,t) = \sum_{k,\omega} \alpha_{k,\omega} \langle x,t | k,\omega \rangle = \langle x,t | \Psi \rangle \qquad (5.4.14b)$$

But, only certain waves $\langle x,t | \Phi_E \rangle$ satisfy a *Schrodinger energy eigen-equation* $\mathbf{H} | \Phi_E \rangle = E | \Phi_E \rangle$.

$$\langle x,t | KE | \Phi_E \rangle = -\frac{\hbar^2}{2M} \frac{\partial^2}{\partial x^2} \Phi_E(x,t) = (E - V) \Phi_E(x,t) \qquad (5.4.15a)$$

Eigenvalue E is used to define non-relativistic time and frequency relations for stationary state $| \Phi_E \rangle$.

$$i\hbar \frac{\partial}{\partial t} \Phi_E(x,t) = E \Phi_E(x,t) \quad \text{where: } \Phi_E(x,t) = \Phi_E(x,0) e^{-iEt/\hbar} \qquad (5.4.15a)$$

This restatement of Planck's (E=$\hbar\nu$)-axiom is an "improved" derivation of Schrodinger theory, but every step of it further erodes relativity of spacetime. To arrive at (5.4.15) we must *(1)* discard proper frequency ($\hbar\mu = Mc^2$), *(2)* consider only non-relativistic low-(ω,ck) approximations, *(3)* introduce a scalar potential $V(x)$ without a relativistic vector potential companion (in QED this is an E•r approximation) , and *(4)* define energy eigenstates by single-frequency time dependence. The last step precludes the first example in Fig. 4.3.3 from being viewed as an energy state in any but the one frame of Fig. 4.3.3(a) that is monochromatic $E_0=\hbar\omega_0$. Again, the proper Dirac derivation of (5.4.15) and solutions are in Unit 4. But, proper or not, Schrodinger theories all have difficulties due to their ignoring relativity.

Schrodinger difficulties

Failure to treat time, frequency, and energy on the same footing as, respectively, space, k-vector, and momentum leads to a logically tangled web. Repair of Schrodinger theory with perturbative patching is difficult, misleading, and lacking physical insight. This leads to many longstanding difficulties that go untreated since Schrodinger's equation has for so long been so successful in its realm of approximation.

A key Schrodinger difficulty involves the concepts of inertia and mass. The *wave effective inertial mass M_{eff}* (5.2.20a) is inversely proportional to the curvature of the dispersion function (5.2.8) and *not* a constant except for the quadratic case $\omega=B\,k^2$. For low velocity ($\beta = u/c << 1$) M_{eff} approaches the *rest mass $M=\hbar\mu/c^2$* given by (5.2.5b), a constant $\hbar/c^2$ times proper-frequency μ.

$$M_{eff} = \frac{F}{a} = \frac{1}{\left(\frac{d^2E}{dp^2}\right)} = \frac{M}{\left(1-\beta^2\right)^{3/2}} \xrightarrow[\beta\approx 0]{} M \qquad (5.4.16)$$

At high β , M_{eff} differs from the *momentum mass M_{rel}* of relation (5.2.5c). M_{rel} also is M at slow u.

$$M_{rel} = \frac{M}{\left(1-\beta^2\right)^{1/2}} \xrightarrow[\beta\approx 0]{} M \qquad (5.4.17)$$

Photon dispersion is linear $(\omega = c|k|)$ so (5.4.16) does not apply. Indeed, photon effective mass is *infinite* since its group and phase velocity are invariant. But, effective mass of any wave at $k=0$ is its *invariant rest mass M*. Higher $M=\hbar\mu/c^2$ makes waves harder to accelerate (unless M is zero as for photons). Then the optical dispersion function ($\omega = c|k|$) in Fig. 5.1.1 has a kink with infinite curvature at the origin $k=0$. So, by equation (5.4.16a), photon rest mass is indeed zero but photon M_{eff} is infinite everywhere else!

The standard Schrodinger equation (5.4.15) is ill equipped to handle variable effective mass, and it literally falls apart for problems involving *negative energy states* with *negative dispersion (μ<0)* or *tachyon states (imaginary μ)*. It might seem that the Newtonian $k^2/_{2M}$ dispersion plot in Fig. 5.2.1(b) is a strategically placed "fig-leaf" covering an embarrassment of Dirac negative-μ (anti-particle) bands for which (5.4.16a) gives negative M_{eff} . The negative-energy or negative-μ bands are states whose phasors run in reverse, that is, counter-clockwise and a world going back in time! Some of the seemingly bizarre wave behavior due to abnormal or anomalous dispersion has been shown in Fig. 5.3.5. The behavior of high-energy matter-anti-matter reactions has to involve similarly bizarre wave dynamics. So will exciton states involving combinations of conduction-band "carriers" and valence-band "holes" in semiconductors.

Classical relativistic Lagrangian derived by quantum theory

The classical Hamiltonian H is derived from the Lagrangian L (5.4.1) so action $S=\int L\,dt$ is arguably a more fundamental quantity than energy. The quantum energy or frequency $\omega=E/\hbar$ is a negative time derivative (5.4.3b) of the phase $\Phi=S/\hbar$, which arguably is the most fundamental quantity of all.

The preceding discussions of these quantities give some idea why classical mechanics could seem to be so prescient about concepts that only make sense in light of quantum wave mechanics. Perhaps, the key link is when Poincare's invariant (5.4.2) is related to the phase invariance axiom (4.3.6). One may view families of classical trajectories fanning out like rays from each spacetime point. Normal to the classical momentum $\mathbf{p}=\nabla S$ (5.4.3a) of each ray are the wavefronts of constant phase Φ or action S. Then, according to a "matter-wave" form of Huygen's principle, new wavefronts are continuously built as in Fig. 5.4.1 through interference from "the best" of all the little wavelets emanating from a multitude of source points.

The "best" are the ones that are extremes in phase, so-called *stationary-phase* rays, who thereby satisfy *Hamilton's Least-Action Principle* requiring that $\int Ldt$ is minimum for "true" classical trajectories. This in turn enforces Poincare' invariance by eliminating, through destructive interference, any "false" or non-classical paths because they do not have an invariant (and thereby stationary) phase, and therefore cancel each other in a cacophonous mish-mash of mismatched phases.

The idea of phase invariance that began this chapter may be restated using the classical ideas of action and Lagrangian functions. Plane phase $\Phi = kx-\omega t$, in the mass rest frame where $x=0=k$, is a product $-\mu\tau$, of minus the proper frequency $-\omega=-\mu$ multiplying the proper time $t=\tau$. The differential of this phase by Einstein-Planck mass-energy-frequency equivalence relation (5.2.5b) is

$$d\Phi = k\,dx-\omega\,dt=-\mu\ d\tau = -(Mc^2/\hbar)\ d\tau. \qquad (5.4.18)$$

τ-Invariance (5.1.4) (or Einstein time dilation (4.4.1a)) gives $d\tau$ in terms of velocity $u=\frac{dx}{dt}$.

$$d\tau = dt\ \sqrt{(1-u^2/c^2)} \qquad (5.4.19)$$

Combining definitions for action $dS=Ldt$ (5.4.2) and phase $dS = \hbar d\Phi$ (5.4.5) gives

$$L =-\hbar\mu\tau = -Mc^2\sqrt{(1-u^2/c^2)}. \qquad (5.4.20)$$

This is a *relativistic matter Lagrangian* whose action integral $S=\int Ldt$, says Hamilton, must be *minimized*.

Feynman's clever interpretation of the S minimization as sketched in Fig. 4.5.2 is that a massive projectile flies in such a way that its "clock" τ is *maximized*. Since proper frequency μ is constant for a given type of matter, this is the same as minimizing $-\mu\tau$ or maximizing $+\mu\tau$. What *does* minimize τ? Answer: Huygen's wave interference demands stationary and extreme phase, that is, the fastest clock!

So, the mechanically ordered Newtonian "clockwork-world" appears then to be the perennial "cosmic gambling house winner" in a kind of wave dynamical lottery occurring in an underlying quantum wave fabric. Since it seems to be such a winner for so long, many physicists find it difficult to say good-bye to a purely classical paradigm even as it becomes more and more clear that it's all "faked" by interfering waves. The classical period of physics was made a huge success by Newton and others who began the great enlightenment period of the 18th century and proceeded through the 20th. We only hope the 21st century will be at least as enlightening as we move on to examining a very wavy universe.

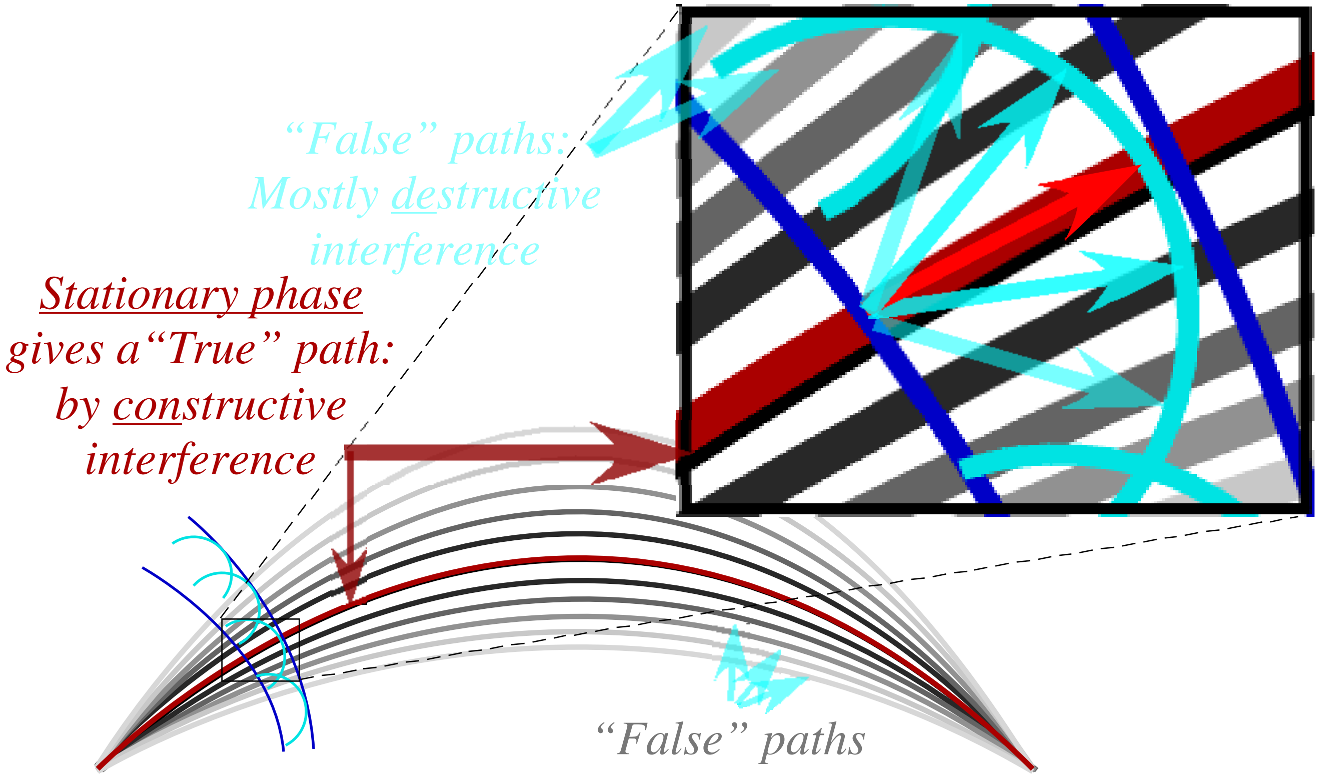

Fig. 5.4.1 Quantum waves interfere constructively near "True" path. Waves mostly cancel elsewhere.

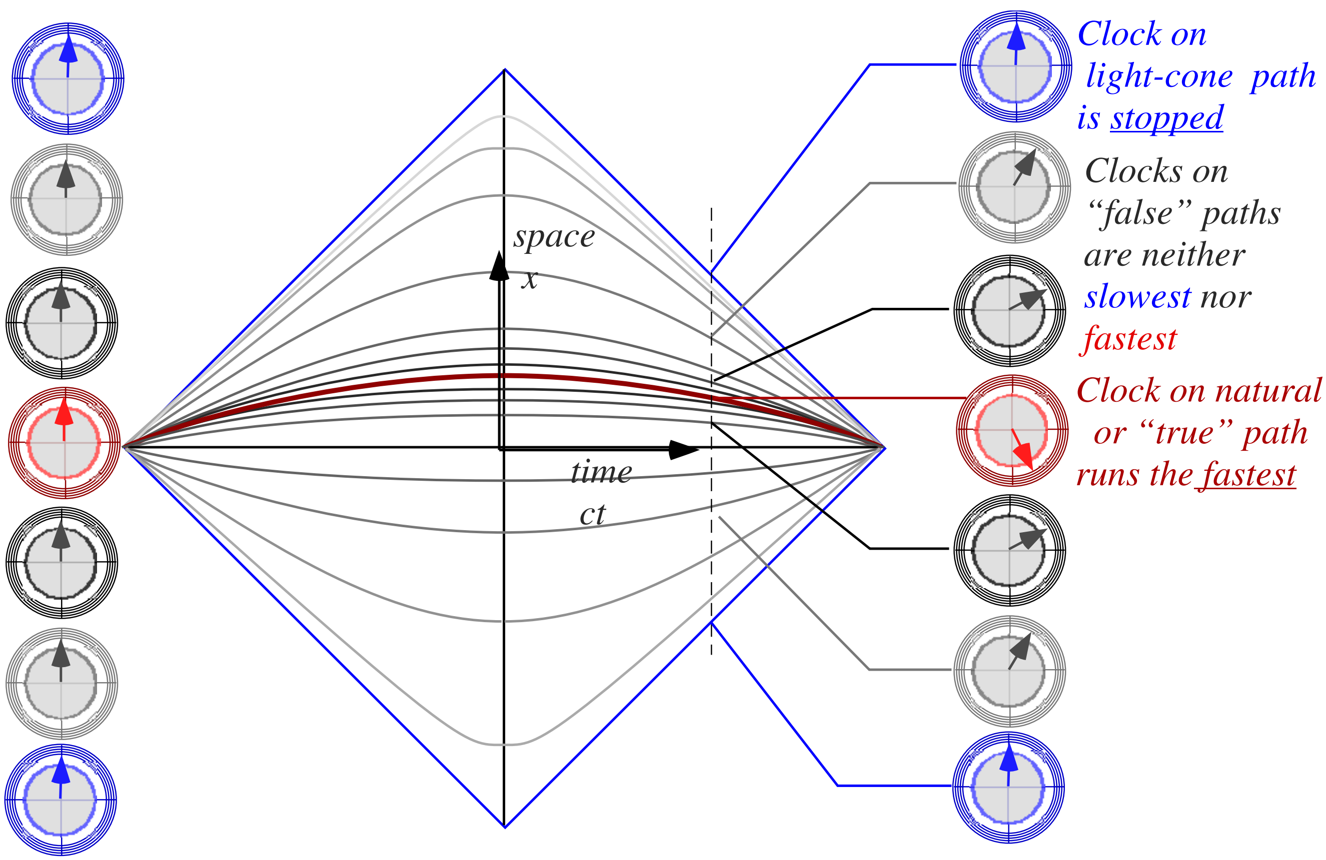

Fig. 5.4.2 "True" paths carry extreme phase and fastest clocks. Light-cone paths carry stopped clocks.

5.5 Relativistic acceleration: Newton's invariants

The theory of special relativity is one of inertial frames and constant velocity. At first this might seem to preclude discussion of frames with non-constant velocity such as linear acceleration (changing inclination in space and time) or rotating frames (changing inclination in space).

Linear accelerated Lorentz frames in just one-space dimension provide a glimpse of some of the issues of Einstein's general theory for curved spacetime and gravity. Einstein's *equivalence principle* claims that a g-accelerated frame or "Einstein elevator" has the same *local* physics as a frame fixed in a uniform g-field. We now consider accelerated frames by classical theory and then by wave mechanics.

(a) Classical particle and PW theory of acceleration

A classical theory of an accelerating particle must deal with its mass, which involves rest mass M (5.2.5a), relativistic mass M_{rel} (4.5.16), and effective mass M_{eff} (5.4.17). Definition of mass depends on which time derivatives we use, proper time differentials $d\tau$ or coordinate time differential dt. Ordinary u velocity is a ratio of coordinate x and coordinate time t. Equation (5.2.5c) for momentum p involves a ratio of coordinate x and *proper* time τ. (p also has rest mass M multiplying the *proper velocity* $\upsilon=dx/d\tau$.)

$$u=\frac{dx}{dt} \qquad (5.5.1a) \qquad\qquad p=M\upsilon=M\frac{dx}{d\tau} \qquad (5.5.1b)$$

The ratio of t and τ differentials follows from (5.4.19) or from definition (5.1.4) of proper time τ.

$$d\tau=dt\sqrt{1-u^2/c^2} \qquad (5.5.1c)$$

The ratio of proper time derivatives of momentum and velocity is the effective mass in equation (5.4.17).

$$\begin{aligned}\frac{dp}{d\tau}&=\frac{d}{d\tau}\frac{Mu}{\sqrt{1-u^2/c^2}}=\frac{M\frac{du}{d\tau}}{\sqrt{1-u^2/c^2}}+\frac{\frac{Mu^2}{c^2}\frac{du}{d\tau}}{\left[1-u^2/c^2\right]^{\frac{3}{2}}}\\&=\frac{M}{\left[1-u^2/c^2\right]^{\frac{3}{2}}}\frac{du}{d\tau}=M_{eff}\frac{du}{d\tau}\end{aligned} \qquad (5.5.2)$$

In quantum dynamics and related Newtonian sub-relativistic classical dynamics, wavevector k (that is, momentum $p=\hbar k$) in (5.2.5c) grows linearly with boost velocity u from its zero-k resting value, while frequency ω (that is, energy $E=\hbar\omega$) in (5.2.5b) grows quadratically with u from its resting value of proper frequency μ (that is, rest energy $\hbar\mu=Mc^2$). If u grows linearly with time $\tau\sim t$, as it would at first with constant acceleration g, then wavevector (momentum) varies initially as $g\tau$ while frequency (energy) varies initially as $g\tau^2/2$. All this recapitulates elementary classical mechanics, as it must. At time $\tau=0$, the τ-derivative of u is g, the τ-derivative of p is Mg, but the τ-derivative of E is zero.

$$\left.\frac{dp}{d\tau}\right|_0=Mg\,, \qquad \left.\frac{dE}{d\tau}\right|_0=0\,. \qquad (5.5.3)$$

Consider a rocket frame (x'',ct'') where $dp''/d\tau$ is *always* a constant Mg. This is an Einstein elevator model of uniformly accelerating gravity. The lab value p at each speed u is a Lorentz boost (5.2.10a).

$$p = \frac{p'' + u\,E''/c^2}{\sqrt{1-(u/c)^2}} \tag{5.5.4}$$

The τ-derivative of p has the same boost since proper time τ is invariant. τ=0 values (5.5.3) are used.

$$\frac{dp}{d\tau} = \frac{\frac{dp''}{d\tau} + \frac{u}{c^2}\frac{dE''}{d\tau}}{\sqrt{1-(u/c)^2}} = \frac{Mg + \frac{u}{c^2}0}{\sqrt{1-(u/c)^2}} = \frac{Mg}{\sqrt{1-(u/c)^2}} \tag{5.5.5a}$$

This reduces to an elementary <u>*pre*-relativistic</u> constant-*g* Newtonian equation by using t/τ-ratio (5.5.1c).

$$\frac{dp}{dt} = Mg \tag{5.5.5b}$$

The velocity is not Newtonian since u cannot grow indefinitely or it will exceed c, but, the momentum p (and wavevector k) as well as energy E (and frequency ω) do grow indefinitely as u approaches c.

Equating (5.5.5a) and (5.5.2) gives an easily integrated equation for velocity u.

$$\frac{dp}{d\tau} = \frac{M\frac{du}{d\tau}}{\left[1-\frac{u^2}{c^2}\right]^{\frac{3}{2}}} = \frac{Mg}{\left[1-\frac{u^2}{c^2}\right]^{\frac{1}{2}}}, \qquad M\frac{du}{d\tau} = Mg\left[1-\frac{u^2}{c^2}\right], \qquad g\tau = \int \frac{du}{\left[1-\frac{u^2}{c^2}\right]} \tag{5.5.6}$$

The integral yields the boost velocity u/c as a hyperbolic tangent of a product of proper time τ and g/c.

$$\frac{u}{c} = \tanh(g\tau/c) = \sinh(g\tau/c)/\cosh(g\tau/c) \tag{5.5.7a}$$

So, hyperbolic rapidity $\rho = \tanh^{-1} u/c = g\tau/c$ increases linearly with proper time τ while velocity u approaches c. Time dilation factor $\cosh\rho$ is a hyper-cosine of proper time $g\tau/c$ consistent with (4.3.7).

$$\frac{dt}{d\tau} = \frac{1}{\sqrt{1-\frac{u^2}{c^2}}} = \frac{1}{\sqrt{1-\tanh^2(g\tau/c)}} = \cosh(g\tau/c) \tag{5.5.7b}$$

Coordinate velocity u (5.5.1a) and proper velocity $\upsilon = p/M$ from (5.5.1b) are also hyper-functions.

$$u = \frac{dx}{dt} = \frac{\frac{dx}{d\tau}}{\frac{dt}{d\tau}} = \frac{\frac{dx}{d\tau}}{\cosh(g\tau/c)} = c\tanh(g\tau/c) \tag{5.5.7c}$$

where:

$$\upsilon = \frac{p}{M} = \frac{dx}{d\tau} = c\sinh(g\tau/c) \tag{5.5.7d}$$

This is no accident. Integrating equations (5.5.7) shows a constant acceleration trajectory is a hyperbola.

$$x = \frac{c^2}{g}\cosh(g\tau/c) \tag{5.5.8a}$$

$$ct = \frac{c^2}{g}\sinh(g\tau/c) \tag{5.5.8b}$$

These are not just any hyperbolas, but *invariant hyperbolas* such as traced by rockets in Fig. 5.5.1.

$$x^2 - (ct)^2 = \left(c^2/g\right)^2 \tag{5.5.8c}$$

A constant-*g* trajectory is invariant since all must agree on the shape of a given constant proper acceleration curve. A ship with a big "g" stamped on its tail doesn't look like a 2g-ship to someone else who happens to moving by outside it. The *g*-number is an intrinsic proper invariant.

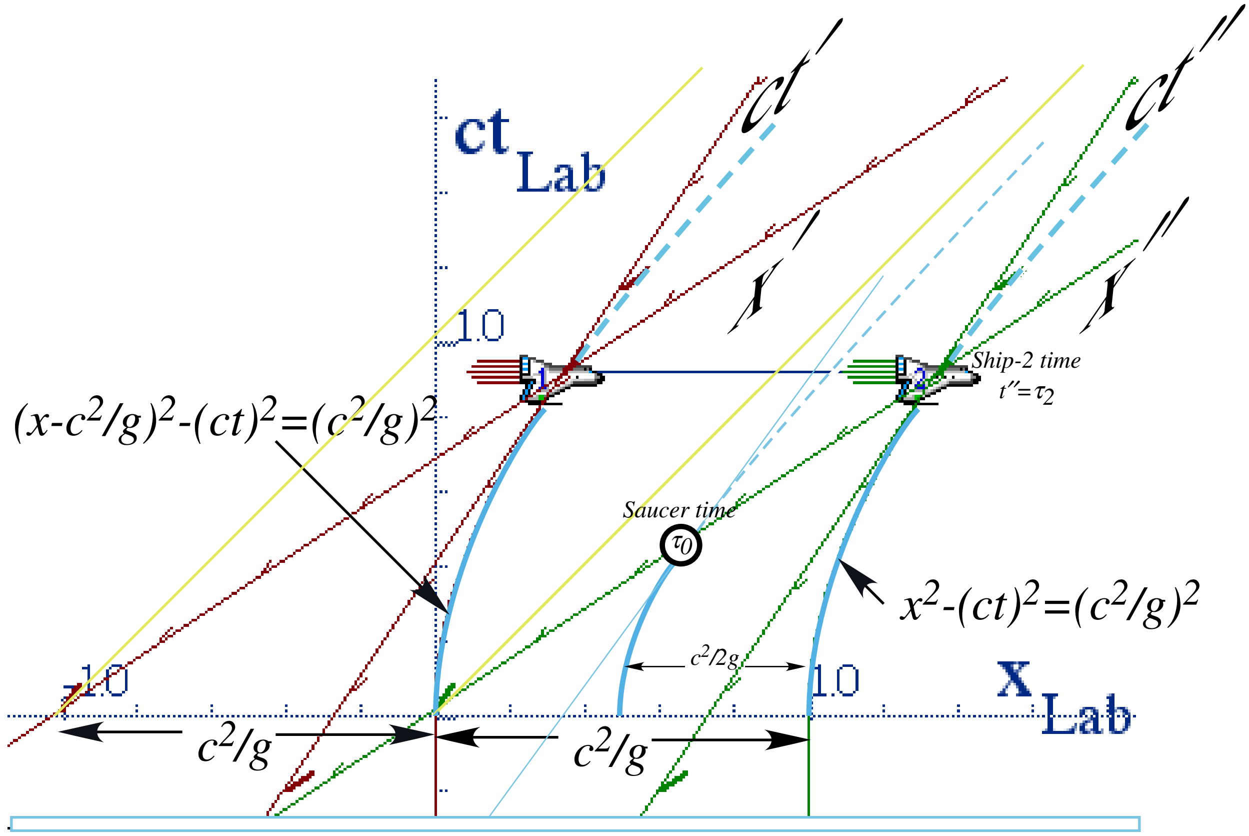

Fig. 5.5.1 Examples of constant acceleration space-time trajectories of ships (g) and saucer (2g).

The relativistic momentum $p=Mv$ is growing as a hyper-sine of proper time in (5.5.7d) and so is lab coordinate time t (5.5.8b). Constant (local) acceleration yields constantly growing (lab) momentum (5.5.5b) just as Newton had claimed all along! So we call the trajectories in Fig. 5.5.1 *Newton's invariants*.

Proper length: Gentlemen start your engines!

Still, there was little to prepare Newton for the modern consequences of his second law in relativistic form (5.5.5). To show this, Fig. 5.5.1 has two identical ships fire their engines at $t=0$ lab time to begin a constant g journey in parallel. What happens next from the point of view of their instantaneous Lorentz frames seems so bizarre that it boggles the mind. If you like paradox, this is a race to watch, a cosmic NASCAR!. The idea of fielding such an event originates with John. E. Heighway around 1967.

The acceleration $g=c^2$ imagined here is astronomical; from zero to half the speed of light in less than a second! Also, there is a "flying saucer" (A circle in Fig. 5.5.1) with *twice* the acceleration located a distance $c^2/2g$ behind ship-2 and the same distance ahead of ship-1 who starts the race at lab origin $x=0$.

Since ship-2 starts at lab $x=c^2/g$ from origin it will trace a hyperbolic invariant trajectory in the lab according to (5.5.8c). So will the alien saucer which starts at $x=c^2/2g$ with acceleration $2g$. You might think that the $2g$ saucer would rapidly catch up with the $1g$ ship-2 it is chasing, and it does appear to do so to the lab observers. As always in relativity, the word we need to question here is "appear."

According to observers at rest in any ship-2 frame, the distance between the saucer and ship-2 *remains fixed at* $x'=c^2/2g$ for as long as both continue their respective acceleration $2g$ and g. And, the lab observers might note that the saucer, in spite of its superior acceleration, never *passes* ship-2. In fact, all they are seeing is gradual Lorentz contraction (4.4.1) of saucer, ship-2, and the distance separating them, while, meantime, the distance separating ship-1 and ship-2 does not shrink at all.

The key idea here is that the saucer and ship-2 are on *concentric* hyperbolic invariants of *proper length* ℓ from the origin. *Proper length* ℓ-curves defined by $x^2-(ct)^2 = \ell^2 = x''^2 - (ct''^2)$ are just the $i\tau$-curves in Fig. 5.1.2(a), that is, the imaginary proper-time $i\tau$-curves that serve as space-axis grid markers. The x''-axis tips for the ship-2 and saucer as they accelerate, but each stays put at the $x''=c^2/g$ and $x''=c^2/2g$ grid marker, respectively. In other words, their proper separation $\Delta x''=c^2/2g$ does not change; it is as though the saucer and ship-2 *were connected by a rigid beam of constant proper length*. Ship-2 has a saucer-trailer! (It is always puzzling that alien flying saucers or other UFO's always visit trailer camps in Alabama, Arkansas, and such places. Perhaps, they just want to *be* trailers.)

Meanwhile, ship-1 follows a hyperbola that is identical to (but not concentric to) that of ship-2. The origin for ship-1 is also fixed a distance c^2/g behind it according to (5.5.8c) and as shown in Fig. 5.5.1. The ship-1 space x'-axis tips just as fast in the lab frame as the x''-axis of ship-2 and its trailing saucer. Along the x'-axis, ship-1 could find ship-2 and its saucer way up in the upper right hand corner of Fig. 5.5.1. He'd better be quick about it because ship-2 and saucer are receding rapidly from ship-1 in its x'-frame. This *Lorentz expansion* is the necessary flipside of Lorentz contraction because the separation Δx of ship-1 and ship-2 is constant in the lab x-frame where their kinetic behavior is identical.

You might think that ship-2 and its saucer-trailer would see ship-1 falling behind them on their x''-axis, and that their view of the Lorentz expansion would equal that of ship-1. But, as indicated in Fig. 5.5.1, the behavior of ship-1 seen by ship-2 is quite extraordinary. In the x''-frame of the trailer-saucer and ship-2, they would see (if they could) ship-1 *stuck at time-zero*. Ship-1's engines won't start, and neither do any of its clocks! Ship-1, in the ship-2 x''-frame, appears to be pretty much a dead parrot.

In spite of this, ship-1 manages to keep up with the very-much-alive ship-2 as does the saucer! Indeed, the Lorentz space-expansion makes the x''-distance from ship-1 and ship-2 stay put at the invariant value $x''=c^2/g$ with the saucer always halfway between at $x''=c^2/2g$. The saucer-trailer acceleration of $2g$ must be twice the rate g of the ship-2 just to remain at $x''=c^2/2g$ behind it.

One key to this strange behavior is in the proper time values of the participants. The instantaneous lab-relative velocity u_2 of ship-2 in Fig. 5.5.2 is equal to the velocity u_0 of its saucer-trailer. Along the x''-axis line, each concentric hyperbolic trajectory has the same tangent slope or velocity but not the same curvature or acceleration. The velocity equation (5.5.7a) gives

$$\frac{u_2}{c} = \tanh\left(g\tau_2 / c\right) = \frac{u_0}{c} = \tanh\left(2g\tau_0 / c\right) \qquad (5.5.9a)$$

This means that the proper time τ_2 on board ship-2 is twice the proper time τ_0 on its saucer trailer.

$$g\tau_2 / c = 2g\tau_0 / c \quad \text{implies:} \quad \tau_2 = 2\tau_0 \qquad (5.5.9b)$$

This means that the ship-2, which is loafing along with *1g* acceleration, is aging twice as fast as its attached saucer-trailer that has to do a 2g acceleration just to keep up. (Exercise keeps us younger!) Also, lab time coordinates t_2 and t_0 (indicated by vertical arrows pointing at ship-2 and saucer, respectively, in Fig. 5.5.2) have the same *2:1* ratio according to (5.5.8b) and (5.5.9b).

$$\frac{t_2}{t_0} = \frac{\frac{c^2}{g}\ \sinh(g\tau_2 / c)}{\frac{c^2}{2g}\ \sinh(2g\tau_0 / c)} = \frac{2\ \sinh(g\tau_2 / c)}{\sinh(2g\tau_0 / c)} = 2 \tag{5.5.10}$$

This checks with the geometry of Fig. 5.5.2. Readings on co-moving clocks along x'' are proportional to distance x'' while the acceleration each one needs to keep up the same velocity is inverse to x''.

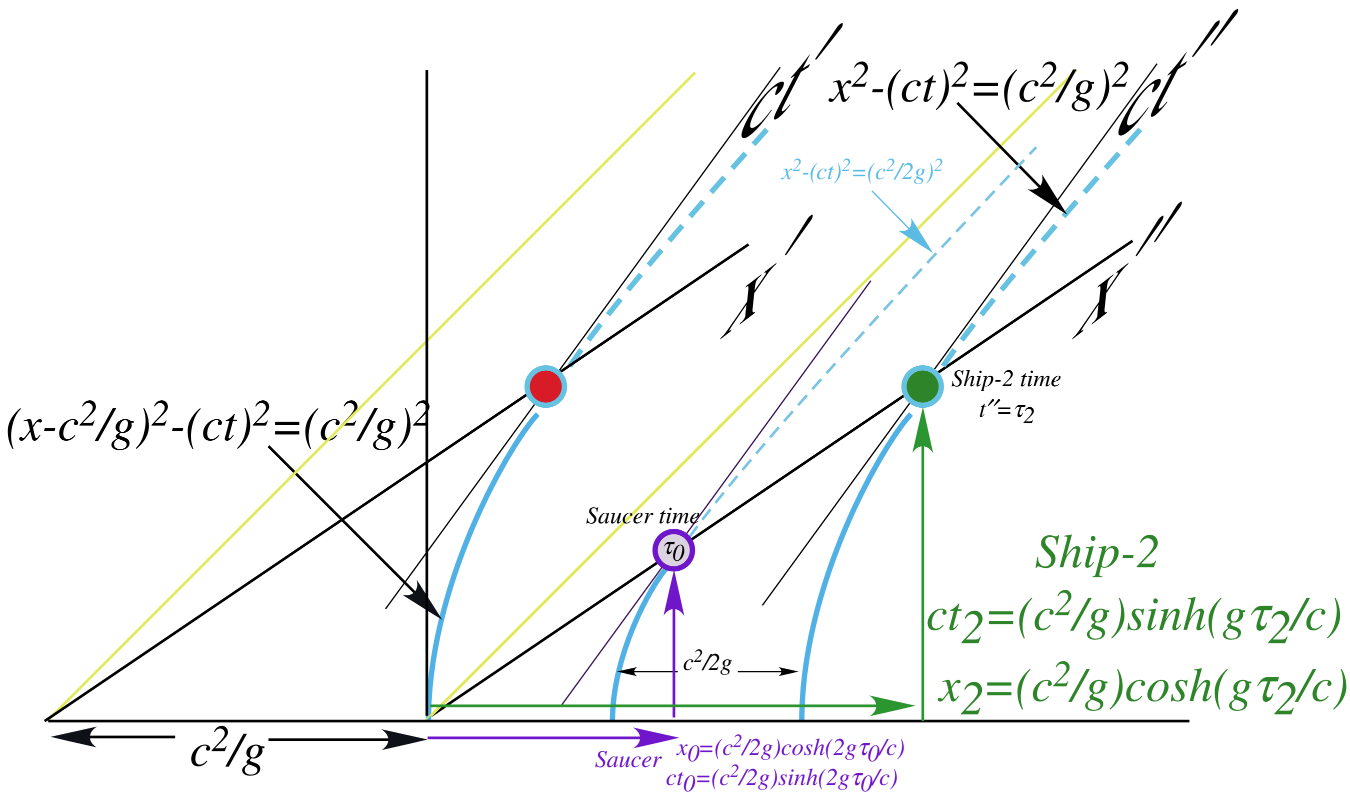

Fig. 5.5.2 Coordinates and proper time relations for ship-1 (one-g) and saucer-trailer (two-g).

Some of the paradox concerning the ship and its length-invariant extension to the saucer-trailer can be resolved by using optical pulse trains bouncing back and forth between ship-2 and its saucer trailer. If the length $x''=c^2/2g$ separating these two objects never changes as long as their accelerations are constant (*1g* for the ship and *2g* for the saucer) then that length can be used as a timing device by bouncing pulses between mirrors held by each of them. The space-time paths of these pulses are shown in Fig. 5.5.3.

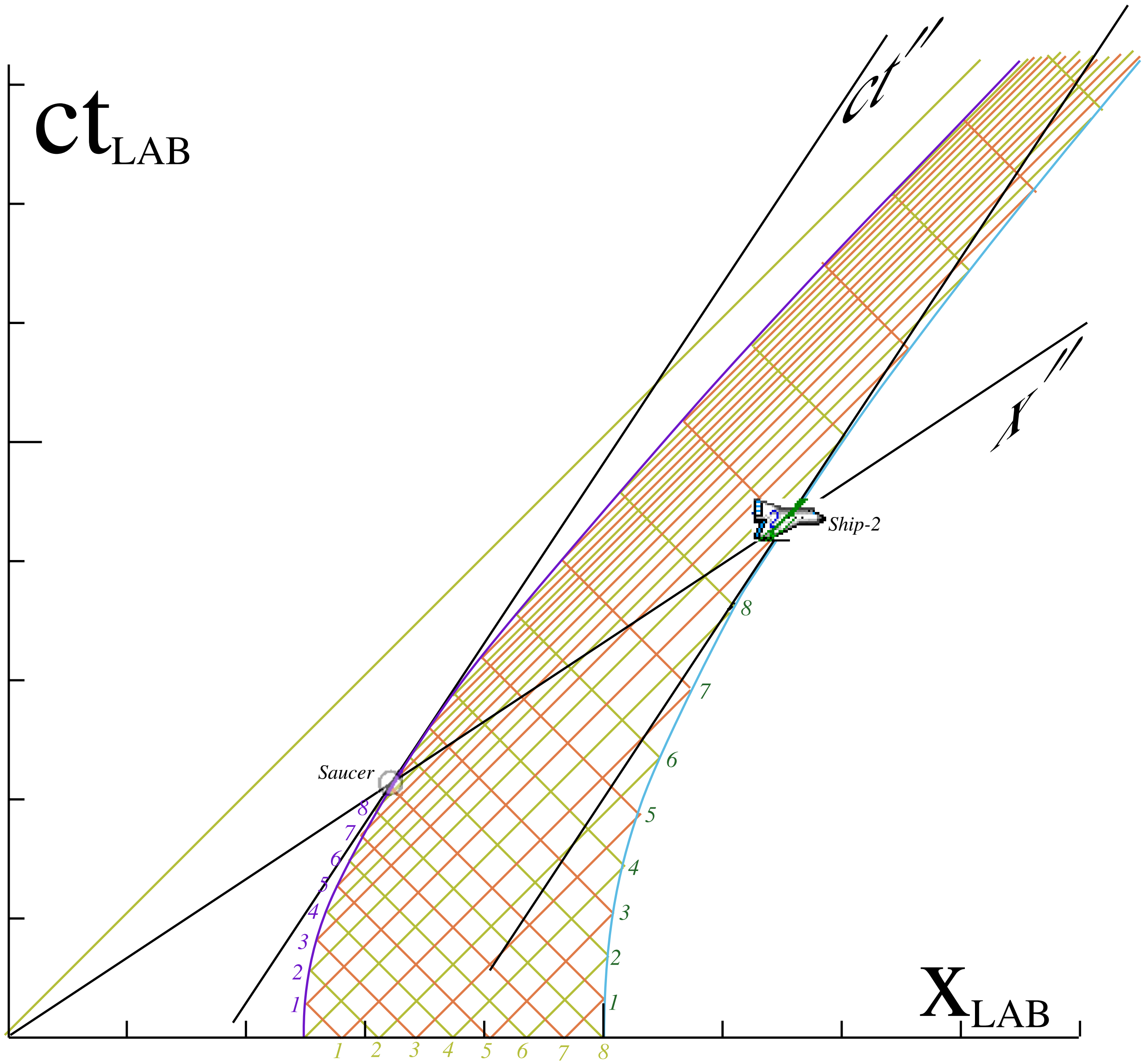

Fig. 5.5.3 Optical pulse wave paths between ship-2 (one-g) and saucer-trailer (two-g) trajectories.

A total of eight pulses are running in each direction along the x''-axis between ship-2 and saucer. At the lab moment when the x''-axis is pictured in Fig. 5.5.3, both the ship and the saucer have bounced eight pulses since departure and are in the process of bouncing a ninth. The *45°* lines in Fig. 5.5.3 could also be paths of continuous wave (CW) ReΨ zeros of moving waves. Interfering wave combinations give local standing wave Minkowski grids (Recall Fig. 4.3.3). The grids start out Cartesian at the bottom of Fig. 5.5.3. (Recall Fig. 4.3.2) Then acceleration makes local Minkowski grids of increasing velocity u. Next we study some detailed properties of accelerated waves. In so doing, we rederive the classical results easily.

(b) Wave interference and CW theory of acceleration

Accelerating Minkowski grids can be made using counter-propagating CW laser beams like the ones making constant-u grids in Fig. 4.3.3. A group velocity u may be achieved by detuning to $\omega_{\leftarrow}=(1/b)\omega'_0$ the laser pointing against u while up-tuning the forward laser $\omega_{\rightarrow}=(b)\omega'_0$, by the same Doppler factor $b=e^{\rho}$ given by (4.3.5b). The exponent ρ is the *rapidity* argument in hyperbolic definitions (4.3.7) of velocity u.

$$b=e^{\rho} \quad (5.5.11a) \qquad\qquad u/c=\tanh\rho \quad (5.5.11b)$$

In Fig. 4.3.3(b) frequency shifting is due to the laser's Doppler b-shifts from motion relative to the atom (or ship) frame. In Fig. 5.5.4 we propose to use *tunable* fixed lasers to accelerate an atom frame (and maybe an atom, too), but now the atom will see a *Cartesian* spacetime grid like Fig. 4.3.3(a) made by *one* green ω'_0 frequency from *either* laser due to its perceived Doppler shifts of $\omega_{\rightarrow}$ and $\omega_{\leftarrow}$.

$$\omega_{\rightarrow}=(b)\,\omega'_0 = e^{\rho}\omega'_0 \quad \text{and} \quad \omega_{\leftarrow}=(1/b)\,\omega'_0 = e^{-\rho}\omega'_0 \qquad (5.5.12)$$

To the atom, both the blue laser $\omega_{\rightarrow}$ off to the left and a red laser $\omega_{\leftarrow}$ off to the right always look green!

This uses tunable versions of grid broadcasting schemes wherein both frequency (5.2.11) and amplitude (5.2.12) would vary in order to achieve a desired instantaneous rapidity ρ at a particular position $(x(t),ct)$ of the atomic (x',ct')-grid-origin in the laser-lab. The trick is to schedule the location and timing of pair(s) of counter-propagating laser beam sources so their beams intersect at the precise spacetime point $(x(t),ct)$ where they can interfere and make the desired local instantaneous atomic (x',ct')-grid of rapidity ρ. In other words, the laser pair on the lightcone of each trajectory point $x(t)$ "paints" a local grid having rapidity ρ so that the specified trajectory $x(t)$ is a continuous spacetime curve.

$$u=\frac{dx}{dt}=c\tanh\rho \qquad (5.5.13)$$

One scheme, shown in Fig. 5.5.4, uses a line of n laser pairs strung out along the lab x-axis. The n^{th} blue-red pair $(\omega_{n\rightarrow},\omega_{n\leftarrow})$ of lasers has the left-hand laser located at $x_{n\rightarrow}$ and the right-hand one at $x_{n\leftarrow}$.

$$x_{n\rightarrow}=x(t_n)-ct_n \quad (5.5.14a) \qquad\qquad x_{n\leftarrow}=x(t_n)+ct_n \quad (5.5.14b)$$

They are set to turn on at lab time $t=t_0=0$ with frequencies $(\omega_{n\rightarrow},\omega_{n\leftarrow})$ given by (5.5.12) so as to produce a desired rapidity ρ_n or velocity u_n (5.5.13) at the n^{th} trajectory point $x_n=x(t_n)$.

Another scheme has just two fixed lasers on the left at $x=a_{\rightarrow}$ and $x=a_{\leftarrow}$ on the right, respectively, but requires each to "chirp" its frequency long *before* $t=0$. As in Fig. 5.5.4(b), the atom accelerates left-to-right if the left-hand laser up-chirps (red to blue) while the right-hand laser down-chirps, and vice-versa.

Invariant atomic proper time τ may be used in time derivatives instead of lab coordinate time t.

$$p\equiv\frac{dx}{d\tau}=\frac{dx}{dt}\frac{dt}{d\tau}=c\tanh\rho\cosh\rho=c\sinh\rho \quad (5.5.15a) \qquad \frac{dt}{d\tau}=\frac{1}{\sqrt{1-u^2/c^2}}=\cosh\rho \quad (5.5.15b)$$

We use (5.4.19) or definition (5.1.4) of proper time τ. Relations for laser scheduling of (5.5.14) follow.

$$\frac{d(x+ct)}{d\tau}=c(\cosh\rho+\sinh\rho)=ce^{\rho} \quad (5.5.15c) \qquad \frac{d(x-ct)}{d\tau}=c(\cosh\rho-\sinh\rho)=ce^{-\rho} \quad (5.5.15d)$$

$$x+ct=c\int d\tau\, e^{\rho} \quad (5.5.15e) \qquad x-ct=c\int d\tau\, e^{-\rho} \quad (5.5.15f)$$

$$x=c\int\sinh\rho\, d\tau \quad (5.5.15g) \qquad ct=c\int\cosh\rho\, d\tau \quad (5.5.15h)$$

This gives the trajectory $x(t)$ given a "local schedule" of rapidity $\rho(\tau)$ as a function of proper time.

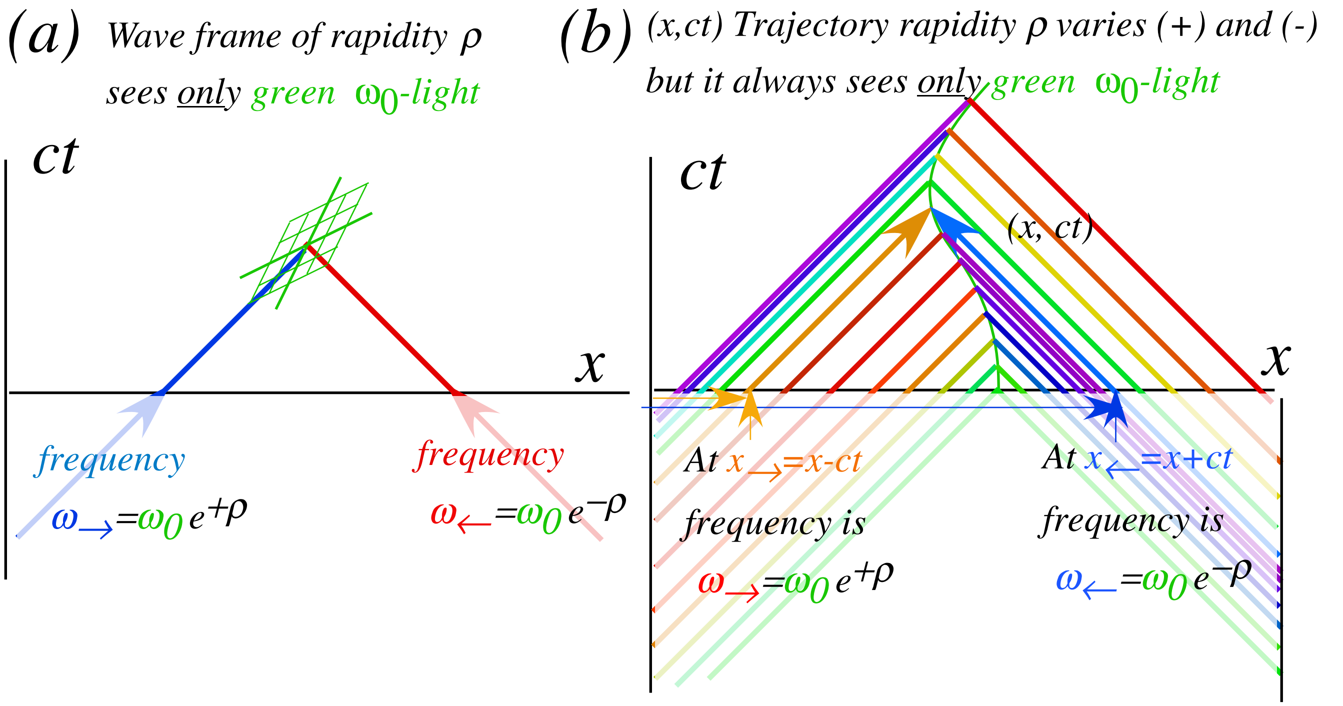

Fig. 5.5.4 Accelerating frames by laser Doppler. (a) Single laser pair. (b) Laser pairs "paint" trajectory.

The simplest choices for a rapidity schedule are *case(a)* $\rho=\rho_0$ (constant) or *case(b)* $\rho=g\,\tau/c$ (linear). The constant *case(a)* gives a straight line trajectory and the usual Minkowski grid in Fig. 5.5.5(a) below. The linear *case(b)* gives the hyperbolic trajectory in Fig. 5.5.5(b). This agrees with (5.5.8) in Sec. (a).

$$x = c\int \sinh\rho_0 \; d\tau = c\tau\sinh\rho_0 \qquad (5.5.16a) \qquad\qquad x = c\int \sinh\left(\frac{g\tau}{c}\right) d\tau = \frac{c^2}{g}\cosh\left(\frac{g\tau}{c}\right) \qquad (5.5.16b)$$

$$ct = c\int \cosh\rho_0 \; d\tau = c\tau\cosh\rho_0 \qquad (5.5.17a) \qquad\qquad ct = c\int \cosh\left(\frac{g\tau}{c}\right) d\tau = \frac{c^2}{g}\sinh\left(\frac{g\tau}{c}\right) \qquad (5.5.17b)$$

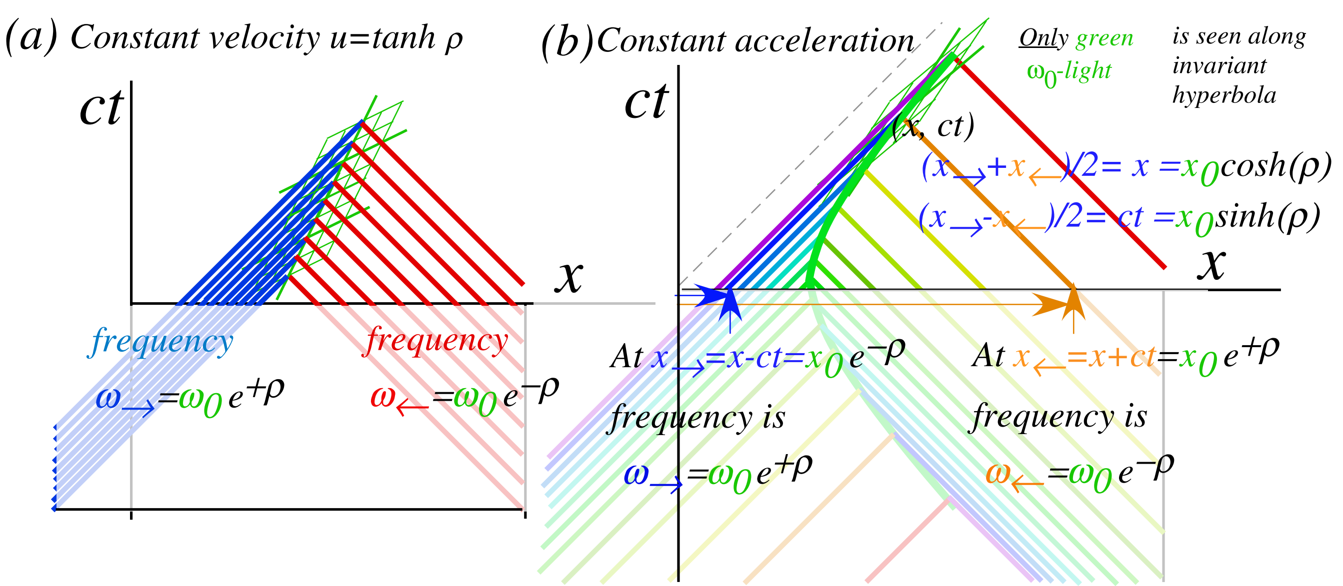

Fig. 5.5.5 Wave paths. (b) Constant velocity and frequency (b) Constant acceleration by exponential chirp.

Describing accelerated frames by CW laser waves leads to a simpler derivation of a trajectory (5.5.16b) than the classical approach that gave (5.5.8) and does so without introducing a massive particle. However, mass-like invariants are hiding in this CW derivation as are the PW rays shown in Fig. 5.5.3.

If the color-varying CW laser beams come from far right and left hand sources as in Fig. 5.5.5(b) they cover the spacetime region as shown in Fig. 5.5.6(a) and generate a curved spacetime manifold of nested constant-acceleration paths as shown in Fig. 5.5.6(b). Among these hyperbolas are the paths of the ship and saucer trailer of Fig. 5.5.3. Fig. 5.5.6(b) is a whole manifold of Newton's invariants.

Atoms (or ships), following the hyperbolic trajectory in Fig. 5.5.5(b), see an invariant green frequency ω'_0 as they run head-on into an ever more red laser beams and run away from ever more blue ones. Each hyperbolic path of Fig. 5.5.6(b) experiences some *single* invariant color. As shown in Fig. 5.5.6(a), each path crosses a variety of red and blue beams but Doppler shifts them all to one fixed hue.

Each path's invariant color is that of whichever laser beams cross the x-axis where that path starts out at $t=0$. The saucer-trailer starts out at the intersection of two blue-green beams. Thereafter, the saucer-trailer sees only the same blue-green color during its trip up its hyperbola just as the ship always lives in the same green light it saw starting further out along the lab x-axis.

Besides invariant frequency $\omega_0=\omega'_0$ for a path starting at lab position x_0 when $t=0$, each path has other constants of motion such as *radius* $x_0=\ell=x'_0$ to origin. The distance between any two paths such as ship-to-saucer-trailer separation $\ell_{-1}-\ell_0$ is *rigid*. By (5.5.12), (5.5.17b) and (5.5.16b), products of frequency and radius *are equal to each other for all paths* in Fig. 5.5.6. The constant P sets the plot scale.

$$\ell_{-2}\,\omega_{-2}=\ell_{-1}\,\omega_{-1}=\ell_0\,\omega_0=\ell_1\,\omega_1=\ell_2\,\omega_2= \;=P \quad (5.5.18a) \qquad c^2/g_n=\ell_n=\sqrt{x_n^2-c^2t_n^2} \quad (5.5.18b)$$

Invariant frequency $\omega=P/\ell$ at radius ℓ must go to zero at large ℓ and approach infinity near origin. Origin in Fig. 5.5.6 is a remarkable singularity, as we'll see. All accelerated frames have singularities. Perhaps, we are a little *too* familiar with the singularity of a rotating frame: its *center of rotation*.

The center of spacetime "rotation" in Fig. 5.5.6 is certainly less familiar. It's an *event horizon*. You cannot communicate with the ship, saucer-trailer, or any of their friends after the $45°$ line through origin (or to the left of it). As long as they continue to accelerate they will outrun your messages! (However, their frame's continued acceleration depends on your left lab laser chirping out an infinite amount of energy *before* the $t=0$ singularity and on having an infinite number of low-ν lasers off to the right.)

Other physical constants of motion for Fig. 5.5.6 are related to the invariant frequency and radius ℓ of each path and have singular behavior, too. One is acceleration g, which by (5.5.16b) blows up at $\ell=0$.

$$g=c^2/\ell=\omega\, c^2/P \qquad (5.5.19)$$

An important invariant is the rate for "aging" or proper time evolution. (This was called proper frequency μ in (5.1.5).) Judging a μ or ω requires *frequency standards* such as an Argon atom that rings for green frequency ω_0 or a Krypton atom that rings for a (very) blue frequency $\omega_{-2}=2\omega_0$. Suppose the ship uses Argon to measure time by the green light it's seeing while a saucer-trailer at $x_{-2}=x_0/2$ uses Krypton to measure time by its local blue-light standard. Then on each *NOW* line between them in Fig. 5.5.6, the ship has counted the same number of green-standard ticks as the trailer has counted blue-standard ticks.

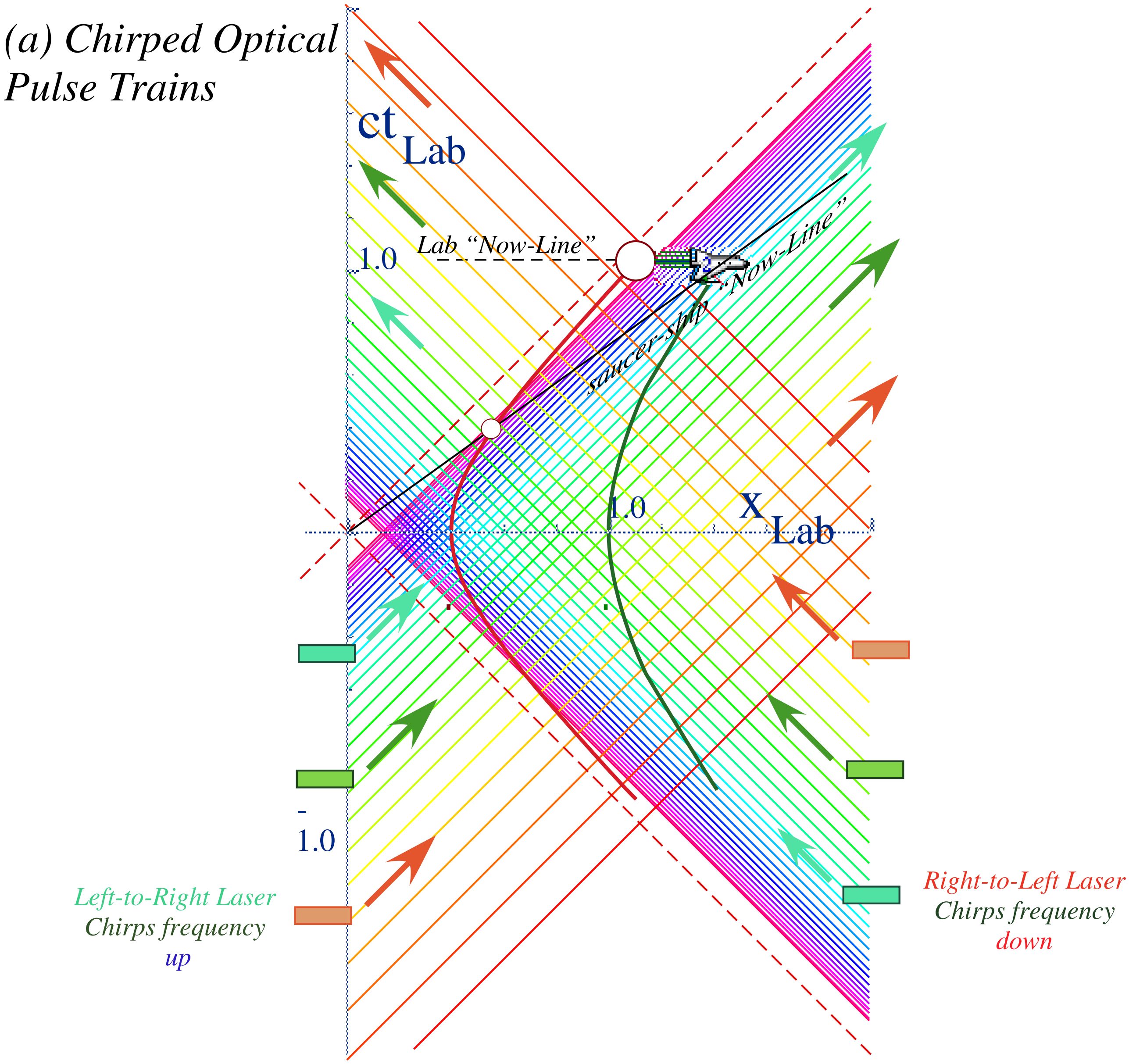

Fig. 5.5.6 Constant-acceleration spacetime (a) Pair(s) of lasers make grid for accelerating paths.

Fig. 5.5.6(b) shows that idea of *NOW* does not imply equal *proper time*. The ship's *NOW* of *10* green ticks includes a trailer who has also seen 10 ticks, just as we noticed in the earlier Fig. 5.5.3 based on pulse waves or in Fig. 5.5.6(a). But that trailer uses blue ticks, and two blue ticks equals one green tick. So the trailer has only "lived" 5 green ticks while the ship has "lived" 20 blue ticks yet they're both on the same *NOW* line. Some *NOW!* Clearly a single frequency standard is needed to properly gauge proper time.

A ship and trailer bouncing the same light wave in a rigid tube would notice it is blue shifted at the bottom but red-shifted (green here) at the high end. A similar effect is present in the equivalent constant gravitational field and is called the *gravitational red (blue) shift*. As long as the constant acceleration g of this system persists, its occupants see a fixed blue-to-red "rainbow" color distribution up an optical tube as in Fig. 5.5.6(b), yet, the entire tube is always (*NOW)* going the same speed relative to the lab!

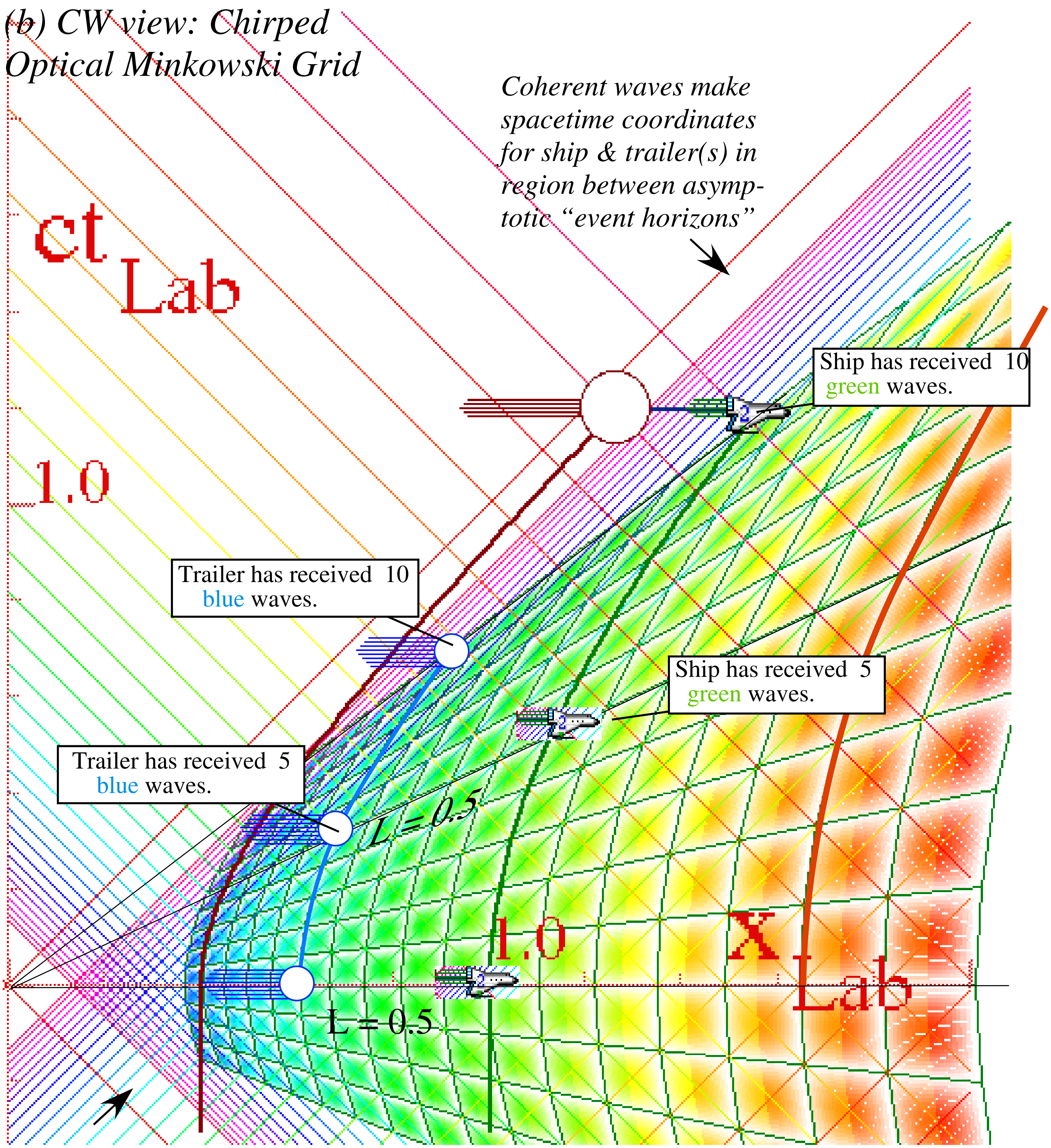

Fig. 5.5.6 Contd. (b) Interfering pair(s) of CW lasers make curved Minkowski grid for accelerating paths.

Fig. 5.5.6(b) shows hyperbolic-polar coordinates (ℓ,ρ) where (5.5.16b) gives rapidity "angle" $\rho = g\tau/c$ to accompany the hyperbolic "radius" ℓ. So proper time τ is a hyperbolic "arc-length" as Fig. 5.5.6 suggests.

$$\rho = \frac{g\,\tau}{c} = \frac{\omega\, c\tau}{P} = \frac{c\tau}{\ell} \quad (5.5.20a) \qquad\qquad c\tau = \ell\,\rho \quad (5.5.20b)$$

Per-spacetime diamond geometry

It is remarkable that proper time τ-evolution or "aging" is in direct proportion to one's hyperbolic radius or distance "up-field" from the singular origin. Spacetime is mirrored in per-spacetime as described in Sec. 4.2. Spacetime "particle" path vectors **X**=*(x,ct)* match per-spacetime-vectors **K**=*(ck,ω)* that define local energy-momentum grids according to the baseball diamond wave geometry of Fig. 5.1.1.

$$X_{particle}: \begin{array}{l} x_p = \ell \cosh\rho \\ ct_p = \ell \sinh\rho \end{array} \quad (5.5.21a) \qquad K_{group}: \begin{array}{l} \omega_g = \omega_0 \sinh\rho \\ ck_g = \omega_0 \cosh\rho \end{array} \quad (5.5.21b) \qquad K_{phase}: \begin{array}{l} \omega_p = \omega_0 \cosh\rho \\ ck_p = \omega_0 \sinh\rho \end{array} \quad (5.5.21c)$$

This geometry is sketched in Fig. 5.5.7 for two different speeds or rapidity values *u/c=1/5* and *3/5* using laser ray lines excerpted from Fig. 5.5.6. The geometric growth of wavelength for increasing radius in spacetime is shown by a series of diamonds made by echoing rays off each *NOW* line of fixed rapidity. A similar diagram in per-spacetime would mirror a growth in wave*vector* or frequency, that is, the inverse of Fig. 5.5.7 as in (5.5.18). Having each echo give a constant δλ/δℓ yields an exponential chirp (5.5.12).

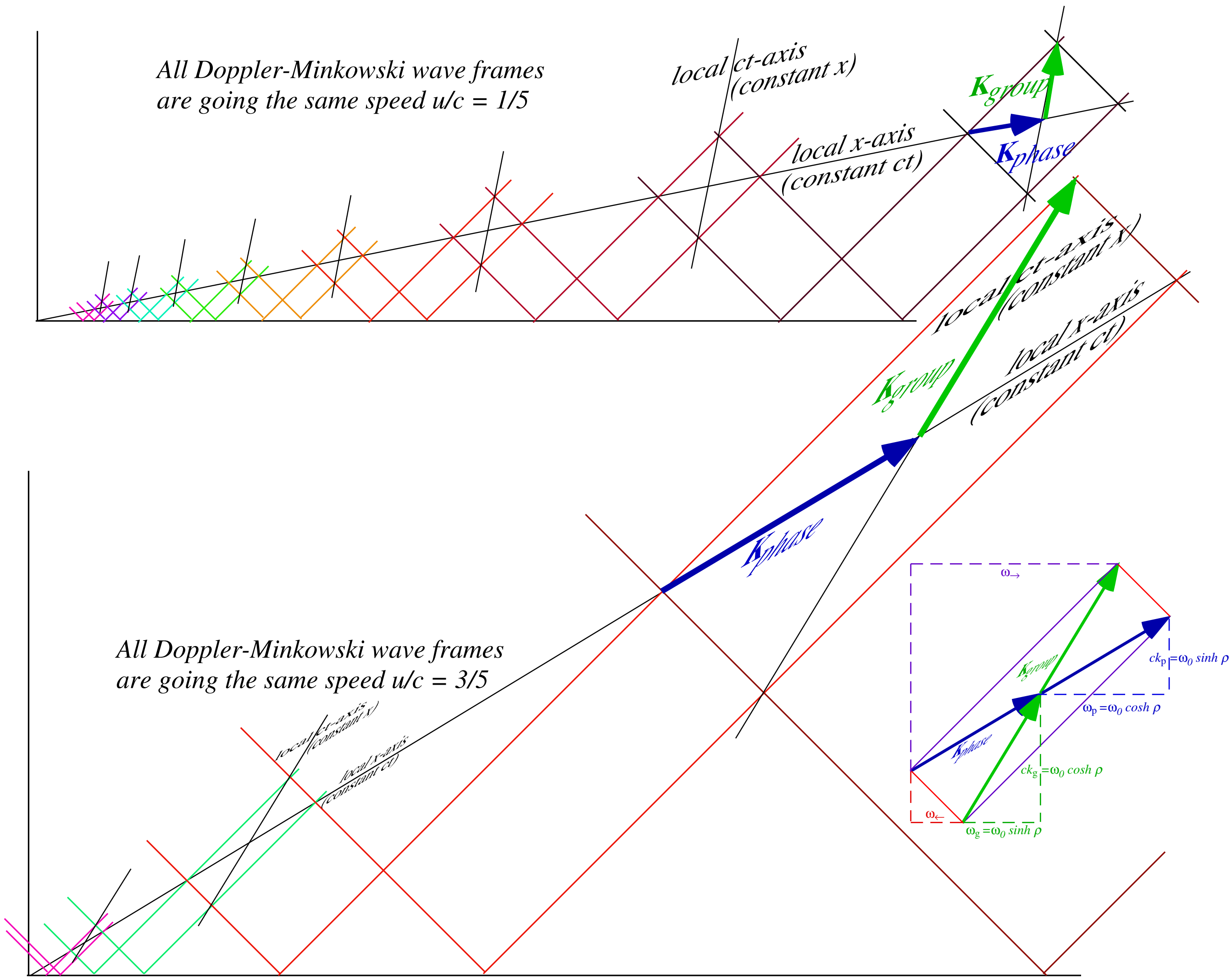

Fig. 5.5.7 Geometric growth of PW ray spacing or CW wavelength or wave vectors.

Acceleration by Compton scattering

The basic parameters of an elementary Compton scattering process in Fig. 5.5.8(a) are sketched in a right hand inset. The *IN* parameters are a fixed mass M_0, or wave proper frequency $\mu_0 = M_0c^2/\hbar$ with zero rapidity $(\rho_0=0)$ and a colliding photon frequency ω_1 or energy $E_\gamma(initial)=\hbar\omega_1$.The *OUT* parameters are a Compton scattered photon frequency ω_2 or energy $E_2(final)=\hbar\omega_2$ and the final velocity u_2 of mass M_0 or else its final rapidity ρ_2 by the usual definition $u_2=\tanh \rho_2$. Geometry helps relate the parameters.

The small μ_0-diamond is stretched by the *IN* photon ω_1 vector $\mathbf{K}_{\rightarrow}(\omega_1)_{intial}$ going from the 2nd-base point μ_0 to point I on the 1st-2nd baseline of a larger μ_2-diamond. By emitting an *OUT* photon with vector $\mathbf{K}_{\leftarrow}(\omega_2)_{final}$ going from point F to point I, the mass returns to its μ_0-hyperbola. But it's boosted to a final rapidity ρ_2, as its $\mu_0/\sqrt{2}$-by-$\mu_0/\sqrt{2}$ diamond shifts to the narrow $\mu_0 exp(\rho_2)/\sqrt{2}$-by-$\mu_0 exp(-\rho_2)/\sqrt{2}$ rectangle of the same area. Its length $\mu_0 exp(\rho_2)/\sqrt{2}$ equals $\mu_2/\sqrt{2}$ in Fig. 5.5.8(a).

$$\mu_2 = \mu_0\, exp(+\rho_2) \quad , \qquad \text{or,} \qquad \rho_2 = ln\,(\mu_2 / \mu_0) \tag{5.5.22}$$

The diagonal length $\sqrt{2}\omega_1$ of the *IN* photon vector $\mathbf{K}_{\rightarrow}(\omega_1)_{intial}$ is the difference between the μ_2-diamond baseline $\mu_2/\sqrt{2}$ (or length $\mu_0 exp(+\rho_2)/\sqrt{2}$ of the rectangle) and $\mu_0/\sqrt{2}$. This gives ω_1 in terms of μ_0 and ρ_2.

$$2\omega_1 = \mu_2 - \mu_0 = \mu_0 exp(+\rho_2) - \mu_0 \tag{5.5.23}$$

The diagonal length $\sqrt{2}\omega_2$ of the *OUT* photon vector $\mathbf{K}_{\leftarrow}(\omega_2)_{final}$ is the difference between the μ_0-diamond baseline $\mu_0/\sqrt{2}$ and the width $\mu_0 exp(-\rho_2)/\sqrt{2}$ of the rectangle. This gives ω_2 in terms of μ_0 and ρ_2.

$$2\omega_2 = \mu_0 - \mu_0 exp(-\rho_2) = 2\omega_1\, exp(-\rho_2) \tag{5.5.24}$$

Inverting (5.5.24) and taking $exp(+\rho_2)$ with $\mu_0 = M_0c^2/\hbar$ in (5.5.22) gives a famous Compton relation.

$$1/\omega_2 = 1/\omega_1\, exp(+\rho_2) \;= 1/\omega_1\, (\mu_2 / \mu_0) = 1/\omega_1\, ((2\omega_1 + \mu_0) / \mu_0) = 2/\mu_0 + 1/\omega_1 \tag{5.5.25a}$$

$$\lambda_2 = 2\pi c/\omega_2 = 4\pi c/\mu_0 + \lambda_1 = 2\lambda_{Compton} + \lambda_1 \,, \quad \text{where: } \lambda_{Compton} = 2\pi\hbar/M_0c = h/M_0c \tag{5.5.25b}$$

Photon wavelength jumps by twice a *Compton wavelength h/Mc* in back-scattering from mass M. That represents a momentum "kick" given by the photon to mass M. A photon thus acts "like a particle."

Suppose the *IN* ω_1 photon excites a state of higher proper energy $\hbar\mu_1 = M_1c^2$. To do this, the μ_0 particle must have an existent μ_1–excited state and ω_1 must be tuned to satisfy its recoil equations.

$$\mu_2 = \mu_1\, exp(+\rho_1) = \mu_0\, exp(+\rho_2) \tag{5.5.26a}$$

$$\mu_1 = \mu_0\, exp(+\rho_1) \tag{5.5.26b}$$

$$\omega_1 = \mu_1 \sinh(\rho_1) \tag{5.5.26c}$$

The $\mathbf{K}_{\rightarrow}(\omega_1)_{intial}$ jump goes from point μ_0 to point I and "sticks" at intermediate recoil ρ_1 without emitting ω_2 and recoiling further to $\rho_2 = 2\rho_1$. Photo *absorption* or "gulp" of photon ω_1 is the reverse of photo *emission* "patooey" discussed earlier. Here, the required *IN* frequency ω_1 is *greater* than the gap $\Delta=\mu_1-\mu_0$ whereas the *OUT* frequency ω_1 in (5.2.22) is *less* than Δ as is ω_2 in (5.2.24) above. However, the recoil $\rho_1=\rho_2/2$ rapidity of the *IN* process equals that of the *OUT*. Each is *half* of the Compton recoil ρ_2 by (5.5.26).

Fig. 5.5.8(b) shows back-to-back Compton processes with the ρ_2–moving particle hit by a second photon of lab frequency $\omega_3 = \omega_1\, exp(+\rho_2)$ so Doppler-blue-shifted to appear as a ω_1–photon. The second scattering yields another ω_2 photon, but it appears as a red-shifted frequency $\omega_4 = \omega_2\, exp(-\rho_2)$ in the lab. Continued bombardment by geometric progression of up-chirped light gives a quantum version of constant acceleration pictured in Fig. 5.5.7 wherein the particle "feels" the same Compton kick from each chirp.

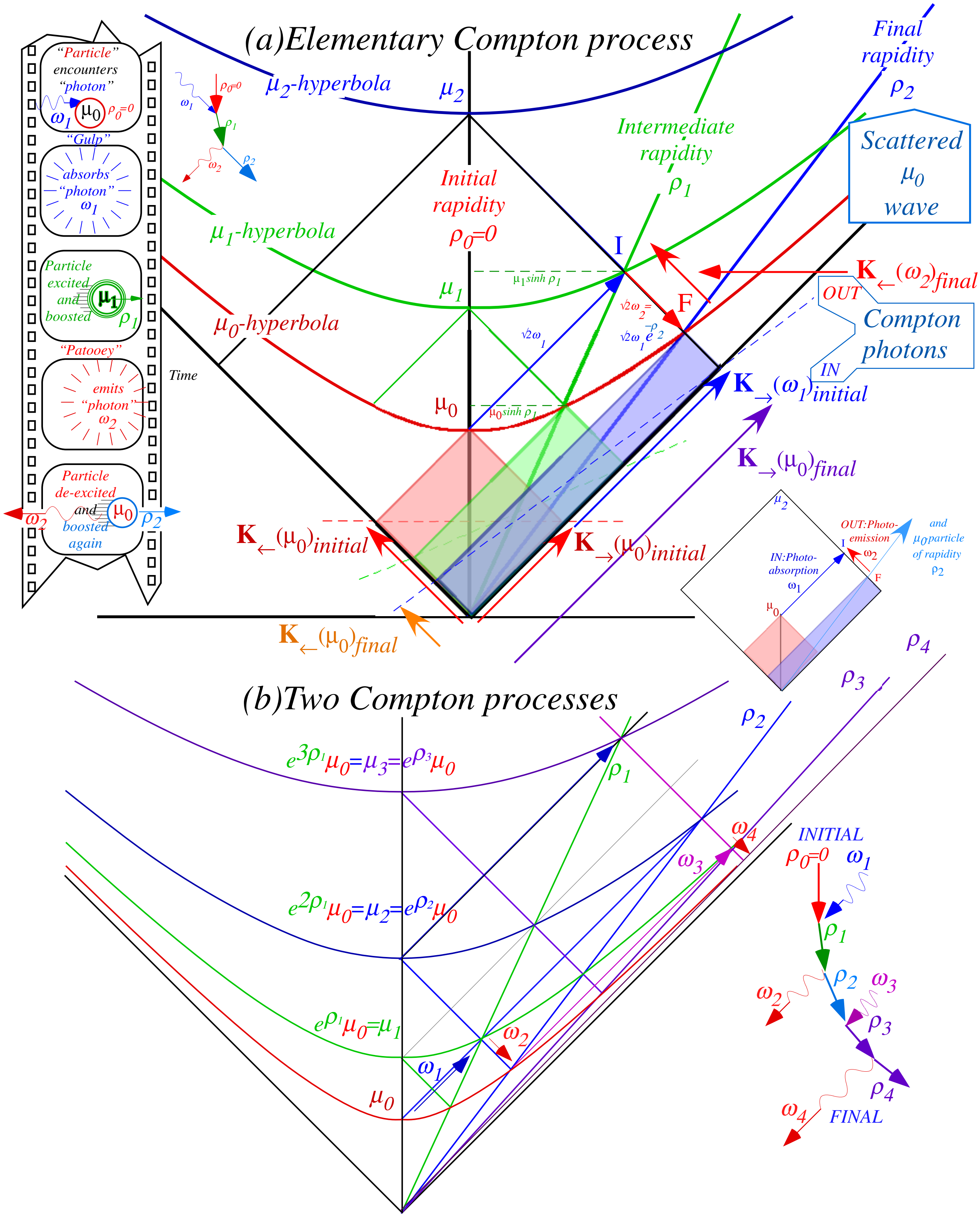

Fig. 5.5.8 Compton scattering (a) Elementary geometry. (a) Geometry of quantum acceleration

5.6 Bohr-Orbitals and Higher Energy Physics

Most of atomic, molecular, and optical physics is concerned with energy on the order of a few *electron Volts* or *eV*. One *eV* is *e*-Joules or *1.6E-19 J*, the energy acquired by an electron falling through one *Volt* of electric potential. Here we introduce atomic Bohr orbitals and some high(er) energy physics.

(a) Dirac's anti-matter

The square root in energy dispersion $E=\sqrt{[(cp)^2+(mc^2)^2]}$ should have ±signs. At least P.A.M. Dirac thought so. He is credited with recognizing the negative energy terms as the representation of *anti-matter* that follows an up-side-down hyperbolic dispersion relation. Examples involving the photon and electron are shown in Fig. 5.6.1 below. Dirac made the extraordinary suggestion that the empty space vacuum is actually a sea of electrons (and other Fermions) occupying the negative energy states in a kind of cosmic valence band. Only when we come along with energy of a little over *1MeV* do we actually see a pair creation of an electron popping out of the sea and leaving behind a "hole" or *positron*, the anti-electron. (Actually, two photons of *0.511MeV* each are needed because of symmetry and conservation requirements.)

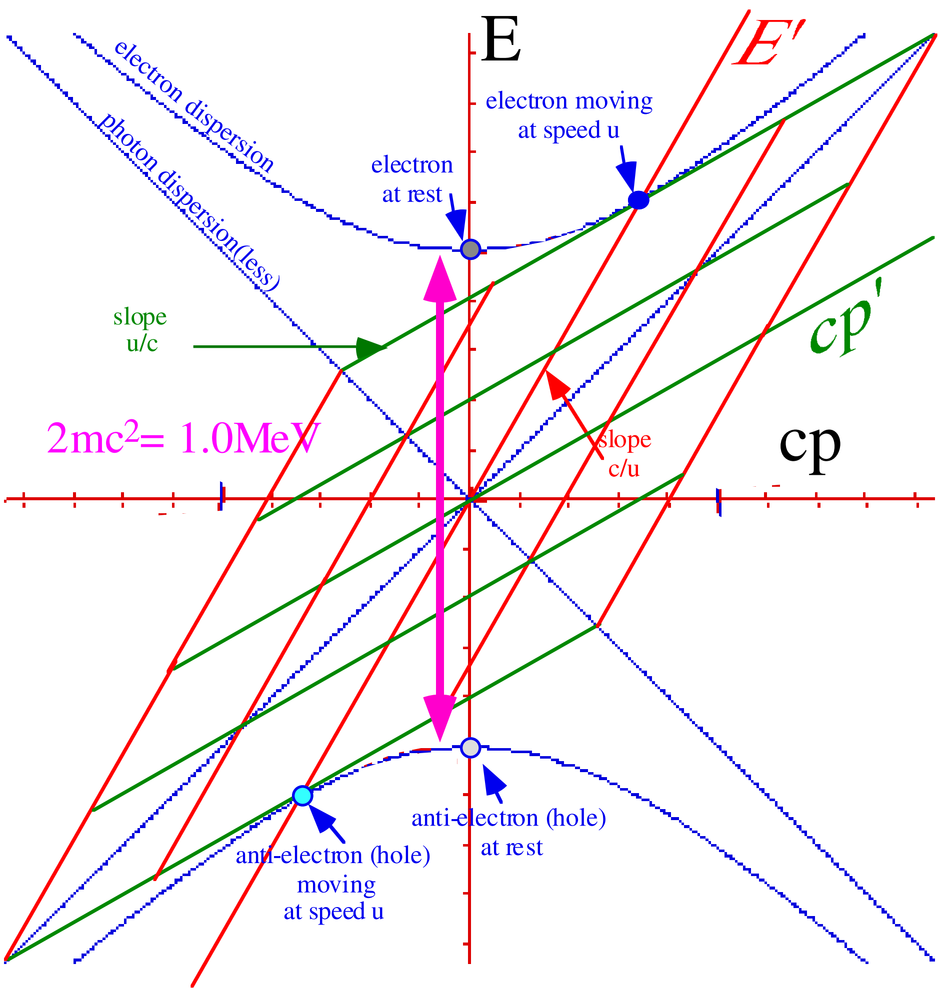

Fig.5.6.1 Relativistic dispersion relations for a photon and an electron and their anti-particles

Dirac's relativistic electron theory is wonderful but mysterious one.As we will see (much later) it shows that the electron is made of something zipping around in its "belly" with an average speed of c. If we identify this "ticking" frequency (It's called "Zwitterbegung" which sounds impressive until hearing the German translation for "trembling motion.") with a beat frequency equal to the band-gap difference $2mc^2$ between the positive and negative energy bands we get *1.5 thousand ExaHertz*.

$$\omega_{\text{zwitterbegung}} = 2\mu_\varepsilon = 2mc^2/\hbar = 1.56E21(radian)Hz \qquad (5.6.1)$$

An electron has a pretty fast "ticker" and its "heartbeat" is observable!

(b) Numerology: Bohr electron radii and Compton wavelength

Since the advent of the Bohr model of the hydrogen atom, the idea of particles being composites of other particles zipping around has been used a lot in the development of quantum theory. Briefly, the Bohr model imagined an electron orbiting in a circle of radius r so that the centrifugal force just balanced the Coulomb attraction to the opposite charged proton.

$$\frac{mv^2}{r} = \frac{e^2}{4\pi\varepsilon_0 r^2} \qquad (5.6.2a)$$

This combined with the Bohr hypothesis that orbital momentum ℓ was a multiple N of $\hbar$ or

$$\ell = m\,v\,r = N\,\hbar \qquad (N = 1, 2,...) \qquad (5.6.2b)$$

gives the *atomic Bohr radius a_0*

$$r = \frac{4\pi\varepsilon_0\hbar^2}{me^2}N^2\left(= r_{Bohr} = 5.28E-11\ m. \ = 0.528\ \ddot{A} \text{ for } N = 1\right) \qquad (5.6.3a)$$

and quasi-relativistic electron speed of

$$\frac{v}{c} = \frac{\ell}{mrc} = \frac{1}{N}\frac{e^2}{4\pi\varepsilon_0\hbar c}\ \left(= 7.31\text{E-}3 = \frac{1}{137.} \text{ for } N = 1\right) \qquad (5.6.3b)$$

The ratio $\alpha = e^2/(4\pi\varepsilon_0\hbar c) = 1/137.036$ is called the *fine-structure constant* α. It shows up a lot in atomic physics. Dirac was concerned with working out the relativistic corrections to the energy of atoms. While a hydrogen electron goes less than 1% of the speed of light, a heavily charged atomic ion would increase (5.6.3b) in proportion to its charge and make relativistic effects large.

If we imagine that whatever Dirac said was going c inside an electron is going around in a circle of radius r at speed c and "ticking" or orbiting at the zwitterbegung frequency then

$$\omega_{\text{zwitterbegung}}\, r = c \qquad (5.6.4a)$$

or

$$r_{Dirac} = c\,/\,\omega_{\text{zwitterbegung}} = \hbar\,/2mc = 1.93\ E\ \text{-}13\ m. \qquad (5.6.4b)$$

Now, it needs to be said that most of the preceding calculations are what is known as *numerology*; simple estimation exercises done to get a rough order of magnitude for the size of things. Occasionally, as in the case of (5.6.3), these rough estimates hit right on, but one shouldn't expect such luck. There is no immediately obvious reason for us to expect that Dirac's "thing" is oscillating on a circle, and there was little reason for Bohr to expect the right answer by just considering circular orbits. Indeed, the lowest atomic H-orbital is a "diving" orbit of maximal unit eccentricity and zero angular momentum.

But still we ask, "How big would it be if it were a circle?" This gives some idea about the relative size of an electron in these two situations. The Dirac answer is about one-hundredth that of the Bohr radius (5.6.3a), but about one hundred times that of a nucleus (Nuclear radii are typically a few Fermi: *1 Fm = 1 Fermi = 1.0E-15 m. = 1 femto meter = 1 fm*; this is one case where a unit abbreviation is correct in lower and upper case!) Being more precise, and this may be a silly numerological exercise, it is interesting to note that the ratio of the Dirac radius to the Bohr radius is

$$\frac{r_{Dirac}}{r_{Bohr}} = \frac{\hbar \;/\; 2mc}{4\pi\varepsilon_0 \hbar^2 \;/\; me^2} = \frac{1}{2}\cdot\frac{e^2}{4\pi\varepsilon_0 \hbar c} = \frac{1}{2}\cdot\frac{1}{137.} = \frac{\alpha}{2} \qquad (5.6.5)$$

This is exactly one-half the fine-structure constant $\alpha=1/137$.

The preceding quantum numerology can be compared to some older classical numerology. The *classical radius of the electron* is defined as the radius an electron would have to have in order to have its electrostatic energy $e^2/(4\pi e_0\, r_{classical})$ equal to its rest energy mc^2. (Remember, this is numerology, not physics. Electrostatic energy depends sensitively on charge distribution. Nevertheless, the classical radius appears more legitimately in the theory of Rayleigh scattering.) Here is the classical radius.

$$e^2/(4\pi e_0\, r_{classical}) = mc^2 \quad \text{or} \quad r_{classical} = e^2/(4\pi e_0\, mc^2) = 2.8\text{E-}15 \text{ m.} \qquad (5.6.6)$$

Now this is about the size of a nucleus and about a hundred times smaller than the "quantum" electron Dirac-radius estimated in (5.6.4b). In fact it is exactly another fine-structure ratio to r_{Bohr}.

$$\frac{r_{Classical}}{r_{Bohr}} = \frac{e^2 \;/\; 4\pi\varepsilon_0 mc^2}{4\pi\varepsilon_0 \hbar^2 \;/\; me^2} = \left(\frac{e^2}{4\pi\varepsilon_0 \hbar c}\right)^2 = \left(\frac{1}{137.}\right)^2 \qquad (5.6.7a)$$

It happens that the "quantum electron diameter", that is ($2r_{Dirac}$), relates to a legitimate experimental constant; $2r_{Dirac}$ happens to be the *Compton (angular) wavelength* ($\lambdabar_{Compton}$)

$$2r_{Dirac} = \lambdabar_{\text{Compton}} = \hbar / mc = 3.86\, E\text{-}13\ m. \qquad (5.6.7b)$$

The "straight" *Compton wavelength* $\lambda_{Compton}$

$$2\pi \cdot 2r_{Dirac} = \lambda_{\text{Compton}} = h / mc = 2.43\, E\text{-}12\ m. \qquad (5.6.7c)$$

is the wave length of the γ-radiation needed to excite pair-creation of electron and anti-electron from the vacuum. (Recall we mentioned that this is a two-photon process.) The quantity $2\lambda_{\text{Compton}}$ is the change in wavelength that a photon suffers in a head-on collision with an electron. λ_{Compton} is less than 1% of a typical X-ray wavelength but it is 100% of the wavelength of the photons needed to create an electron-positron pair.

As a final numerological exercise, we derive the angular momentum $\ell = m\, v\, r$ of the fictitious "zwitterbegung" orbit inside the electron. With $v=c$ and $r = r_{Dirac}$ the following is obtained.

$$\ell = m\, c\ r_{Dirac} = m\, c\, \hbar / 2mc$$
$$= \hbar / 2$$

We did mention that numerology occasionally gives the correct answer, in this case, the spin angular momentum of an electron! We won't give this equation a number since it is not (yet) legitimate physics. As we said, numerology is just that, estimating some numbers and their orders of magnitude, and that's all we should expect at first.

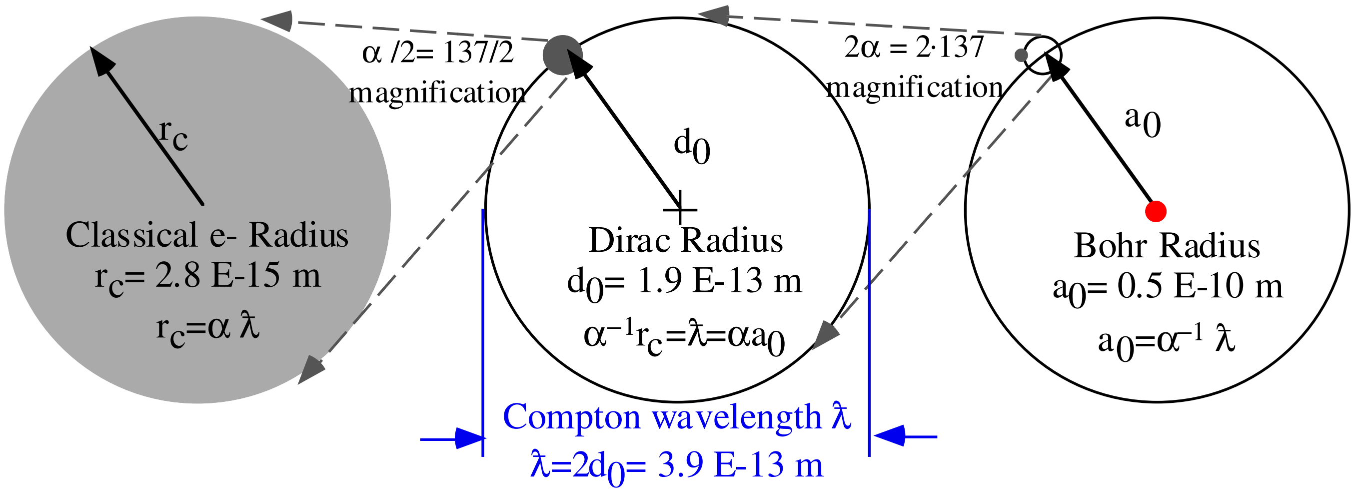

Fig.5.6.2 Various electron radii and their relative sizes related by fine-structure constant α *= 1/137.*

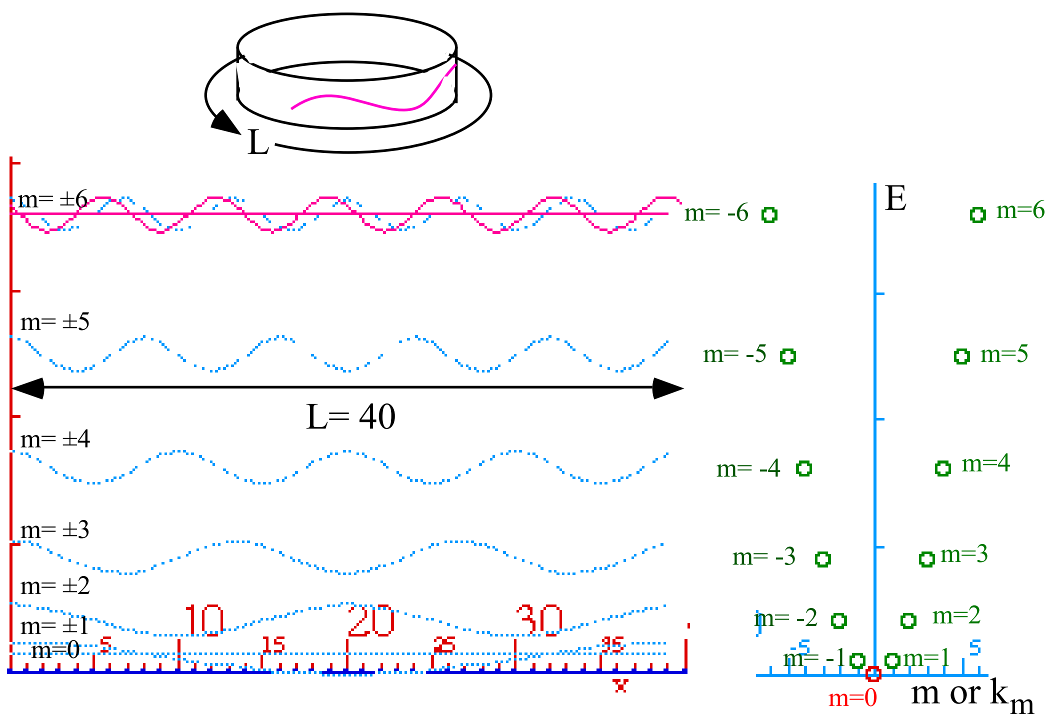

Fig. 5.6.3 Sketches of Bohr waves confined to 1-D L-interval and quantum energies (for m=0 to 6).

(c) Bohr matter-wave PW revivals: When μ-waves party!

Bohr's simplest model is called the *quantum rotor* and consists of a μ-wave wrapped around a ring of fixed radius *r*. The Bohr atomic model contains rings having Bohr radii r_N (5.6.3) for all radial quantum numbers $N=1,2,3\ldots\infty$. Here we will study just one such ring with large *N* and circumference $L=L_N= 2\pi r_N$ as sketched at the top of Fig. 5.6.3. As sketched in the lower part of Fig. 3.6.3, the waves on this ring must have an integral number *m* of wavelengths within its circumference *L*.

$$m\,\lambda_m = L \quad \text{or:} \quad k_m = 2\pi/\lambda_m = m\,2\pi/L = m/r \;(m=0,\ 1,\ \pm 2,\ \pm 3,\ldots) \tag{5.6.8}$$

This *m* is called the *magnetic* or *angular momentum quantum number* and quantizes the amount of *angular momentum* circulating the ring. Quantization is necessary to have phase matching at each 2π turn.

As we will see, even this simple quantum rotor model is capable of extraordinary wave dynamics. Wrapping waves onto a ring, along with their spacetime or per-spacetime, introduces some big problems, only a few of which we can deal with here. While this ring wave is on a one-dimensional path, it is really a wave in two or three-dimensional space and time, the subject of the following Chapter 6.

Bohr-Schrodinger dispersion and group velocity

Here we use the Bohr-Schrodinger approximation to the dispersion function in (5.2.8).

$$E_m = \hbar\omega_m = \frac{p_m^2}{2M} = \frac{\hbar^2 k_m^2}{2M} \tag{5.6.9}$$

The quantized k_m values in (5.6.8) gives quantized energy or frequency values plotted in Fig. 5.6.3.

$$\omega_m = \frac{\hbar k_m^2}{2M} = \left(\frac{\hbar(2\pi)^2}{2ML^2}\right)m^2 = \left(\frac{\hbar}{2Mr^2}\right)m^2 \equiv \omega_1 m^2 \tag{5.6.10a}$$

From this dispersion we get group velocity values by (4.7.8), one for each line between quantum points in Fig. 5.6.4. With $L=2\pi\,r$ and $k_m=m/r$ it gives $V_g(m,n)$ as multiples of *fundamental velocity* $V_1=\omega_1 r$.

$$V_{group}(m,n) = \frac{\omega_m-\omega_n}{k_m-k_n} = \frac{h}{2Mr}\left(\frac{m^2-n^2}{m-n}\right) = \omega_1 r(m+n) \tag{5.6.10b}$$

V_1 is the lowest quantum orbit speed and ω_1 is the *fundamental transition* or lowest *beat frequency*.

$$V_1 = \omega_1 r = \left(\frac{h}{2Mr}\right) \tag{5.6.10c}$$

So, if a Bohr quantum rotor has, say, range of *m*-wave states excited from $m=0$ to $m=\pm 4$, then the possible velocity values given by (5.6.10b) range from *0* to *but not including* $\pm 8V_1$. Because the $m=4$ state cannot interfere with itself, the maximum slope in Fig. 5.6.4 is 7 V_1, just shy of tangent-slope derivative $d\omega/dk= 8$ at $m=4$. This shows why the conventional $d\omega/dk$–formula for group velocity should not be used in most quantum mechanical applications.

In the wave business, it's generally considered "impolite" to just cut-off the wave *m*-distribution at, say, $m=\pm 4$ as imagined in Fig. 5.6.4. Doing so leads unnecessary complications of "ringing" shown in Fig. 5.3.2. Better is a tapered distribution such as a Gaussian (5.3.6) that yields unwrinkled waves like Fig. 5.3.3. This will be applied to the Bohr waves below.

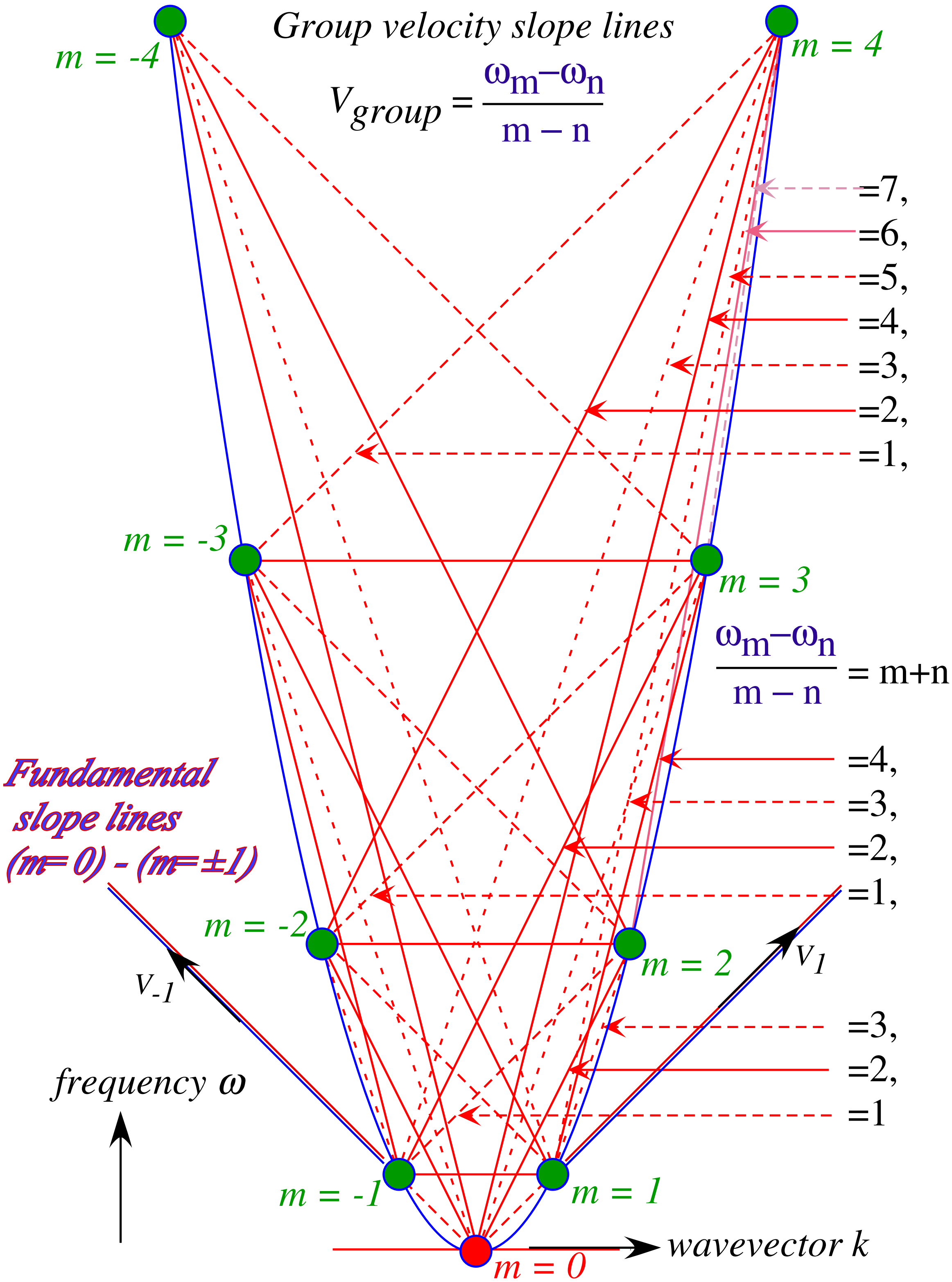

Fig. 5.6.4 Bohr per-spacetime plot and group velocity lines for combinations of m=0 to m=±4.

Bohr μ-wave quantum speed limits

Instead of $d\omega/dk$, one needs to consider a *lattice* of per-spacetime **K**-vectors such as Fig. 5.6.4 or an *array* $V_g(m,n)$ of velocity values given in (5.6.10b). Here, the $V_g(m,n)$ array given by (5.6.10d) is a simple one.

$$V_{group}(m,n)_{\leq 4} = \begin{array}{cc|ccccccccc} E_m & m/n & \cdots & -4 & -3 & -2 & -1 & 0 & 1 & 2 & 3 & 4 \\ \hline & \cdots & & & & & & & & & \\ 16 & -4 & & -8 & -7 & -6 & -5 & -4 & -3 & -2 & -1 & 0 \\ 9 & -3 & & -7 & -6 & -5 & -4 & -3 & -2 & -1 & 0 & 1 \\ 4 & -2 & & -6 & -5 & -4 & -3 & -2 & -1 & 0 & 1 & 2 \\ 1 & -1 & & -5 & -4 & -3 & -2 & -1 & 0 & 1 & 2 & 3 \\ 0 & 0 & & -4 & -3 & -2 & -1 & 0 & 1 & 2 & 3 & 4 \\ 1 & 1 & & -3 & -2 & -1 & 0 & 1 & 2 & 3 & 4 & 5 \\ 4 & 2 & & -2 & -1 & 0 & 1 & 2 & 3 & 4 & 5 & 6 \\ 9 & 3 & & -1 & 0 & 1 & 2 & 3 & 4 & 5 & 6 & 7 \\ 16 & 4 & & 0 & 1 & 2 & 3 & 4 & 5 & 6 & 7 & 8 \end{array} \qquad (5.6.10d)$$

Even so, the array gives a clear picture of the number of each type of *(m,n)-beat* or *(m-n)-transition* giving rise to equal group velocity *(m+n)* V_1. Apart from the zero velocity entries (standing waves) it is clear that the greatest number *2N* of contributors are for *fundamental (m+n)=±1* transitions giving group velocity $V_{\pm 1} = \pm\omega_1 r$ of (5.6.10c). Next in line is double-group-speed $V_2 = 2\omega_1 r$, then triple-group-speed $V_3 = 3\omega_1 r$, and so on, each with one less contributing *(m-n)*-pair, up to $V_{2N} = 2N\omega_1 r$, the *quantum speed limit* for a m=(- N^{th})-to-(+N^{th}) harmonic wave combination. But, Gaussian distributions "spill over" their *N*-limits.

An *(N=4)*-Gaussian distribution of Bohr-μ-wave harmonics is plotted in Fig. 5.6.5. Waves up to the 4^{th} or 5^{th} harmonic dominate while 6^{th} and 7^{th} *m*-values lie in the distribution tail ends. Compare the Bohr μ-wave to an optical pulse train (OPT) γ-wave having a similar Gaussian in Fig. 5.3.3(b).

What a difference! While the spacetime picture of the γ-wave OPT makes a single "baseball diamond" path, the μ-wave harmonics plotted in Fig. 5.6.5 show many overlapping diamonds. The m^{th}-group speed V_m is *m*-times the fundamental V_1, so the m^{th}-harmonic diamond takes a fraction *(1/m)* of the fundamental diamond time period τ_1 and then repeats *m* times in that period. The result is more than *N* overlapping diamonds made of wave nodes or anti-nodes, most squashed by some fraction *1/m>1/N*.

Follow the zeros!

If there is one rule for learning wave theory, it is, *"Follow the zeros!"* Zeros of ReΨ are spacetime coordinate grids in Chapter 4, beginning with Fig. 4.2.11 and Fig. 4.3.3. Here the zeros of probability or group wave magnitude $|\Psi|$ show prominently in Fig. 5.6.5. The $|\Psi|$-zeros (white-regions) stand out more clearly than the fainter and more broken diamonds that emanate from the original Gaussian pulse wave at the bottom center of the Fig. 5.6.5. In contrast, just one centered diamond is clearly visible in the γ-wave OPT plots of Fig. 5.3.2 and Fig. 5.3.3 while near-zero gallop-scallops fill the rest of those figures.

A $|\Psi|$-plot like Fig. 5.6.5 shows mainly group-wave $|\Psi|$-zeros or *nodes*. Phase wave (ReΨ)-zeros are more complicated and require some more theory and technology that will be introduced in Unit 3.

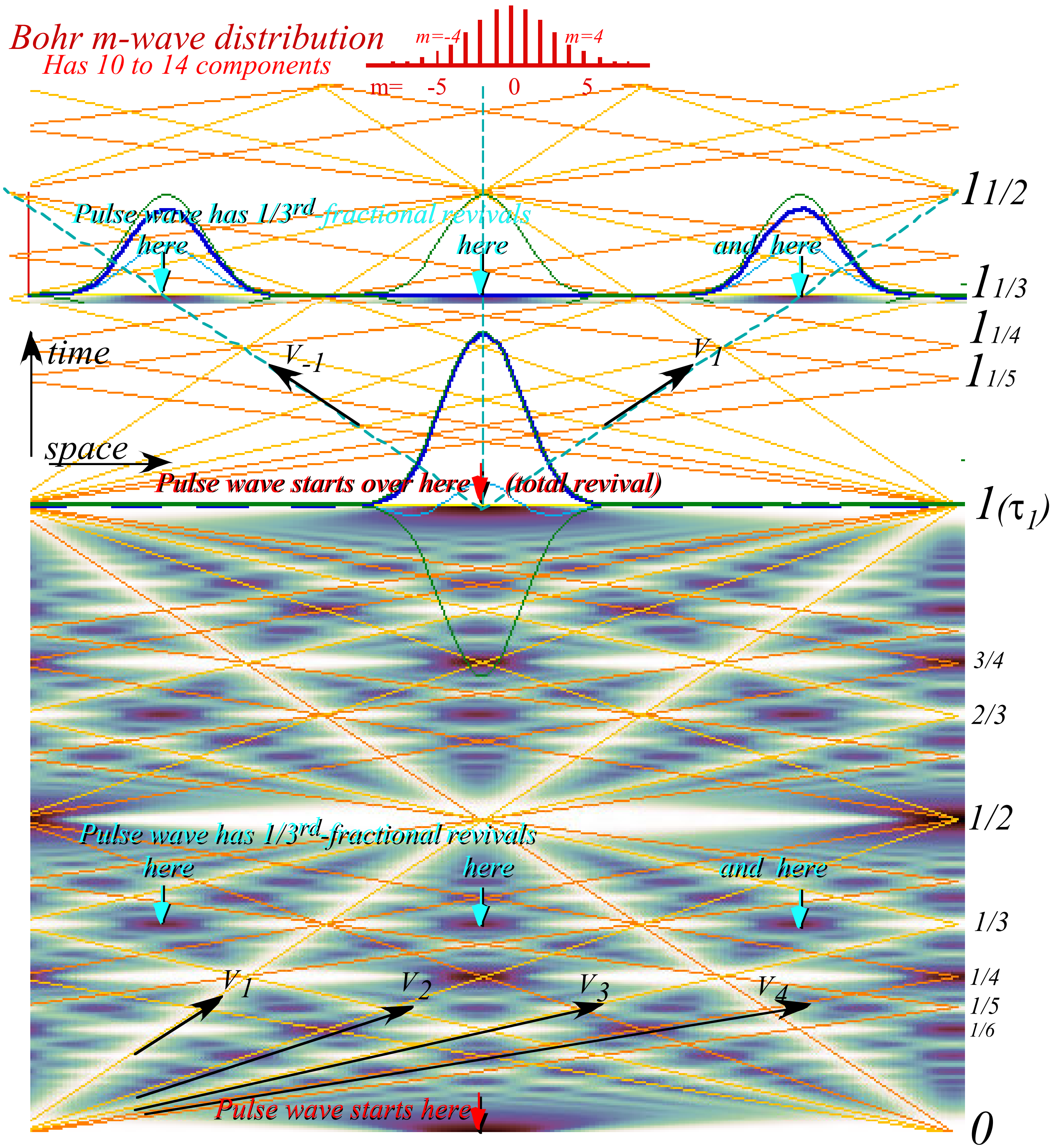

Fig. 5.6.5 (N=4)-Gaussian Bohr μ-wave pulse in spacetime |Ψ|-plot shows multiple group velocities.

Nodes tell a primary story of quantum wave interference. Instead of first asking the question of why and where a physical system or "particle" *IS*, we should first ask a more Zen-like question, that is, "*Where is it NOT!* As Holmes remarked, it was the dogs that *didn't* bark who first revealed the truth.

One reason for such a nihilistic philosophy is a simple emerging fact. There *ARE NO* Newtonian "particles" or corpuscles, only waves that often masquerade as particles. More to the point, $|\Psi|$-zeros are robust indicators of interference because, by being completely zero, they are not as sensitive as their still-breathing neighbors who, so being, are tossed up and down with each passing wavelet. In other words, if you're already dead, who can hurt you anymore? Nodes ($|\Psi|$-zeros) cut clear and contiguous paths in the spacetime plots while the anti-nodes ($|\Psi|$-peaks) leave fuzzy and broken paths.

Bohr μ-wave pulse train dephasing and revival

The initial pulse wave at the bottom of Fig. 5.6.5 starts out with an "expansion" phase before its quantum diamond paths can be seen emerging sometime between $1/12^{th}$ or $1/14^{th}$ of the fundamental period τ_1. That is just enough time for the fastest components, who travel above the quantum speed limit of $2NV_1 = 8V_1$, to make one trip around the ring. The $m=\pm 5$, $m=\pm 6$, and $m=\pm 7$ harmonics are in the "tails" of the *(N=4)*-Gaussian distribution plotted at the top of Fig. 5.6.5. A *(6+7)*-combination has group velocity $13\ V_1$ and exceeds the quantum speed limit of $5V_1$. That's a quantum *50 mph* over the speed limit. Off to jail!

When these "outlaws" first run into each other coming around the ring, they make the very finest gallop-scallops near the bottom of Fig. 5.6.5. These scallops are part of the very finest group velocity zero-lines emanating from the initial antipodal node (at the point on the Bohr ring opposite to the initial anti-node), that is, from either side of the x-axis in Fig. 5.6.5. The pulse wave then begins to *dephase* as a dozen or so velocity components spread out while literally cutting the pulse into ribbons of nodes!

However, after a whole period τ_1, the whole bloody mess reassembles or *revives* into a perfect reconstruction of the original pulse as plotted just above the center of Fig. 5.6.5. The concept of *rephasing* or *revival* was pointed out relatively recently by Joseph E. Eberly in a much more complicated system, the Jaynes-Cummings quantum electrodynamic model of an atom in a cavity.

For the Bohr model plotted in Fig. 5.6.5, a *total revival* is possible after each period τ_1, because all Bohr frequencies ω_m (5.6.10a) are an integral multiple m^2 of the fundamental transition frequency ω_1 . Also, there are *(1/m)-fractional revivals* in which the initial pulse appears to be "cloned" into m or $m/2$ copies that pop-up at uniform intervals of space and time between that of the main revivals. Their node or anti-node spacing depends on intersections of the group-velocity diamonds as do *(1/3)*-fractional revivals indicated in Fig. 5.6.5. One could argue that the *(1/3)*-clones in the upper part of Fig. 5.6.5 are due to the "particle" traveling at V_1 from its initial pulse origin. However, such a Newtonian picture is misleading. (Just look what happened to that clone on its way to the forum!)

If only the fundamental *(m=0)*-to-*(m=±1)* transitions are excited, only speed V_1 is possible as in Fig. 5.6.6 . Now the resulting spacetime plot resembles a 2-component γ-wave pulse plot in Fig. 5.3.2(b) or Fig. 5.3.3(a). Again, one could argue for a "particle" going velocity $\pm V_1$ from its initial pulse origin, but here wave interference or beat makes a Newtonian theory laughable. Less laughable are the quite clearly defined "X" nodal paths having velocity $\pm V_1$ in Fig. 5.6.6. It *is* more difficult to laugh at the deceased!

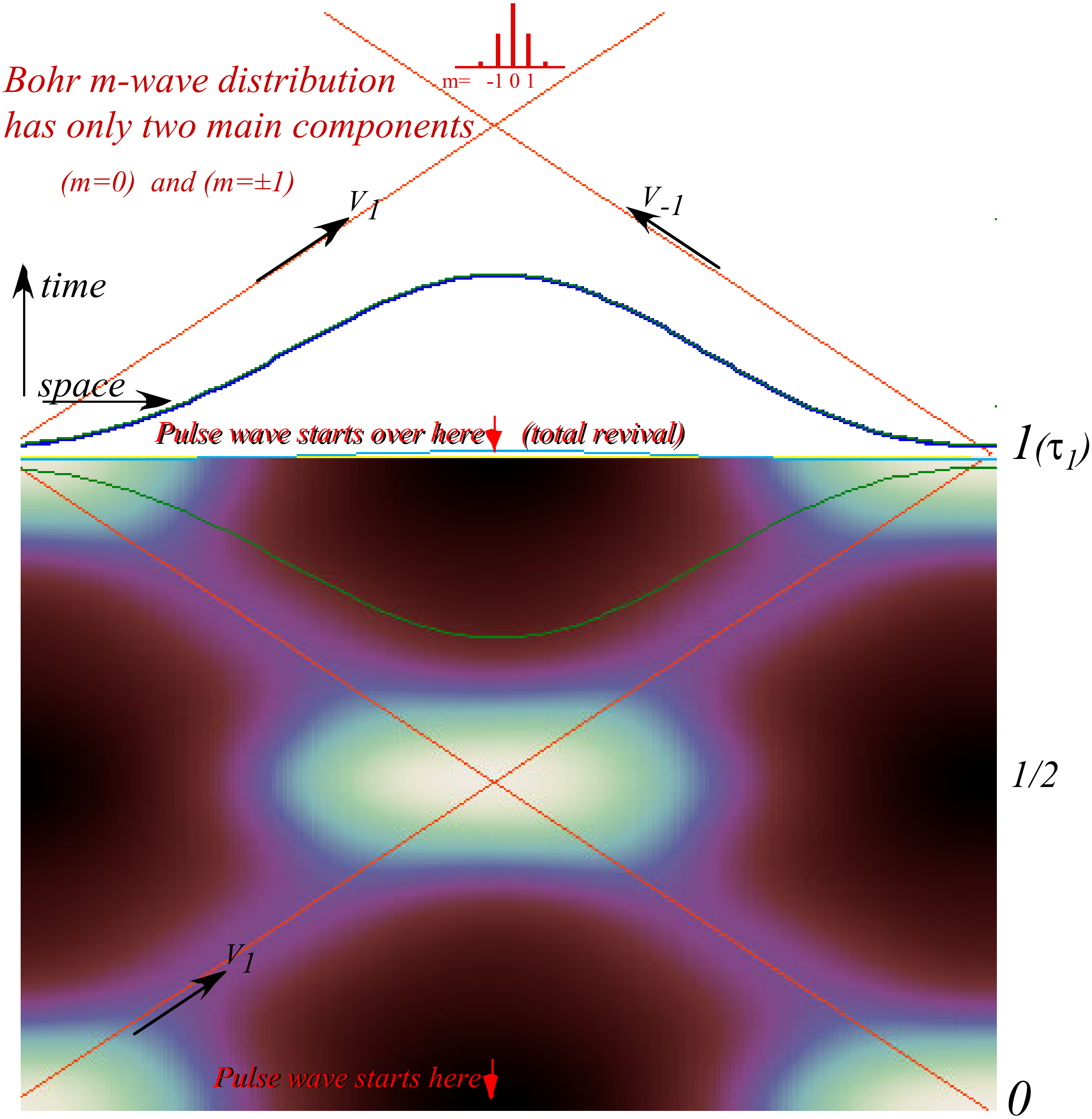

Fig. 5.6.6 (N=4)-Gaussian Bohr m-wave pulse in spacetime |Ψ|-plot shows multiple group velocities.

Ignored in all the |Ψ|-plots above are the wave phase, phase velocity, and ReΨ-zeros which, even for the simplest non-trivial 2-state case above in Fig. 5.6.6, have much more detailed structure than do the group waves and probability distributions plotted so far. To tell a comprehensible story about phase requires some symmetry group algebra of Fourier theory and its number-theoretic ancestry as given in Unit 3. In our wave-world, phase is the key, and the devil is definitely in its details.

Problems for Chapter 5.

Aquatic Dispersion *(revised 10.15.03)*

5.1.1 Suppose a dispersion function $\omega_{Aqua}(k)=ak^{1/2}$ describes water waves. (It does approximately.)
(a) Find phase and group velocity as a function of wavelength λ and wavevector k. Find V_{phase}/V_{group}.
(b) Water waves are peculiar by being both transverse and longitudinal. Suppose each surface point follows both the $Re\Psi$ and $Im\Psi$ parts of its phasor instead of just $Re\Psi$ (transverse wave) or just $Im\Psi$ (longitudinal wave), that is, goes around in a circle. Will the surface shape still be a sine wave?
If not, tell what sort of curve it might be under different conditions. (What amplitude "breaks" a wave)
(c) Does $\omega_{Aqua}(k)$ have Lorentz invariance?.,.i.e., is same for ship and any moving observer?
Compare $\omega_{Aqua}(k)$ to $\omega_{Newton}(k)$ below by comparing V_{phase}/V_{group}. for each.

Holiday Dispersion

5.1.2 Suppose that no matter what amplitudes or phase you attached to each wave point, the wave phasors would all rotate at exactly 1 Hz without any change of amplitude. (Call this a "Movie Marquis" or "Christmas Tree" system after the string of uncoupled blinking lights in it.)
(a) Derive and plot a dispersion function $\omega_{Xmas}(k)$ that would describe this system.
(b) Tell what V_{phas} and V_{group} you expect to see as a function of wavelength λ and wavevector k.
(c) Does $\omega_{Xmas}(k)$ have Lorentz invariance.i.e., is same for all observers? . approximately… sometimes?

Fig-Newton Dispersion

5.1.3 Suppose a dispersion function $\omega_{Newton}(k)=ak^2$ describes matter waves. (It does approximately.)
(a) Give V_{phas} and V_{group} velocity as a function of wavelength λ and wavevector k. Find V_{phase}/V_{group}.
(b) Does $\omega_{Newton}(k)$ have Lorentz invariance?. approximately… sometimes?

Deer in the headlights

5.1.4--Imagine a deer crosses the East bound lane of a superhighway on which all cars have the same source frequency ω_0 for headlights and tailights. The deer sees frequency ω_W to the West and ω_E off in the East.
(a) If the deer knows all cars go the same speed u, can it find u and ω_0 from ω_W and ω_E? How or why not?
(b) Now, what if the headlight source frequency ω_{0Head} and tailight source frequency ω_{0Tail} are different?
(c) If cars go different speeds u_1 and u_2, can deer find the speeds and source frequencies from ω_W and ω_E? How or why not? What if $\omega_{0Head} = \omega_{0Tail}$? Would knowing source frequency(s) help? Explain.
(d) Suppose instead each car has head-matter-asers putting out kinkless wave (ω_H , ck_H=0) and tail-matter-asers putting out (ω_T , ck_T=0), and the deer (crafty doe) can measure (ω_W , ck_W) in the west and (ω_E , ck_E) in the East. Is this enough for the deer to determine both cars' speed and frequency? How or why not?

Really-really fast

5.2.1.At ultra-relativistic speeds it may be useful to use the parameter $\delta=1-\beta$ instead of $\beta=\tanh(\theta)$ since the latter gets so close to unity that numerical underflow problems may arise. Find approximate and exact expressions relating δ to (and from): (a) Rapidity θ, (b) Doppler red/blue shift *b*. (c) Lorentz contraction (d) Time dilation.

How long does it take to get to α-Centauri in 6 months?

5.2.2. Suppose we define a velocity we will call $v_{ignorant}$ as that speed that someone ignorant of relativity would say a spaceship had to go to get to a distant star in a given time. For example, if we ask how fast a ship would have to go to get to α-Centauri (~4 light years away) in 6 months then the "ignorant" person would say it had to go $v_{ignorant} = 8c$, that is, eight times the speed of light, so if super-luminal travel is prohibited 6 months is too short.

But the relativity expert says that there is a speed v_{expert} which will get the ship to α-Centauri in 6 months according to the ship's passengers, who, after all, are the ones counting.
(a) Compute v_{expert} for this 6-month α-Centauri trip and derive general algebraic relations giving v_{expert} in terms of $v_{ignorant}$ and vice-versa.
(b) How long does it really take to get to α-Centauri in 6 months? (Lighthouse time.)

The cost of ignorance::NASA goes for broke

5.2.3 Use the velocity $v_{ignorant}$ defined in the preceding problem and results concerning the *α-Centaur* voyage.

(a) Relativistic momentum of particle m can be expressed nicely in terms of $v_{ignorant}$. Do so.

(b) Given the proposed journey to α-Centauri in 6 months work up a budget estimate. How many GNPU (1 GNPUnit = $\$10^{12}$=$1 Trillion) will it cost to get a ship of mass 10^6 kg (1,100 tons) up to speed at the prevailing rate of power: $0.10/kWHr. ? (1 kWHr = 3600x10^3 J) Note: Don't count the rest mass energy of the ship in your cost...assume NASA (i.e. you the taxpayer) has already bought that.

` Bottom line: Cost=___________________

A Long Way to Go for a Beer

5.5.1 Suppose you have been accelerating at 9.8m/sec^2 since birth. (You have been!) By the time you are 21 and can legally order a drink you have traveled a long way relative to the inertial "birth" frame in which you were born. How long? Let's see!

All this is derived using a relativistic Newton's law in your (proper) local time τ. Recall (5.5.3)

$$\frac{dp_x''}{d\tau} = mg, \qquad \frac{dE''}{d\tau} = 0$$

Since all observers should agree that you are experiencing constant 1 g acceleration they will all see your trajectory as a single invariant curve. You should plot this curve in (x,ct) and (cp,E) graphs.

(a) At 1 year of age what is your hyperbolic rapidity angle relative to the inertial frame? ρ_u=_______

(b) At 1 year of age what is your speed relative to that frame? u/c=____________

(c) When you are 1 year old how much time has passed in that "birth" frame? ________sec. and__________yr.

(d) When you are 1 year old how far have you gone in that frame? ________m.

(e) At 21 years of age what is your hyperbolic rapidity angle relative to the inertial frame? ρ_u=_______

(f) At 21 years of age what is your speed relative to that frame? 1-u/c=____________ (Use δ in *Really-really fast*.)

(g) When you are 21 years old how much time has passed in that frame? ________sec. and __________yr.

(h) When you are 21 years old how far have you gone in that frame? ________m.

Homecoming or Born again!

(i) At what age do you have enough kinetic energy relative to the birth frame to recreate all your mass there?

Boom and BOOO-OOM!

5.6.1 Suppose your job is to estimate and compare the energy yields per kilogram of conventional chemical explosives and of nuclear fission devices. You have at your disposal only the topics of this chapter, particularly the famous $E=Mc^2$ result of (5.2.5b), the Bohr radius of (5.6.3), the Coulomb energy $V(r)=q^2/4\pi\varepsilon_0 r$ from (5.6.2), approximate nuclear size of 5 Fermi, and Avagodro's number of *6.02e23* nuclei per mole.

(a) Estimate the yield of a kg of $^{92}U_{235}$ assuming it splits roughly in half. (First, do you follow the suggestions of the popular literature and use the Mc^2 formula? Why, how, or why not?)

(b) Estimate the yield of a kg of Lead Azide PbN_6 assuming it splits completely. (Is Mc^2 formula at all applicable here? Why, how, or why not?) For lead and Nitrogen you may assume 2 Bohr radii each and that all electrons disappear. (This maximum energy estimate exceeds true yield. By roughly how much?)

Bleep the phase, maybe

5.6.2 Details of wave phase dynamics have been such nebulous and complicated subjects that some physicists have simply said, "(Bleep) the (bleeping) phase!" Can you help this situation?

(a) Consider the possible phase velocity or velocities for an Bohr matter wave excited as it was in Fig. 5.6.5 and Fig. 5.6.6. Give formulas and construct tables as was done for the group velocity in (5.6.10).

(b) Give a geometric construction of Bohr-Schrodinger phase velocity that relates to the group velocity construction of Fig. 5.6.4. Does Schrodinger's ignorance of Mc^2 for his quantum theory affect this? Discuss why or why not.

3's Company

5.6.3 Find what group velocity values would show up for a 3-level excitation of m=0,±1, and ±2, only. Sketch the reulting wave-probaility-zero paths or nodal lines and anti-nodal lines in space time for one fundamental period. (Optional: Compare to a plot of (Δm~±2)-range $^{\sin x}/_x$ and Gaussian packets by BohrIt or equivalent.)

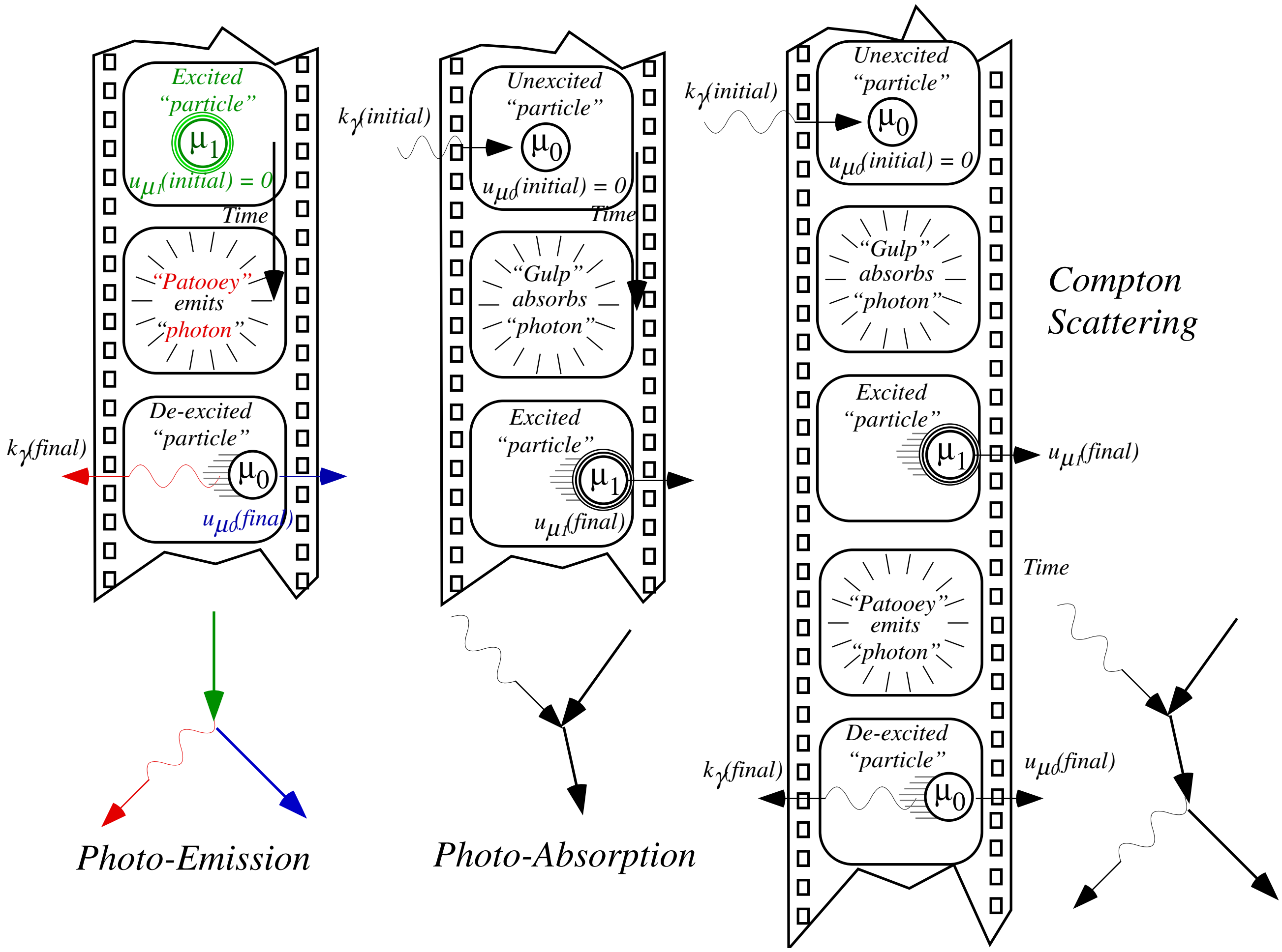

"Patooey"- Compton emission recoil

5.6.4 When an excited stationary molecule, atom, or nucleus emits a photon (γ-wave) during a quantum transition, it ends up on a lower μ-hyperbola, that is, it gets lighter by starting out at k_1=0 on a μ_1-hyperbola and ends up with a non-zero k_0 on a lower μ_0-hyperbola. This is called a *Compton recoil* process.

Suppose that the recoil process conserves the sum $\mathbf{K}_\gamma + \mathbf{K}_\mu = \mathbf{K}_{Total}$ of the μ-wave and γ-wave **K**-vectors $\mathbf{K}_\gamma$=(ck(γ), ω(γ)) and $\mathbf{K}_\mu$=(ck(μ), ω(μ)). Given the initial and final μ-levels μ_1 and μ_0 derive equations for the final momenta and energies of the μ-wave and γ-wave. Solve by geometry or algebra in terms of μ_1 and μ_0.

(a) Graph the transition on a per-spacetime graph for the case μ_1 = 2 and μ_0 = 1. (High energy physics)
(b) Graph the transition on a per-spacetime graph for the case μ_1 = 2 and μ_0 = 1.8. (Lower energy physics)
(c) Consider an H atom state or level whose μ_1 value is 10 eV higher than μ_0. (Way low energy physics) (Recall that its ground energy is ~Mc^2 where $M=m_{proton}$.) Give recoil momenta and velocity in mks units but energy in eV. Compare the shift in energy to 10eV? Is it big enough to be observed easily?

"Gulp"- Compton absorption recoil

5.6.5 The quantum absorption process is essentially the reverse of the emission process in Prob. 5.6.4 but as shown in the middle figure the μ_0 particle is initially stationary. For cases (a-c) work out the corresponding algebra, graphs, and numerical results (for (c)). For part (c) let a stationary H atom be excited from its ground state to a state or level whose μ_1 value is 10 eV higher than μ_0.

"Gulp & patooey"- Compton scattering

5.6.6 A photon backscattering (180°) off of a particle is the most extreme form of *Compton scattering*. As shown in the 3rd figure, this process is equivalent to absorption followed by emisssion. While this is the key to analyzing scattering crossections, it is not necessary for deriving final recoil and frequency shift values. These may be found using the techniques sketched in Sec. 5.2(g) and should depend only on initial light frequency and ground state paricle mass or proper frequency μ_0 . Derive formulas using geometry as in Fig. 5.2.6 wherever possible.

Fast company (Based on Lab booklet for RelativIt)
5.RelativIt.1. Consider *Relativit* Fig. 2a showing an elastic collision between identical m=1MeV particles with equal but opposite momenta in the Lighthouse frame. (It is called a center-of-momentum (CM) frame.)
(a)Given Fig. 2a compute correct relativistic momentum components for the same identical particle collision seen by the ship in Fig. 2b. Is this momentum conserved?
(b) Suppose instead that the particles scattered at Θ_{CM}=180° instead of Θ_{CM}=90° as in the figure, that is both come in and go out with the same speeds u=±c/2 in the Lighthouse frame along the ship's path. Derive the final velocities and momenta according to the ship going v=-c/2 (RLH).
(c) Plot the initial and final (cp, E) vectors of the two particles in (b) for the Lighthouse frame.
(d) Plot the initial and final (cp', E') vectors of the two particles in (b) for the Ship frame.
(e) If the collision is totally inelastic, that is, results in one big "Glunkon" particle, show momentum energy of the resulting Glunkon in both plots (c) and (d).
(In each plot show the vector sum of the (cp, E) vectors before collision and the sum after collision. Should this sum be conserved? Use the mass shell hyperbolas.)

Relativistic decadence (Based on Lab booklet for RelativIt)
5.RelativIt.2. Suppose a 2MeV "Slobon" particle sitting in Lighthouse frame decays into a rest mass 1MeV "Skinon" particle and a photon which is emitted in the direction of the ship's travel. (Ship goes v=-c/2 (RLH).)
(a) Compute all final energies and momenta and plot this event according to the Lighthouse.
(b) Compute all final energies and momenta and plot this event according to the Ship.
(You should do plots on (cp, E) and (cp', E') graphs first, but also sketch results on (x, ct) plot.)